EUROPEAN SCHOOL OF MOLECULAR MEDICINE

SEDE DI NAPOLI

UNIVERSITA' DEGLI STUDI DI NAPOLI "FEDERICO II"

Ph.D. in Molecular Medicine – Ciclo IV/XXII

Curricula Human Genetics

The Oral-facial-digital type I syndrome: a model to study renal cystic disease in ciliopathies

Tutor:
Prof. Brunella Franco

Internal Supervisor:
Prof. Domenico Grieco

External Supervisor:
Prof. Mario Pende

Coordinator:
Prof. Francesco Salvatore

Ph.D. student:
Dr. Daniela Iaconis

Academic Year: 2010-2011

TABLE OF CONTENTS

ABBREVIATIONS

AA – aminoacids

ADPKD – Autosomal dominant polycystic kidney disease

ARPKD – Autosomal recessive polycystic kidney disease

DMEM – Dulbecco's modified Eagle's Medium

eIF3 – eukaryotic initiation factor 3

eIF4E – eukaryotic initiation factor 4E

FAK – focal adhesions

FBS – Fetal Bovine Serum

GFR – Glomerular Filtration Rate

GH – Growth hormone

HBSS – Hank's balanced salt solution

HEK293 - Human Embryonic Kidney 293 cells

IND - *Ofd1*$^{fl/y}$;*cre*$^{ER\text{-}TM}$ mutants

Ksp mutants – *Ofd1*^{fl};*cre*^{Ksp} conditional mutants

MDCK – Madin-Darby Canine Kidney Cells

mTOR – mammalian target of rapamycin

NPHP – nephronophthisis

OFDI – Oral -Facial-Digital type I syndrome

Pc 1 and 2 – polycystin1 and 2

PIC – pre-initiation complex of translation

PKD – Polycystic Kidney Disease

RT – Room Temperature

SEM – Scanning electron microscopy

siRNA - small interfering RNA

TSC – tuberous sclerosis

WT – wild type

FIGURE INDEX

ABSTRACT

The Oral-Facial-Digital type I syndrome (OFDI; MIM 311200) is a rare syndromic form of inherited renal cystic disease. It is transmitted as an X-linked dominant, male lethal disorder and is caused by mutations in the *OFD1* gene. Previous studies demonstrated that OFDI belongs to the growing number of disorders ascribed to dysfunction of primary cilia. Among the different clinical signs OFD type I is characterized by the presence of renal cystic disease, which is present in over 60% of cases. With the purpose of studying the role of the *Ofd1* transcript in renal cystic disease, we generated two conditional *Ofd1* deficient mouse models (*Ksp* and IND), which resulted in viable mice characterized by renal cystic disease and progressive impairment of renal function. The study of these models allowed us to demonstrate that primary cilia initially form and then disappear after the development of cysts, suggesting that the dysfunction of primary cilia is a consequence rather than the primary cause of renal cystic disease. Immunofluorescence and western blotting analysis revealed upregulation of the mTOR pathway in both dilated and non dilated renal structures. Treatment with rapamycin, a specific inhibitor of the mTOR pathway, resulted in a significant reduction in the number and size of renal cysts and a decrease in the cystic index compared with untreated mutant animals, suggesting that cystogenesis in our model is mTOR-dependent. mTOR is frequently deregulated in inherited forms of cystic kidney although the molecular mechanisms underlying this phenomenon are still to be determined. The use of both *in vitro* and *in vivo* systems allowed us to demonstrate that OFD1 has a role in the formation of the pre-initiation complex of translation (PIC). We showed that OFD1 coimmunoprecipitates with two subunits (η and δ) of the eIF3 complex and colocalizes at the centrosome with subunits of the PIC. In addition, we also demonstrated that OFD1 is present in polysomes extracted from kidneys and interacts *in vivo* with subunits of the eIF3 complex. Microarray experiments performed on mRNA extracted from polysomes indicate impaired translation for a number of transcripts. These results indicate for the first time a role of OFD1 in the formation of the PIC and in the regulation of translation. Among the putative targets we focused our attention on GH and our data suggest that higher levels of the GH due to the impairment of translation may be responsible for the upregulation of the mTOR pathway.

All together our results shed light on the pathogenetic mechanisms underlying this rare inherited form of renal cystic disease and propose new possible link between renal cystic disease and deregulation of the mTOR pathway.

INTRODUCTION

1. The molecular basis of OFDI syndrome

1.1. Clinical features observed in OFDI syndrome

Oral-facial-digital type I (OFDI; MIM 311200) syndrome is an X-linked dominant male lethal disorder and belongs to the heterogeneous group of developmental disorders known as Oral-facial-digital syndromes (OFDs) (Toriello 1993) (Gurrieri, Franco et al. 2007). OFDI syndrome was reported in 1954 (Papillon and Psaume 1954) and further defined by Gorlin and Psaume in 1962 (Gorlin and Psaume 1962). OFDI has an estimated incidence of 1:250,000 live births (Wahrman, Berant et al. 1966) and it has been described in different ethnic backgrounds (Salinas, Pai et al. 1991). This syndrome is transmitted as an X-linked dominant condition with embryonic male lethality, which usually occurs in the first and/or second trimester of pregnancy (Doege, Thuline et al. 1964; Wettke-Schafer and Kantner 1983). However, 75% of the cases are apparently sporadic. OFD type I, similar to all other OFDs, is characterized by malformations of the face, oral cavity and digits with a high degree of phenotypic variability. The central nervous system is frequently involved. Dysmorphic features affecting the head and face include facial asymmetry, hypertelorism, micrognathia, broadened nasal ridge, hypoplasia of the malar bone and of the nasal cartilage, and frontal bossing (Gorlin 2001). Craniofacial abnormalities include facial anomalies in 69.1% of cases (downslanting palpebral fissures, hypoplasia of the ala nasi, hypertelorism, telecanthus, microretrognathia, epicanthus, flat face, and low-set ears); evanescent milia (29.4%) of the face and ears, which usually disappear before the third year of life; and dryness, brittleness, and/or alopecia of the scalp hair (21.5%). Also, cleft lip and pseudocleft of the upper lip are observed in 32.6% of patients (**Table I**). Oral abnormalities are consistently reported in this condition and include oral aberrant frenula (63.7%), tongue abnormalities (84.1%) (lobulated tongue, lingual hamartomas, clefts), clefts of the alveolar ridge (22.2%), cleft/high arched palate (49.6%), and teeth abnormalities (43.3%) (**Table I**) (Macca and Franco 2009). These clinical features overlap with those reported in the other forms of OFDs (Toriello 1993), although among these, OFDI can be easily distinguished because of its X-linked dominant inheritance pattern and because of the renal cystic disease, which is specific to type I (Connacher, Forsyth et al. 1987; Donnai, Kerzin-Storrar et al. 1987; Scolari, Valzorio et al.

1997). Examples of the clinical signs observed in OFD type I are reported in **Figure 1**. Histochemical analysis of cystic renal tissues from OFDI patients demonstrate a predominantly glomerulocystic kidney disease with a minor population of tubular cysts (Feather, Winyard et al. 1997). The age of onset of cystic disease in patients with OFDI is most often adulthood (second and third decades) but cysts have been occasionally described in children in the first decade (Stapleton, Bernstein et al. 1982; Salinas, Pai et al. 1991; Odent, Le Marec et al. 1998). The overall incidence of renal cysts in this condition is 37.3%, if we consider all patients regardless their age (**Table I**). However, if we consider the subset of cases >18 years this incidence goes up to 63%, thus indicating that most cases are detected in adulthood due to both the delayed age of onset and to more frequent monitoring of the renal function. Systematic monitoring from early years could reveal that cystic kidney disease is more frequent than previously estimated in this condition. This observation represents a strong indication for renal function monitoring (both morphological and biochemical) in OFDI patients from childhood (Prattichizzo, Macca et al. 2008).

1.2. The Identification of the gene responsible for OFD type I syndrome

The locus of OFD type I was first mapped by linkage analysis to the Xp22 region (Feather, Winyard et al. 1997; Gedeon, Oley et al. 1999). The gene responsible for this rare genetic disorder, named *OFD1*, was identified by using a positional candidate gene approach in 2001 (Ferrante, Giorgio et al. 2001). The *OFD1* gene comprises 23 exons encoding a 1011 amino acid protein that shares no sequence homologies with proteins of known function. Interestingly, the *OFD1* gene has been found to escape X-inactivation in human while the murine counterpart is subject to X-inactivation (Ferrante, Barra et al. 2003). A total of 67 different mutations in OFDI patients have been reported to date, including frameshifts, splicing, non-sense and missense mutations. The vast majority is represented by frameshift mutations resulting in premature protein truncation (Ferrante, Giorgio et al. 2001; Rakkolainen, Ala-Mello et al. 2002; Romio, Wright et al. 2003; Thauvin-Robinet, Cossee et al. 2006; Prattichizzo, Macca et al. 2008). Most of the *OFD1* mutations identified to date in patients lead to a premature truncation of the protein in its N-terminal region and are therefore predicted to act with a loss of function mechanism. However, the

possibility that truncated forms of the OFD1 protein may have a dominant-negative effect on the wild type protein has not been formally ruled out.

The *OFD1* transcript has been shown to be expressed in both human and murine structures in all tissues affected by the disorder from early stages of development to adulthood. Studies have shown that *OFD1* is expressed in all adult human tissues examined (pancreas, kidney, skeletal muscle, liver, lung, placenta, brain, and heart)(de Conciliis, Marchitiello et al. 1998). In the laboratory were I completed my PhD project, RNA in situ studies on mouse-embryo tissue sections at different developmental stages starting from E12.5 were performed to investigate the spatiotemporal expression of the *Ofd1* transcript during development. The first site of expression was sharply and exclusively detected at 12.5 days of gestation in the genital ridges. At later stages (E14.5 and E16.5), *Ofd1* expression is not only confined in the developing gonads, but high to moderate levels of expression are detected in various craniofacial structures and in the nervous system. In particular, *Ofd1* resulted to be highly expressed in the epithelium lining the oral and nasal cavities, including the tongue and the gum region, in the developing tooth buds, in the Rathke's pouch (primordium of the adenohypophysis), and in the vibrissae follicles. The transcript is also highly represented in the proliferative and postmitotic layers of the cerebral cortex and ganglionic eminences (anlage of the basal ganglia), the neural retina, the inner ear, and the dorsal root ganglia and the kidneys (Ferrante, Giorgio et al. 2001). Concerning the expression of the *Ofd1* transcript in the kidney immunohistochemical studies demonstrated that the Ofd1 protein localizes in the fetal developing metanephros, in particular in the outer nephrogenic zone of the cortex in the mesenchyme. Minimal positive signal was detected in later nephron precursors, including vesicles, comma, and S-shaped bodies. Consistent staining was not observed in developing glomeruli (Romio, Wright et al. 2003) even if a glomerular function for Ofd1 was demonstrated using different animal models, namely the mouse (see below) (Ferrante, Zullo et al. 2006) and the zebrafish (Ferrante, Romio et al. 2009).

1.3. The OFD1 protein: putative functions and subcellular localization

The *OFD1* gene encodes a 1011 amino acid protein, which shares no sequence homologies with proteins having known function. Five predicted coiled coil domains (hereafter CC) occupy almost the entire length of the molecule

(de Conciliis, Marchitiello et al. 1998) whereas the N-terminal region shares a Lis1 homology motif (LisH) with over 100 eukaryotic intracellular proteins (Emes and Ponting 2001). Several studies indicate that the alpha-helical CC, is a highly versatile folding motif found in proteins with different functions and is described to mediate subunit oligomerization (Burkhard, Stetefeld et al. 2001). The biological function of the LisH motif is still unknown, although it has been postulated to be involved in cell migration, nucleokinesis, and chromosome segregation (Emes and Ponting 2001).

Previous studies had shown that OFD1 co-localizes with γ-tubulin and is a centrosome-associated protein (Romio, Wright et al. 2003). Data from different laboratories also indicate that OFD1 localizes to the basal body of primary cilia in fully differentiated renal epithelial cells and in MDCK (Madin-Darby Canine Kidney Cells) (**Figure 2 B and C**) (Romio, Wright et al. 2003; Giorgio, Alfieri et al. 2007). In addition, it was recently described that OFD1, is a component of the distal centriole in the centrosome and controls centriole length and building (Singla, Romaguera-Ros et al. 2010). The centrosome is an organelle that serves as the main microtubule organizing center (MTOC) of the animal cell as well as a regulator of cell-cycle progression. Moreover, centrosomes can act as basal body at the cell cortex, promoting cilia assembly and function. The centrosome and the primary cilium are strongly linked both structurally and functionally; a consistent number of centrosomal proteins were found to localize to the centrosome, the basal body and the ciliary axoneme during different phases of the cell cycle.

In addition data generated in the laboratory when I performed my PhD project also demonstrated a nuclear localization for the OFD1 protein (**Figure 2 F, G and H**) (Giorgio, Alfieri et al. 2007). In the same report Giorgio G. and coauthors also demonstrated that OFD1 is able to self-associate through its CC rich region and it interacts with RuvBl1. RuvBl1 belongs to the AAA-family of ATPases, is involved in transcriptional regulation and cell division and it has been associated to ciliary assembly and function in *Chlamydomonas reinhardtii* (Stolc, Samanta et al. 2005). OFD1, together with RuvBl1, is also able to coimmunoprecipitate with subunits of the human TIP60 histone acetyltransferase (HAT) multisubunit complex, suggesting that OFD1 may be part of a multi-protein complex and could play different biological functions in the centrosome-primary cilium organelles as well as in the nuclear compartment (Giorgio, Alfieri et al. 2007).

2. Animal models for OFDI syndrome

2.1. Generation of a null murine model for OFDI syndrome

To gain insights into the pathogenetic mechanisms underlying OFDI syndrome, a murine animal model for this condition was generated in Prof Brunella Francos's laboratory (Ferrante, Zullo et al. 2006). Exons 4-5 of the Ofd1 murine homolog were cloned between two loxP sites. The *Ofd*^{fl} line was crossed with pCX-NLS-Cre mice, a generale deletor cre line that expresses the Cre recombinase ubiquitously starting at the four-cell-stage (Nagy 2000). This cross would allow to obtain null mice with ubiquitous *Ofd1* inactivation from early stages of development. Exicision of these exons by a cre/loxP strategy resulted in the generation of a shorter, presumably non-functional form, of 106 AA. This strategy was selected to reproduce the pathological condition observed in humans since many non-sense or frameshifts mutations leading to the production of a short and truncated form of the protein have been identified in exon 3 in OFDI patients. Heterozygous females (*Ofd1*$^{\Delta 4\text{-}5/+}$), reproduced the main features of the human disease, albeit with increased severity, probably due to differences between the X-inactivation patterns observed in human and mouse (Ferrante, Barra et al. 2003; Morleo and Franco 2008). Female mutants died at birth, displaying craniofacial and skeletal abnormalities including polydactyly or polysyndactyly, with seven to nine digits. The tibia and fibula in the hindlimb were invariably bent and in some cases fused and additionally, abnormalities of the ribs and of the sternum, which was not fused along the midline have been observed (Ferrante, Zullo et al. 2006).

Autopsy of the newborn *Ofd1*$^{\Delta 4\text{-}5/+}$ females showed also disorganization of the brain, reduction of the lungs, defects in the great vessels and a highly penetrant renal cystic disease of glomerular origin (**Figure 3**). Immunofluorescence analysis with an antibody that preferentially labels the ciliary axoneme of primary cilia showed the absence of cilia on the luminal surfaces of cells that lined the cysts, thus implicating ciliogenesis as a mechanism underlying cyst development in OFD type I (**Figure 3 F**). Cilia were present in noncystic glomeruli and in normal tubules adjacent to the cysts (**arrows in Figure 3 F**); due to the fact that heterozygous females are mosaics and for the X inactivation phenomenon we have the presence of both cells expressing the mutated X and cells expressing the normal X chromosome (Ferrante, Zullo et al. 2006).

Complete inactivation of *Ofd1* in hemizygous males (*Ofd1*$^{\Delta 4\text{-}5}$) causes male embryonic lethality, as the majority of *Ofd1*$^{\Delta 4\text{-}5}$ male embryos die by E12.5, and early developmental defects, mainly neural tube, heart and laterality defects were observed. Some *Ofd1*$^{\Delta 4\text{-}5}$ male embryos display *situs inversus* and abnormal expression of the asymmetrical markers *Nodal* and *Pitx2* at E8 suggesting that heart position is randomized due to loss of molecular asymmetry. In addition, electron microscopy analysis demonstrated absence of primary cilia in the embryonic node of these embryos at E7.5 (Ferrante, Zullo et al. 2006).

These results are consistent with the subcellular localization of OFD1 in the basal body and indicate that Ofd1 is required for primary cilia formation and left right axis specification (Ferrante, Zullo et al. 2006). In addition these results demonstrate that OFD type I syndrome should be included in the growing number of disorders associated to ciliary dysfunction.

2.2. Generation and characterization of model for OFD type I syndrome in zebrafish

Recently Ofd1 function was also studied in developing zebrafish (*Danio rerio*) embryos (Ferrante, Romio et al. 2009). The Zebrafish homolog, *ofd1,* encodes a protein with a LisH domain and coiled-coil domains with a 29.6% identity with the human OFD1. Transcription of *ofd1* occurs ubiquitously in embryos with noticeably higher levels in ciliated organs such as otic vesicles and neuromasts and the protein has the same centrosome/basal body localization previously described in human and mice. Injection of antisense morpholinos (MOs) in one-cell stage embryos, determines a typical ciliary phenotype with bent body, laterality defects and oedema. In this model, cilia are shorter then normal and show an altered ultrastructure leading to an alteration of the fluid flow and laterality defects as a consequence. Interestingly, they show a role for *ofd1* in convergent extension (CE) during gastrulation, consistent with other studies linking cilia and non-canonical, PCP, Wnt signalling (Benzing, Simons et al. 2007; Corbit, Shyer et al. 2008). This could be an indirect result of a requirement for Ofd1 in normal ciliary structure and function, or could occur directly through interaction with Wnt signalling components, further analysis are necessary to address this point. However, while cystic disease was not observed, the described CE defects could be responsible also for delayed glomerular fusion observed in *ofd1* morphants. In addition, glomerular vascolarization is also compromised (Ferrante, Romio et al. 2009). Very little is known about a

glomerular function for *ofd1* and the paper by Ferrante et al., opens new insights in renal involvement for the protein. Altogether the phenotype observed in the zebrafish model together with the phenotype described in the null murine model indicate that Ofd1 plays an important role in the pathogenesis of inherited renal cystic disease and in normal renal function.

3. Renal cystic disease: genetic causes and pathogenetic mechanisms

3.1. Introduction and definition

Renal cystic disease is a pathological condition characterized by the growth of numerous cysts in the kidneys. The cysts are filled with fluid and can replace much of the mass of the kidneys, reducing kidney function and leading to end stage renal failure with indication for dialysis or renal transplantation. One third of people older than 50 years develop renal cysts with multiple aetiologies:

- Genetic diseases in which renal cyts are the prevalent clinical sign – Autosomal recessive polycystic kidney disease (ARPKD), Autosomal dominant polycystic kidney disease (ADPKD), nephronophthisis (NPHP), medullary cystic kidney disease (MCKD), glomerulocystic kidney disease (GCKD).
- Cysts associated with systemic genetic disease – Autosomal Dominant syndromes: Von Hippel-Lindau syndrome (VHLS), tuberous sclerosis (TS) – Autosomal Recessive syndromes: Meckel's Syndrome; Jeune's Asphyxiating Thoracic Dystrophy; Zellweger's Cerebrohepatorenal Syndrome; Ivemark's Syndrome (renal-hepatic-pancreatic dysplasia); Bardet-Biedl Syndromes – X linked syndromes: Oro-facio-digital type I syndrome (OFDI).
- Acquired – Simple cysts, acquired cystic renal disease, medullary sponge kidney (MSK).
- Malignancy – Cystic renal cell carcinoma (RCC).

Among the genetic forms of Polycystic Kydney diseases (PKDs), ADPKD is the most common and occurs in 1 in 800 live births. Two genes have been identified for ADPKD: PKD1 and PKD2. These genes encode for two-membrane proteins polycistin 1 (Pc1) and 2 (Pc2), respectively. Pc1 is a mechanoreceptor localized at focal adhesions, cell-cell junctions and primary cilia and transduces signals through phosphorylation cascades to regulate cell transcription (Zhou 2009). Pc1 interacts with Pc2, a calcium-permeable channel that facilitate

calcium influx. Calcium acts as an intracellular second messanger and activates G proteins and the production of cAMP leading to the regulation of multiple signaling pathways (Chapin and Caplan 2010). ARPKD is quite rare and is caused by mutations in the PKHD1 gene encoding for Fibrocystin. This protein is a membrane receptor that is highly espressed in fetal-kidney collecting ducts and it is now firmly established that localizes at the primary cilium (Ward, Yuan et al. 2003). In addition, NPHP is caused by mutations in twelve genes (*NPHP1–11* and *NPHPL1*). The first identified NPHP gene was *NPHP1* that encodes the protein nephrocystin-1, which is mutated in approximately 20% of all cases of NPHP (juvenile NPHP type 1 form) (for a review on nephronophtisis see (Hurd and Hildebrandt 2011). Unlike the Polycystins and Fibrocystin, Nephrocystin is a small protein that does not localize at the membrane, however it localizes at the focal adhesions and at the primary cilium (Donaldson, Dise et al. 2002; Wilson 2004; Fliegauf, Horvath et al. 2006). Also the other proteins associated to NPHP localize at the cilium (Hurd and Hildebrandt 2011). It is interesting to note that despite the clinical differences in the onset of cysts, the portion of the nephron involved and the prognosis, all these proteins show common subcellular localizations and recently a physical interaction between Pc1 and NPHP1 has been described, suggesting a common role in the cell. These observations suggest that common mechanisms may underlie the formation and enlargement of renal cysts. As reviewed in Wilson 2004 different biological processes are involved in renal cystogenesis. A precisely controlled balance between cellular proliferation and cell death (apoptosis) is essential for normal growth and differentiation of the kidney and maintenance of normal renal structure after birth. These fundamental processes are disturbed in PKDs stimulating growth of cysts. An increase of cell proliferation is described in all forms of PKD and one possibility is that the higher amount of calcium influx activates the MAP Kinase pathway (Calvet and Grantham 2001; Zhou 2009). In addition, persistence of apoptosis, due to inactivation of apoptotic inhibitors observed in models for genetic forms of PKD, can destroy much of the normal parenchyma allowing cystic epithelia to proliferate. Another alteration commonly linked to PKD is fluid accumulation due to dysregulation or altered transcription of ion-transporters (Terryn, Ho et al. 2011), such as aquaporins. As described before, proteins involved in genetic forms of PKD localize at focal adhesions (FAK). Several experiments have shown that inactivation of different matrix adhesion receptors and FAK complexes causes formation of the cysts, probably because cells in PKDs are more adherent to matrixes causing defects in migration required for the normal morphogenesis of the kidney. Alteration in proliferation and FAKs determine also loss of

cell polarity in renal epithelial cells with consequent mislocalization of several proteins and impairment of orientation during cell divisions (Gibson, Veldhuis et al. 2011). Many signalling underline these biological processes that was deregulated by mutations in the genes involved in PKDs.

3.2. Molecular mechanisms of cystogenesis

Genes leading to PKDs were extensively studied in the last years and, even if the exact mechanisms that result in cysts development are not well clarified, these genes seem to be involved in the regulation of different intracellular signallings controlling cell proliferation, apoptosis and cell adhesion.

In a recent review by Hannah C. Chapin and Michael J. Caplan (Chapin and Caplan 2010) the more recent insights in the signalling pathways modified by Pc1 and Pc2 were reported (**Figure 4**). To summarize broadly, the evidence highlights three general themes in the relationship between the Pc1 and Pc2 proteins and cellular signalling pathways: negative growth regulation, G protein activation, and Wnt pathway modulation. Elevated cellular growth rates are a hallmark of PKDs, so it is no surprise that the polycystin proteins negatively regulate cellular growth and division through several pathways. One significant effect of PC1 involves inhibition of the mTOR (mammalian target of rapamycin) cascade. PC1 decreases mTOR activity by stabilizing the functional TSC1–TSC2 complex, a known inhibitor of the mTOR pathway. PC1 decreases ERK-dependent phosphorylation of TSC2 at S664 (Distefano, Boca et al. 2009), which allows TSC2 to remain bound to TSC1 (Ma, Chen et al. 2005). The TSC1/2 complex is also stabilized by the binding of PC1 to TSC2 at the plasma membrane, protecting TSC2 from phosphorylation by Akt at S939. Cell cycle progression is also governed by cyclin-dependent kinases (Cdks), and p21 slows or halts cell cycle progression by inhibiting Cdk2. The polycystin proteins act in concert to positively regulate p21 expression and activity. PC1 can increase p21 levels by binding and activating members of the Janus kinase (JAK) and signal transducers and activators of transcription (STAT) pathway, thus elevating p21 levels and decreasing cell growth. This activation requires a PC2-dependent interaction with JAK2 (Bhunia, Piontek et al. 2002). In addition, Pc1 has a direct role in activating G proteins. G protein α-subunits activated by PC1 go on to positively regulate the activity of the c-Jun N-terminal kinase (JNK) and the AP-1 transcription factor (Parnell, Magenheimer et al. 2002). AP-1 controls differentiation, apoptosis, and proliferation through a

complex network of signaling and binding proteins (Shaulian and Karin 2002). The interaction between PC1 and G proteins also activates the nuclear factor of activated T cells (NFAT) that is also connected to PC2 dependent calcium influx. NFAT is activated by calcineurin, which, in turn, is activated by sustained elevation of cytosolic Ca^{2+} levels. Activated calcineurin dephosphorylates NFAT, leading to its nuclear accumulation. The NFAT pathway regulates genes involved in apoptosis, growth, cellular differentiation, and cell adaptation (Horsley and Pavlath 2002). Finally, PC1 seems to have a profound influence on both the canonical (β-catenin dependent) and noncanonical (β-catenin independent) components that make up the Wnt signaling network. In the canonical pathway, the presence of the Wnt ligand induces β-catenin stabilization and nuclear translocation, leading to transcriptional activity. Cleaved PC1 inhibits this pathway by directly or indirectly binding to β-catenin, moving with it to the nucleus, and reducing its ability to promote transcription (Lal, Song et al. 2008). PC1 may also regulate noncanonical Wnt signaling, which is in turn related to the maintenance of planar cell polarity. The cells lining renal tubules generally divide parallel to the tubule's axis, lengthening the tubule rather than expanding its diameter. Tubule-lining cells in models of polycystic kidney disease, however, show a tendency to divide at an angle to the tubule's axis, which could lead to expansion of the tubule diameter. This deviation can occur before cysts appear, suggesting that a loss of this planar cell polarity may be a precursor to cyst formation (Fischer, Legue et al. 2006; Patel, Li et al. 2008). Is interesting to note that Pc1 and Pc2 such as Nephrocystin 1 and almost all proteins encoding transcripts that when mutated cause renal cystic disease localize at the primary cilium. This organelle, which is described in greater detail in the next paragraph, is like an antenna for the cells, senses the extracellular environment and transduces signals inside the cells. Interestingly, mutations in proteins involved in cilia formation and maintenance cause genetic syndromes with common phenotypes, for this reason these group of syndromes are called ciliopathies. One of the main features of ciliopathies, as further discussed in the next section, is the renal cystic disease. This observation suggests an important role for the primary cilium in the formation and/or expansion of renal cysts.

3.3. Primary cilium in physiological and pathological conditions

The primary cilium is an organelle protruding from the cell that consists of a basal body located under the cell surface and a projecting structure called the axoneme. The basal body comprises two centrioles embedded in the pericentriolar material, while the ciliary axoneme contains 9 doublets of microtubules surrounded by a membrane contiguous with the plasma membrane (Satir and Christensen 2007; Satir, Pedersen et al. 2010; Seeley and Nachury 2010). Its peculiar structure is called "9 + 0" for the absence of the central pair of microtubles normally present in motile cilia ("9 + 2" structure) (**Figure 5 A**) (Davenport and Yoder 2005). The inner microtubule pair could be required for back-and-forth movement while in its absence the cilia movement is rotational. Therefore, the primary cilium is considered to be a non-motile organelle. The unique 9 + 0 motile cilium is present on the embryonic node. The specific feature of the 9 + 0 motile cilium is its rotational movement that generates a leftward flow of extraembryonic fluid in the nodal area (Nonaka, Tanaka et al. 1998; Hirokawa, Tanaka et al. 2009). Moreover, a 9+4 structure for motile cilia was also described in the notochordal plate of rabbit embryos (Feistel and Blum 2006).

The primary cilium only assembles when cells exit the cell cycle from mitosis, and it is considered to be an organelle of cells in the quiescent or differentiated state. In fact, the cell cycle is preceded by cilium reabsorption (Quarmby and Parker 2005). The primary cilium is a highly dynamic organelle both because it is assembled only during specific phases of the cell life and because active molecular transport occurs within its axoneme. Given the dynamism of the organelle, ciliogenesis should be tightly regulated, and many modulators have been recently identified by a functional genomic screen (Kim, Lee et al. 2010). Primary cilia are present on a wide variety of cell types and tissues (**Figure 5 B-D**), such as the kidney tubule, the bile duct, neurons, the endocrine pancreas, the thyroid, smooth muscle cells, fibroblasts and others (for a complete list of cells and tissues containing cilia: http://www.bowserlab.org/primarycilia/cilialist.html).

As I stated above, alterations in the structure or function of primary cilia are responsible for a group of diseases known as ciliopathies. As cilia are a component of almost all cells, ciliary dysfunction can manifest as a wide constellation of features that include renal and hepatic cysts, malformations of the central nervous system (CNS), polydactyly and other skeletal defects, retinal degeneration, and obesity (Badano, Mitsuma et al. 2006; D'Angelo and Franco 2009; Lancaster and Gleeson 2009) (**Figure 6**). These phenotypes are quite peculiar of ciliopathies and

recent experimental evidences also suggest a tissue-specific function of primary cilia (Goetz and Anderson 2010; D'Angelo and Franco 2011). Mutations in over 40 genes to date have been associated with ciliopathic features (Waters and Beales 2011). However, with over 1,000 polypeptides currently identified within the ciliary proteome, several other disorders associated with this constellation of clinical signs will likely be ascribed to mutations in other ciliary genes. Genes that are mutated in ciliopathies can affect ciliary signalling in different ways: through changes in cilia structure or in targeting signalling molecules appropriately. As reviewed in Bettencourt-Dias et al., 2011 (Bettencourt-Dias, Hildebrandt et al. 2011), different pathways are involved in ciliopathies. Changes in the Hh pathway are associated with several developmental defects, including polydactyly, neural tube and craniofacial defects. Mouse mutants deficient in specific genes involved in intraflagellar transport (IFT), including the kinesin family member 3A (*Kif3a*), exhibit Hh mutant phenotypes with cystic kidneys. In addition, several molecules associated with cilia-related diseases, play a role in the Wnt pathway. For instance, Inversin/NPHP2 function is necessary to switch from the canonical to the non-canonical Wnt/planar cell polarity (PCP) pathway. Moreover, several BBS proteins cooperate with non-canonical Wnt signalling in PCP. There is aberrant orientation of the mitotic spindle in mouse or rat models with mutation of the cystic kidney disease genes hepatocyte nuclear factor 1 (*Hnf1*), *Pkhd1* and *Kif3a*, suggesting that defective spindle orientation could contribute to kidney cysts. The role of proliferation in the genesis of ciliopathies phenotypes is supported by the fact that the cyclin-dependent kinase inhibitor roscovitine can efficiently treat two renal cystic mouse models (*jck* and *cpk*) (Chang and Ong 2011). It is not clear whether all ciliopathies phenotypes result from dysfunctional ciliary signalling or whether, in some cases, impairment of the centrosome signalling and/or cytoskeleton disorganisation alone trigger the disease and display dysfunction of cilia as a consequence.

3.4. Primary cilium and renal cystic disease

Primary cilia are present on the epithelial cells of renal tubules, and their dysfunction is very often associated to cystic disease (Wilson 2004; Deltas and Papagregoriou 2010). Cystic kidney disease is a common feature of pleiotropic disorders such as Bardet–Biedl (BBS), Joubert (JBTS), Meckel–Gruber, Oral-facial-digital type I (OFDI), and Senior–Loken syndromes. Accordingly, all the protein products encoded by the genes responsible for

the above mentioned inherited forms of cystic kidneys disease are expressed in primary cilia, basal bodies, or the centrosome (Yoder 2007). Ciliary localization is also described for proteins involved in genetic forms of PKD, such as ADPKD, ARPKD and JNPHP, as described in the previous paragraph. Numerous mouse models have revealed kidney polycystic disease to be associated to the dysfunction of primary cilia (Wilson 2008), although the underlying molecular mechanisms are still undetermined.

In the kidney, primary cilia have a mechano-sensory role sensing flow (Praetorius and Spring 2005). Bending of the renal primary cilium initiates a calcium-signaling pathway that is dependent on the ciliary proteins Pc1 and Pc2 (Nauli, Alenghat et al. 2003). In response to fluid flow, the C-terminal tail of the plasma membrane Pc1 is proteolytically removed and the protein translocates to the nucleus where it directly initiates signaling processes linked to proliferation (Chauvet, Tian et al. 2004). In addition to their mechano-sensory role, renal primary cilia contain components of the Wnt pathway that plays an important role during kidney development (Simons, Gloy et al. 2005). Little is known about the role of renal primary cilium during postnatal life.

The main processes involved in renal cyst formation are defects in proliferation, differentiation, matrix adhesion, or polarity (Yoder 2007; Lee, Battini et al. 2011) and more and more evidence link dysfunction of primary cilia to deregulation of different pathways (Winyard and Jenkins 2011). However, ciliary disfunction is unlikely to be the only cause of cystic kidneys (Winyard and Jenkins 2011). Actually, it was reported that non-ciliary proteins give rise to renal cystic disease when mutated. In particular Bicaudal C is a conserved RNA-binding protein that is mutated in two murine models for renal cystic disease, the jcpk and bpk models (Cogswell, Price et al. 2003). Moreover, recent findings link the activity of this RNA-binding protein with the orientation of cilia via Wnt signaling (Maisonneuve, Guilleret et al. 2009). Another example is the FLCN protein, also known as folliculin. Mutations in the BHD/FLCN gene cause the Birt – Hogg – Dube syndrome characterized by renal cystic disease and increased risk for renal neoplasia. The gene product localizes to the cytoplasm and the nucleus and seems to be involved in the regulation of the mTOR pathway (Chen, Futami et al. 2008; Hasumi, Baba et al. 2008; Hasumi, Baba et al. 2009). Even if there is a clear link between ciliary alterations and renal cystic disease, further studies are necessary to address the causal link between cysts development and ciliary functions.

4.1. The mTOR pathway and the translational machinery

The mammalian target of rapamycin (mTOR) is a serine/threonine protein kinase and belongs to the phosphatidylinositol 3-kinase-related kinase protein family. mTOR regulates cell growth, cell proliferation, cell motility, cell survival, protein synthesis and transcription (Beevers, Li et al. 2006; Sonenberg and Pause 2006). It integrates the input from upstream pathways, including insulin, growth factors and amino acids (Sonenberg and Pause 2006). mTOR also senses cellular nutrient and energy levels and redox status (Tokunaga, Yoshino et al. 2004). The mTOR protein can exists in two different complexes: mTOR Complex 1 (mTORC1) and mTOR Complex 2 (mTORC2). The mTORC1 complex includes mTOR, the regulatory-associated protein of mTOR (Raptor), the mammalian LST8/G-protein β-subunit like protein (mLST8/GβL) and other partners (Kim, Sarbassov et al. 2002; Kim, Sarbassov et al. 2003). This complex works as a nutrient/energy/redox sensor and controls protein synthesis. Among the targets of mTORC1, p70-S6 Kinase 1 (S6K1) and the eukaryotic initiation factor 4E binding protein 1 (4E-BP1) have been extensively studied (Sonenberg and Pause 2006) (**Figure 7 A**). The mTORC2 complex, instead, is composed by mTOR, the rapamycin-insensitive companion of mTOR (Rictor), GβL, and the mammalian stress-activated protein kinase interacting protein 1 (mSIN1) (Sarbassov, Ali et al. 2004; Frias, Thoreen et al. 2006). mTORC2 is an important regulator of the cytoskeleton through its stimulation of F-actin stress fibers, paxillin, RhoA, Rac1, Cdc42, and protein kinase C α (PKCα)(Sarbassov, Ali et al. 2004). In order to execute its function, mTORC2 phosphorylates the serine/threonine protein kinase Akt/PKB and appears to be regulated by insulin, growth factors, serum, and nutrient levels (Frias, Thoreen et al. 2006). Originally, mTORC2 was identified as a rapamycin-insensitive entity, as acute exposure to rapamycin did not affect mTORC2 activity or Akt phosphorylation (Sarbassov, Guertin et al. 2005) (**Figure 7 B**).

Translation of an mRNA into its protein is accomplished in three successive steps (initiation of translation, elongation of the native peptide and termination) controlled by a wide range of regulatory factors. During initiation of translation, the tRNA for the Methionine (Met-tRNA) together with the small ribosomal subunit (40S) and eukaryotic initiation factors (eIFs), form a complex onto the mRNA. By doing so, the reading frame for the

protein is determined and the assembled ribosome can start elongation, which is regulated by elongation factors (EFs), by adding amino acids to the growing peptide chain in accordance with the mRNA sequence (Browne and Proud 2002; Frank 2003; Thornton, Anand et al. 2003). The termination phase begins after recognition of a stop codon. Subsequently, the 80S ribosome is released from the protein and dissociates into its subunits to be recycled in another round of peptide synthesis (Van Der Kelen, Beyaert et al. 2009).

The mTOR pathway plays a role in the phosphorylation of a number of components of the translation machinery. mTOR signaling appears to be important for both short-term (minutes) and long-term (hours) induction of translation by increasing the levels and activation of ribosomes and translational factors (Dennis, Jaeschke et al. 2001). Upon activation, S6K1 can in turn stimulate the initiation of protein synthesis through phosphorylation and thus activation of S6 Ribosomal protein (a component of the ribosome) and other components of the translational machinery (Raught, Peiretti et al. 2004; Holz, Ballif et al. 2005; Shahbazian, Roux et al. 2006) and recent reviews on this topic (Ma and Blenis 2009; Van Der Kelen, Beyaert et al. 2009). Moreover, non-phosphorylated 4E-BP1 binds tightly to the translation initiation factor 4E (eIF4E), preventing it from recruiting to the ribosomal initiation complex. Upon phosphorylation by mTORC1, 4E-BP1 releases eIF4E, allowing it to perform its function (Schalm, Fingar et al. 2003). **Figure 8** shows in details the events leading to initiation of translation. mTOR binds the eukaryotic initiation factor 3 (eIF3) after aminoacids stimuli and exposure to nutrients and their binding is prevented by rapamycin. After this binding, mTOR is able to phosphorylate both S6K and 4E-BPs. Phosphorylated S6K dissociates from eIF3 and activates S6 ribosomal protein. After this phosphorylation event, the 40S ribosomal subunit is recruited by eIF3 (Holz, Ballif et al. 2005). In addition, phosphorylated 4E-BP1 dissociates from eIF4E, allowing the recruitment of eIF4G, eIF4B and eIF4A to the 5′ end of an mRNA. Finally, eIF3, the small ribosomal subunit (40S) and the ternary complex (comprising eIF2, Met-tRNA and GTP) are recruited to the cap, resulting in the assembly of the 48S translation pre-initiation complex, ribosome scanning and translation initiation (Ma and Blenis 2009). More than one ribosome can translate an mRNA at one time, making it possible to produce many polypeptides simultaneously from a single mRNA. The mRNA molecule bound by a cluster of ribosomes are called polyribosomes (or polysomes) and were first discovered and characterized by Jonathan Warner, Paul Knopf, and Alex Rich in 1963. The mTOR pathway was associated with an increase of polysomes due to its role in translation. Deregulation of the mTOR pathway has been demonstrated in

pathological conditions including cancer (Beevers, Li et al. 2006) and, more recently, in polycystic kidney disease (Lieberthal and Levine 2009).

4.2. The mTOR pathway and cell cycle in renal cystic disease

The mammalian target of rapamycin (mTOR) is a key regulator of cell growth and proliferation. The mTOR pathway integrates signals from nutrients, energy status and extracellular growth factors to regulate translation of many proteins involved in cell cycle progression, angiogenesis, ribosome biogenesis, and metabolism. Growth factors such as insulin-like growth factor, epidermal growth factor and vascular endothelial growth factor bind to and activate their corresponding tyrosine kinase receptors (TKR) located on the cell surface, to induce signal transduction to the nucleus. TKR induces intracellular signalling cascades via the phosphorylation of the phosphatidylinositol 3-kinase, which in turn phosphorylates Akt and then the Akt target, mTOR (Azim, Azim et al. 2010). Because of the involvement of the mTOR pathway in cell progression, mTOR deregulation is associated with many types of human cancer (Beevers, Li et al. 2006). Mutations in the PTEN gene affect mTOR signaling and are commonly found in a spectrum of cancers including prostate, breast, lung, bladder, melanoma, endometrial, thyroid, brain, renal carcinomas and others, making it one of the most frequently mutated tumor-suppressor genes (Beevers, Li et al. 2006). In addition, mutations in PTEN lead to Akt activation. It is known that active Akt regulates cell survival, cell proliferation and metabolism by controlling positively the mTOR signaling and negatively cell cycle inhibitors like p21 and apoptosis activators (Guertin and Sabatini 2005). However, cell cycle alteration is also described in different models of renal cystic disease (Lee, Battini et al. 2011). This is not surprising since many proteins involved in renal cystic disease show a centrosomal localization (Yoder 2007) and centrosome is the main coordinator of cell division (Nigg and Stearns 2011). In addition treatment with different drugs that inhibit cell proliferation leads to an improvement of renal function and to a slowing down of cyst development (Ibraghimov-Beskrovnaya 2007; Okumura, Sugiyama et al. 2009; Masyuk, Radtke et al. 2011). However, it is not still clear if the deregulation of the cell cycle is a consequence rather than the cause of the molecular mechanisms linked to cysts progression, such as the mTOR pathway activation. Further analysis will be necessary to elucidate this point.

4.3. The mTOR pathway, cilia and renal cystic disease

The link between mTOR signaling, PKD and ciliary biology is more and more evident. Among the available experimental evidences the mTOR pathway has been implicated in tuberous sclerosis (TSC), a tumor suppressor gene syndrome associated with renal cystic disease. TSC is an autosomal dominant condition characterized by the formation of hamartomas in multiple tissues and organs. Renal cysts are observed in ~ 30% of patients with TSC, while a minority of these patients develop severe PKD. This condition is caused by mutations in the TSC1 and the TSC2 transcripts. The proteins encoded by the TSC1 and TSC2 genes, hamartin and tuberin, respectively, physically interact with each other inhibiting the mTOR pathway (Potter, Huang et al. 2001; Inoki, Li et al. 2002; Potter, Pedraza et al. 2003).

Interestingly, TSC1 was shown to localize to the cilium and basal body (Yoder, Tousson et al. 2002; Nauli, Alenghat et al. 2003; Bonnet, Aldred et al. 2009; Hartman, Liu et al. 2009). Interestingly, the *TSC2* and *PKD1* genes lie adjacent to one another on human chromosome 16p13.3, and contiguous deletions of both genes have been identified in patients with this early onset ADPKD (Brook-Carter, Peral et al. 1994). This observation suggests that TSC and PKD genes interact functionally in the pathogenesis of PKD. This is also supported by the observation that loss of one allele of *Pkd1* worsens the renal cystic phenotype of $Tsc1^{+/-}$ and $Tsc2^{+/-}$ mice (Bonnet, Aldred et al. 2009; Winyard and Jenkins 2011).

It was also described that, in different animal models, silencing of *Tsc1* leads to renal cystic disease with upregulation of the mTOR pathway (DiBella, Park et al. 2009; Zhou, Brugarolas et al. 2009) and presence of longer cilia in the cells that line renal cysts (DiBella, Park et al. 2009). Moreover, mouse embryonic fibroblasts from $Tsc1^{-/-}$ and $Tsc2^{-/-}$ mutants show an increased number of cilia, which is not rescued by treatment with rapamycin, suggesting that the enhanced cilia formation is mTOR-independent (Hartman, Liu et al. 2009).

The upregulation of the mTOR pathway was also described in different inherited forms of renal cystic disease (Shillingford, Murcia et al. 2006; Fischer, Jacoby et al. 2009; Becker, Opazo Saez et al. 2010; Dere, Wilson et al. 2010). Furthermore, rapamycin, a specific inhibitor of the mTORC1 complex, causes regression of renal cysts in several rodent models, suggesting a role for mTOR signaling in the pathogenesis of renal cystic disease

(Shillingford, Murcia et al. 2006; Wu, Arcaro et al. 2009; Shillingford, Piontek et al. 2010; Zafar, Ravichandran et al. 2010).

Finally recent data seem to mechanically link cilia with mTOR signaling. Indeed, in renal tubules bending of cilia due to fluid flow has been shown to down-regulate mTOR signaling (Boehlke, Kotsis et al. 2010). These data suggest that the absence of cilia observed in a number of renal cystic diseases determines failure to sense urine flow and the upregulation of the mTOR pathway as a consequence.

A number of studies indicate different possible links between mTOR, cilia and cysts and further analysis will be necessary to clarify and understand the connections.

4.4. The mTOR pathway and autophagy

Autophagy is a cellular degradation system in which cytoplasmic components and organelles are sequestered by double membrane structures called autophagosomes and then degraded by lysosomal hydrolases to supply amino acids and to regulate cellular homeostasis. Efficient sequestration and clearance of unneeded damaged or nonself components is crucial for cell survival and function and thus malfunction of autophagy contributes to a variety of diseases, including cancer, neurodegeneration, cardiovascular disorders and microbe infection (He and Klionsky 2009). Autophagy is accurately regulated and the mTOR pathway is one of the main actors. This complex biological process is induced in response to nutrient deprivation and mTORC1, which is a downstream factor in insulin and/or amino acid signals, controls autophagy. Under nutrient-rich conditions, mTORC1 is incorporated into the ULK1 complex and subsequently phosphorylates ULK1 and Atg13, which suppress autophagic activity. In response to starvation, mTORC1 dissociates from the ULK1 complex, resulting in dephosphorylated ULK1 and Atg13 thus allowing the formation of autophagosomes (Ichimura and Komatsu 2011). In **Figure 9** (modified from (Maiuri, Zalckvar et al. 2007)) (Rajawat and Bossis 2008), a schematic explanation for autophagy progression is shown, even if the molecular events are not well clarified. The mTOR pathway controls the first steps of autophagy induction and membrane recruitment (steps 1 and 2). Vesicles will elongate and extremities will fuse to complete the double-membrane structure (step 3 and 4). Most of the proteins involved in vesicle expansion and maturation steps are retrieved to the original pool because they do not associate with the complete and mature

autophagosome. Therefore, it has been suggested that the proteins involved in autophagosome formation are retrieved for future use. Atg8 (LC3) is the exception; it is found on the mature autophagosome and can be used as a valuable marker to track these structures. The next critical step is transport and fusion of the autophagosome with the lysosomes (step 5). The machinery required for the process of vesicle fusion includes SNARE proteins and the class C Vps/HOPS complex. The last step (step 6) in the autophagic process is degradation of the autophagic body content by lysosomal enzymes, which ensures recycling of essential cytoplasmic contents. Another important actor in autophagy is the p62 protein. This protein interacts with ubiquitinated proteins and LC3 and seems to drive autophagic substrate selection (Riley, Kaiser et al. 2010).

Until now, there are no evidences of the involvement of autophagy in renal cystic disease. However, several laboratories are looking for autophagy impairment in animal models of renal cystic diseases due to the experimental observation described above (paragraph 4.2. and 4.3.).

MATERIALS AND METHODS

Generation of Ofd1^{fl};cre^{Ksp} mice and PCR genotyping

Ofd1$^{fl/+}$ females (Ferrante, Zullo et al. 2006) were crossed with creKsp male mice containing 1.3 kb of the Ksp-cadherin promoter linked to the coding region of cre recombinase (Shao, Somlo et al. 2002). Animals were genotyped for the presence of the cre gene using the primers cre1 (GGACATGTTCAGGGATCGCCAGGCG) and cre2 (GCATAACCAGTGAAACAGCATTGCTG) as described in Lakso et al., PNAS, 89:6232-6 (Lakso, Sauer et al. 1992).

All animal experimentation was performed under regulation of the Internal Ethical Committee and authorized by the Italian Ministry of Health.

Generation of Ofd1$^{fl/y}$;CAGGcre$^{ER\text{-}TM}$ mice, tamoxifen injections and PCR genotyping

Ofd1$^{fl/+}$ females (Ferrante, Zullo et al. 2006) were crossed with pCAGGCre-ERTM mice, a generale deletor cre line that expresses Cre recombinase ubiquitously due to the presence of the β-actin promoter/enhancer CAGG

(Hayashi and McMahon 2002). In addition, the protein is fused with the mutant form of the ligand-binding domain of the estrogen receptor (ER^{TM}). This domain sequesters the Cre in the cytoplasm. Its translocation to the nucleus and its activity are induced after tamoxifen administration. We treated pregnant mothers with a single intraperitoneal injection of 100ug tamoxifen / g of weight at Embrionic stage 18.5 (E 18.5). Injections in adult mice were performed at P60 with a single intraperitonel injection at the dose described before. Tamoxifen was diluted in 10% ethanol and 90% sesam oil (SIGMA) at a final concentration of 10 mg/ml.

Animals were genotyped using two couple of primers: cre1 (GGACATGTTCAGGGATCGCCAGGCG) and cre2 (GCATAACCAGTGAAACAGCATTGCTG) to detect the cre gene as described in Lakso et al., PNAS, 89:6232-6 and Fsui3 (CATTCCTGTTAGTATTTGGAGG) and RperFRT (CGACACTGCAGAGACCTACTTC) to detect the floxed allele.

RT-PCR and real-time PCR

For the *Ksp* model, effective production of a deleted allele in the kidney was confirmed by RT–PCR (One-step system, Invitrogen) on kidney RNA or lung RNA, from WT and conditional mutants at P21, extracted with Trizol (Invitrogen), using primers Fsu1mcx and To-14020 (Ferrante, Zullo et al. 2006). Quantification of *Ofd1* inactivation was assessed by real-time PCR on cDNA (SuperScript First-Strand, Invitrogen) synthesized from RNA from the kidney of P20 of both *Ksp* and IND conditional mutants and controls. Primers used to amplify specifically the *Ofd1* WT allele were A (TGGCAGACCACTTACAAAGATG), A′(AGACTGGATGAGGGGTTAATC), B (CATTCCTGTTAGTATTTGGAGG) and B′ (GTGTTAGGAGGGTATGAACATG). A set of primers, GapdhF (TCTTCTGGGTGGCAGTGAT) and GapdhR (TGCACCACCAACTGCTTAGC), that amplify the Gapdh gene were used as internal reference.

Glomerular filtration rate assay

Glomerular filtration rate (GFR) measurements were performed on adult mice at P28, P35 and P45. A thiobutabarbital sodium (Inactin, Sigma-Aldrich) intraperitoneal injection (120 mg/kg body weight) was given as

anethesthetic. The animals were surgically prepared as follows: after tracheotomy, the left carotid artery and left jugular vein were cannulated with polyethylene tubing. The arterial catheter was then connected to a pressure transducer to monitor blood pressure and to take blood samples, while the venous catheter was connected to a syringe pump for saline infusion. After replacing surgical fluid loss with isotonic saline, the mice were given a priming dose of 10μCi of [methoxy-3H] inulin, followed by a maintenance infusion in isotonic saline containing 10μCi/h at a rate of 0.4 ml/h. The bladder was cannulated with a PE 50 tube for urine collection. After a 60 minutes balance period, 30-minute urine samples were collected. Blood samples were taken after each clearance period. A total of 4 urine and blood collections were made. GFR was calculated by standard methods.

Scanning electron microscopic analysis

For SEM analysis kidneys from P7 and P14 *Ksp* and WT animals were fixed in Karnovsky fixative, postfixed with 1% osmium tetroxide in 0.1 M cacodylate buffer for 1 hour at 4°C. Kidneys were sliced with a razor blade, dehydrated, dried with critical point-drying apparatus, and mounted on aluminium stubs coated with palladium-gold using a cold sputter-coater. Analysis was performed with a Philips XL-20 microscope. SEM analysis on *Ksp* mutants was performed in close collaboration with Pascal Dollé (Institut de Génétique et de Biologie Moléculaire et Cellulaire, BP 10142, 67404 Illkirch Cedex, France).

For SEM analysis on IND mice kidneys were fixed with 2%Glutaraldhehyde/2%Paraformaldehyde in 0.1M phosphate buffer. This analysis was performed in collaboration with Dr. Caroline Miller and Dr. Vincent Gattone (Electron Microscopy Center; Indiana University School of Medicine) following the Electron Microscopy Center procedures (http://anatomy.iupui.edu/core-facilities/electron-microscopy-center/emc-affiliations/emo-pkd/).

Histological and Immunofluorescence assays on kidney sections

Isolated kidneys were fixed in paraformaldeyde 4% in PBS buffer at 4°C overnight. Haematoxylin-eosin stainings were performed on OCT (Kaltek) sections. For immunofluorescence experiments the OCT sections were incubated for 30 min with 0.1% BSA, 10% goat serum in TBS before incubation with the primary antibody at 4° over night. Sections were then washed with TBS and incubated with secondary Abs goat anti-mouse IgG

conjugated to Cy3 and anti-rabbit IgG conjugated to FITC (Jackson ImmunoResearch). Stained sections were mounted with Vectashield (Vector Laboratories). The primary antibodies used were: anti-acetylated tubulin antibody (T6793, Sigma-Aldrich), anti-NaPiII cotrasporter {Custer, 1994 #8151}, anti-PCNA (sc-56, Santa Cruz Biotechnology), anti-Cleaved Caspase-3 (9661) and anti-phosphoS6 (Ser235/236) (2211) from Cell Signaling Technology (US).

Staining for collecting ducts and distal tubules was performed with lectin from Arachis hypogaea (L7759, Sigma-Aldrich), and with anti-Tamm-Horsfall Glycoprotein (CR2027SP, Europa Bioproducts) for detection of the thick ascending limb of Henle, according to manufacturer's instructions. PAS staining (395, Sigma-Aldrich) was performed on kidneys from *Ofd1*^{fl}*;cre*^{Ksp} mice at stage P23.

Microscopy was performed with a Zeiss Axioplan 2 microscope and a Leica TCS SP2 AOBS confocal microscope with a 63x Neofluor Pan-Apo 1.3 nm oil objective.

Rapamycin treatment and cystic index caculations

To evaluate the response to rapamycin treatment, mice received daily intraperitoneal injections of 2.5 mg/kg rapamycin dissolved in vehicle (10% DMSO, 10% ethanol, and 80% saline) or vehicle alone. Rapamycin was administered starting at postnatal day 14 for a period of 10 days. For these experiments three sets of animals (mutants and controls) from three different littermates were analysed.

Representative images of Haematoxylin-eosin -stained kidneys were acquired. A grid was placed over the images, and the cystic index was calculated as the percentage of grid intersection points that bisected cystic or noncystic areas, as previously described (Shillingford, Murcia et al. 2006).

Cell lines

Two different cell lines were used to obtain the results described in this thesis, namely HEK293 (Human Embryonic Kidney 293) and MDCK (Madin Darby Canine Kidney). In particular HEK293 and MDCK. HEK293 and MDCK cells were both cultured in high glucose Dulbecco's modified Eagle's Medium (DMEM) medium with 10% Fetal Bovine Serum (FBS).

All the transfections performed for HEK293 cells were made using TransIT®-LT1 Transfection Reagent from Mirus. MDCK cells were transfected with the Amaxa Nucleofactor system according to manufaturer's instructions (Cell Line Nucleofector®Kit L).

For immunofluorescence assay a HEK293 clone stably expressing mycGFP-OFD1 was used. To obtain a stable clone, HEK293 cells were transfected with an empty pCDNA vector and a pCDNA vector carrying the mycGFP-OFD1 gene, both vectors carry the resistence for the G418 antibiotic. After 48h from the transfection, the cells were incubated for 15 days in DMEM medium with 10% FBS and 0.5 mg/ml of G418 for selection of non-transfected cells and few clones were picked. Clones were expanded and then analyzed by immunofluorescence for the expession of the GFP-OFD1 fusion protein. Western blot analysis was performed to check the levels of expression of the mycGFP-tagged fusion protein. Two clones were isolated that showed a convenient OFD1 overexpression.

Immunofluorecence assyas on HEK293 cells

Cells were fixed in methanol for 6 minutes at -20^0 C, then washed with PBS saline solution and incubated for 1 hour with a blocking solution (0,2% Triton X-100, 10% goat serum in PBS). The primary antibodies were diluted in blocking solution and cells were incubated for 2 hours at RT. Cells were then washed with PBS and incubated with Alexa Fluor® Dyes from Invitrogen. Before mounting with 50% glycerol in PBS nuclei were stained with Hoecst for 10 minutes at RT. We used the following antibodies: eIF4E (9742 Cell Signaling Technology) γ-tubulin (clone GTU-88 T6557 SIGMA), centrin (S-19 sc-27794 Santa Cruz), eIF3δ (R-20 sc-16362 Santa Cruz).

Immunoblot analysis

Western blot studies were performed in duplicate and at least two different animals were analyzed for each group. Kidneys were isolated and homogenized in lysis buffer (Tris 50mM pH 7.9, 1% triton X-100, 0.1% Tween20, 150mM NaCl, 10% glycerol, 5mM $MgCl_2$) with protease inhibitors from SIGMA (P8340) and phosphatase PhosSTOP inhibitors from Roche. Western blot analysis of total proteins extracts was performed with antibodies for S6 (2317), P-S6 (2211), Akt (9272), P-Akt (Ser473 9271 and Thr308 9275), mTOR (2983), P-mTOR (2971),

p70S6Kinase (9202), P-p70S6Kinase (Thr421/Ser424 9204 and Thr389 9205) from Cell Signaling Technology (US), GH (sc-10364), eIF3δ (sc-16362) and eIF3η (sc-28857) from Santa Cruz Biotechnology, INC. Polyvinylidene difluoride (PVDF) membranes were used for Immunoblot (Millipore, US) and ECL western blotting reagent (Amersham, UK) or Femto (Pierce, US) for detection.

RNAi in MDCK cells

We designed two different pairs of DNA oligonucleotides (si254 and si1257) containing siRNA-expressing sequence targeting two regions of the canine *OFD1* mRNA (XM_537958) using the software available at www.qiagen.com/GeneGlobe. We then cloned the annealed oligos into the expression vector pSuper (oligoengine). The cells were transfected with the Amaxa Nucleofactor system according to manufaturer's instructions (Cell Line Nucleofector®Kit L). RNA sequences were GATCCCCGTGGTTTGGCCAAAGAAAATTCAAGAGATTTTCTTTGGCCAAACCAC and GATCCCCGGCCCAGATACGTGATTATTTCAAGAGAATAATCACGTATCTGGGCC for si254 and si1257, respectively. The sequence for the scrambled oligo is GATCCCCACTACCGTTGTTATAGGTGTTCAAGAGACACCTATAACAACGGTGTTTTTT. Cells were collected after 48 hours after transfection.

RNAi in HEK293 cells

HEK 293 cells were plated to a confluence of 30% the day before transfection. To silence *OFD1* transcript we used the ON-TARGET plus smart pool against human *OFD1* transcript and controls from *Darmachon RNAi technology* to a final concentration of 100uM. The transfection reagent was INTERFERIN from Polyplus. Cells were used for both WB analysis and immunofluorescence analysis after 72 hours from transfections.

Co-immunoprecipitation experiments

Co-IP experiments were performed to demonstrate the interaction between eIF3 subunits and OFD1. We used HEK293 cells both non transfected or transiently transfected with a construct expressing 3XFlagOFD1, however all the cells were transfected with a vector overexpressing p70S6 kinase1. In addition, quantitative Co-IPs were performed to check the amount of endogenous P-S6 bound to endogenous eIF3η to study the formation of the PIC in WT HEK293 cells. Both sets of Co-IP experiments were performed with the following protocol. After 48 hours from plating, the cells were lysed in Buffer A (50mM Tris-HCl/1mM EDTA, 10mM $MgCl_2$, 5mM EGTA, 0.5% Triton X-100 [pH 7.28]) and 250ug of total lysates were incubated for 1 hour with 5ug of specific antibodies or rabbit IgG as control, followed by for 1 hour of incubation with protein A-Sepharose beads. The unbound proteins were washed out twice with the Buffer A and once with the Buffer ST (50mM Tris-HCl, 150mM NaCl [pH 7.28]), while the bound fraction was analyzed by Western Blot with an antibody against the putative interactor. Buffer A and Buffer ST used were: Buffer A; Buffer ST The protocol used, the lysis buffer and the washing buffer are modified from what previous described in (Holz, Ballif et al. 2005). Proteases Inhibitors from SIGMA (P8340) and phosphotase inhibitors (PhosSTOP) from Roches were freshly added.

Bicistronic Luciferase assay

For luciferase reporter experiments, HEK293 cells were transfected with pRL-HCV-FL reporter plasmid (provided by John Blenis - Professor of Cell Biology. Department of Cell Biology Harvard Medical School 240 Longwood Avenue Boston and previously described in Kruger et al., 2001 (Kruger, Beger et al. 2001)). Forty-eight hours post-transfection, cells were harvested, and the luciferase activity was measured using Dual-Luciferase Reporter Assay System (Promega) and Glomax 96 microplate luminometer from Promega according to the manufacturers' instructions.

Polisome fractionation

HEK293 CELLS: Cells were transfected with siRNA against *OFD1* and with control oligos. After 48 hours cells were treated for 10 minutes with 100ug/ml cycloheximide (C-7698 from SIGMA) and then washed twice with

Hypotonic buffer (5mM Tris-HCl pH 7.5, 1.5mM KCl, 2.5mM $MgCl_2$). Cells were lysed in 400ul of extraction buffer (hypotonic buffer, 0.5% triton X-100, 0.5% Na-deoxycholate, 120 U/ml RNAse inhibitors [AM2692 from Ambion], 3mM DTT, 100ug/ml cycloheximide) and after quantification 1mg/ml of heparin was added.

KIDNEYS: Tissues were lysed in 1 ml of buffer 3 (50mM Tris-HCl pH 7.8, 240mM KCl, 10mM $MgCl_2$, 250mM sucrose) with 5mM DTT, 100ug/ml cycloheximide, 2% triton X-100, 100 U/ml RNAse inhibitors and after quantification 1mg/ml of heparin was added.

The extracts were rapidly frozen into liquid nitrogen and stored at –80°C.

After sample preparation (which is specific for tissues or cells, see above) 1.2 mg of total lysates were layered on a 0.5–1.5 M linear sucrose gradient (20mM Tris-HCl, pH 7.5, 80mM NaCl, 5mM MgCl2, 1mM dithiothreitol) and centrifuged in a SW41 rotor at 160,000 g for 2 hours at 4°C. After centrifugation, the gradient was displaced upward through a flow cell recording absorbance at 260 nm with the use of the density gradient fractionation system (Isco) and fractionated in 12 fractions as described in (Espeillac, Mitchell et al. 2011). Fractions were rapidly stored at –80°C. Absorbance at 260 nm was registered in a curve. The area below the curve was calculated using Adobe Photoshop program and the output is a read-out of general translation.

RNA extraction from polysomes

We added 1ml of isopropanol to each fraction and put the mixed fractions at –20°C over night. After 16 hours, the fractions were centrifuged for 30 minutes at 15000 rpm at 4°C. The pellets were resuspended in solution D (4M Guanidinium thiocyanate, 25mM Sodium Citrate pH 7, 0.5% Sarcosyl, 100mM 2-MeSH Mercaptoethanol) and 180mM NaAc pH4. The RNA was extracted by phenol/chloroform protocol. After centrifugation the supernatants were collected and mixed. The same volume of isopropanol was added and the samples were put at –20°C over night. After 16 hours, the fractions were centrifuged for 30 minutes at 15000 rpm at 4°C. The pellets were washed with 80% of ethanol, then dryed and resuspended in water.

Microarray experiments

For microarray analysis we collected polysomal and total RNA from kidneys of both IND and WT mice at P8. We used the Affymetrix Mouse 430A 2.0 array, 3'-IVT array, ~ 23,000 transcripts platform. The experiments were performed by Prof. Norman P. Gerry at the Genotyping and Microarray Center Coriell Institute for Medical Research (403 Haddon Ave Camden, NJ 08103).

Bioinfomatic analysies

Bioinformatic analysis was performed on the mouse Ofd1 protein sequence obtained from UCSC genome browser (http://genome.ucsc.edu/), we looked for known RNA binding region in the Ofd1 protein using two different bioinformatic tools: BindN (http://bioinfo.ggc.org/bindn/) and RNABindR (http://bindr.gdcb.iastate.edu/RNABindR/). For the analysis of microarray results we used the PUMA methods (Propagating Uncertainty in Microarray Analysis) (Rattray, Liu et al. 2006; Pearson, Liu et al. 2009).

All the analysis were performed in collaboration with the Bioinformatic core at TIGEM.

RESULTS

1· Conditional models for Ofd1

1.1. Generation and characterization of a conditional model with Ofd1 kidney-specific inactivation

To study the role of Ofd1 protein in cysts development and to overcome the problem of embryonic male and perinatal female lethality observed in *Ofd1* knockout ($Ofd1^{\Delta 4\text{-}5}$ and $Ofd1^{\Delta 4\text{-}5/+}$) mutant animals (Ferrante, Zullo et al. 2006), a mouse line with kidney-specific inactivation of *Ofd1* was generated in professor Franco's laboratory where I performed my PhD training. Females from the *Ofd1*-floxed line ($Ofd1^{fl}$) were crossed with the *Ksp-Cre* transgenic line in which cre recombinase is under the control of the Ksp-cadherin (Cdh16) gene promoter, that is specifically expressed in renal tubular epithelial cells and developing genitourinary tract from E15.5 (Shao, Somlo et al. 2002). The resulting mice, both females ($Ofd1^{fl/+}$;cre^{Ksp}) and males ($Ofd1^{fl/y}$;cre^{Ksp}), were viable and indistinguishable from wild type (WT) animals at birth. RT–PCR analysis of these genotypes confirmed the kidney specific inactivation of *Ofd1*. This analysis revealed that the mutated allele is present only in the kidney of

mutant animals, whereas it is absent in other organs, such as the lung, where only the WT allele could be detected (**Figure 10 A**). To determine more accurately the extent of *Ofd1* inactivation, we performed quantitative RT–PCR with primers that specifically amplify the WT Ofd1 allele on genomic DNA (primers B and B′ in **Figure 10 B**) and on RNA (primers A and A′ in **Figure 10 B**) obtained from kidneys of *Ofd1*^{fl};*cre*^{Ksp}-conditional mutants (*Ksp* mutants) and controls. Primers A′ and B′ do not anneal on the deleted allele, thus allowing to specifically amplify the WT allele. Our analysis revealed the presence of 40 and 30% of the mutated allele on genomic DNA of whole kidneys from *Ofd1*$^{fl/y}$;*cre*^{Ksp} and *Ofd1*$^{fl/+;}$*cre*^{Ksp} mutants, respectively, when compared with controls. Similar results were obtained after analysis of the RNA (**Figure 10 B**). The incomplete inactivation of Ofd1 in the kidneys of *Ofd1*^{fl};*cre*^{Ksp} animals was expected since cre recombinase is not expressed in all renal cells; however, one cannot exclude an incomplete efficiency of cre/loxP recombination. In *Ofd1*$^{fl/y}$;*cre*^{Ksp} males, renal cysts were not observed at P7, whereas dilated tubules were visible starting from P14, after this stage, cysts became larger and more numerous (**Figure 11 B**). By P35, we observed a massive replacement of the renal parenchyma by cysts. Histological examination revealed that cysts progression in *Ofd1*$^{fl/+}$;*cre*^{Ksp} female mutants was similar, although the number of cysts observed was reduced compared to the male mutants, probably due to the X- inactivation phenomenon. Cysts were confined to the medullary portion of the kidney up to P28 in *Ofd1*$^{fl/y}$;*cre*^{Ksp} (**Figure 12 A**). Starting from P35, cysts appear in the kidney cortex (**Figure 12 B**), where expression of Ksp-cadherin has been detected at adult stages (Shao, Somlo et al. 2002). At P70, glomerular cysts were also observed, as reported in other conditional models obtained using the Ksp-Cre line (Gresh, Fischer et al. 2004; Hiesberger, Bai et al. 2004) (**Figure 12 C**). To establish the cellular origin of cysts, we performed staining with antibodies or lectins that specifically label different segments of the nephron. The cysts were preferentially labelled with the antibody against the Tamm–Horsfall protein (THP), which labels the thick ascending limb of Henle's loop, although some cysts were positive for lectin *Arachis hypogaea* (LAH), which labels distal tubules and collecting ducts. Staining with an antibody to the Na-PiII (NaPiII) transporter, which marks the proximal tubules, did not label any cysts until P28. Taken together, these results indicated a primarily distal tubular origin of the cysts. Staining with Na-PiII confirmed the presence of proximal cysts at P35. Staining with periodic acid-Schiff (PAS) allowed us to exclude the presence of fibrosis in mutant kidneys (**Figure 13**). The renal function of *Ofd1*^{fl};*cre*^{Ksp} mutants was assessed by analysis of the glomerular filtration rate (GFR) starting from P28. At this stage, a marked reduction of

the GFR was observed in both male and female mutants, indicating a severe impairment of the renal function. GFR analysis at later stages indicated a progressive deterioration of the renal function (**Figure 14**) (Zullo, Iaconis et al. 2010). The GFR study was performed in close collaboration with Prof. Giovambattista Capasso (Division of Nephrology, Second University of Naples).

1.2. Generation and characterization of an inducible model with Ofd1 time – specific inactivation

In order to obtain a model in which most of the renal cells will be depleted of the *Ofd1* transcript we crossed the *Ofd1*^{fl} line with a transgenic line ubiquitously expressing a tamoxifen-inducible Cre^{ERTM} protein. The *Cre* expression is regulated by the ß-actin promoter/enhancer (CAGG promoter/enhancer) that allows the ubiquitous expression of the gene. In addition, the protein is fused with the mutant form of the ligand-binding domain of the estrogen receptor (ER^{TM}). This domain sequesters the Cre in the cytoplasm. When tamoxifen binds the ER^{TM} domain the entire complex translocate to the nucleus and the Cre-mediated recombination of the DNA is allowed. In this system inactivation of the transcript of interest occurs more or less 24h after injection (Hayashi and McMahon 2002). We decided to start analyzing mice in which *Ofd1* inactivation is induced at E18.5 by intraperitoneal injections of pregnant mothers thus resulting in inactivation of the transcript at birth in newborn mice. The resulting mice, both females (*Ofd1*$^{fl/+}$;*cre*$^{ER\text{-}TM}$) and males (*Ofd1*$^{fl/y}$;*cre*$^{ER\text{-}TM}$), were viable and indistinguishable from wild type (WT) animals at birth. All subsequent experiments on this model were performed in *Ofd1*$^{fl/y}$;*cre*$^{ER\text{-}TM}$ male mutants which will be indicated as IND. The level of inactivation in the kidney was evaluated by quantitative RT-PCR and by Western Blot at different postnatal stage and is on average around 80% (**Figure 15 A**). Haematoxylin-eosin staining of kidney sections from IND mutants at different stages showed that tubules dilatation starts at P10 and by P18 the majority of the parenchyma was replaced by cysts (**Figure 15 B** and **C**). IND mutant mice die around P30. As in the *Ksp* mutants, the cysts were preferentially labelled with the THP antibody although some cysts were positive for LAH while no cysts are positive for the NapiII staining until postnatal stage P25 (**Figure 15 D-F**). The tubular origin of the cysts could not be explained by expression of the Cre recombinase that occurs ubiquitously. However, at P0 glomeruli are already formed while tubules are still growing. One possibility is that after birth tubules are more sensitive to molecular signals compared to glomeruli.

Moreover, glomerular cysts were visible already at P25. Overall this data indicate that the phenotype observed in the inducible model is more severe than that observed in the *Ksp* mutants. This was expected as in this model we obtained inactivation of the *Ofd1* transcript in all renal cells thus obtaining a higher level of gene inactivation.

Moreover, this model also allowed us to obtain a time specific inactivation of *Ofd1*. We wanted to evaluate whether Ofd1 inactivation in adult tissues could also result in the generation of renal cysts. We thus injected intraperitoneally tamoxifen in adult (P60) *Ofd1*$^{fl/y}$;CAGG*cre*$^{ER\text{-}TM}$ mice. These mutants in whom *Ofd1* inactivation is obtained at P60 develop tubular cysts 9 months after *Ofd1* inactivation (**Figure 16).** At the same stage also glomerular cysts could be observed (arrows in **Figure 16**).

Altogether the results obtained by inactivating the *Ofd1* transcript in the mouse at different time points confirms that *Ofd1* inactivation leads to renal cystic disease and indicate that the *Ofd1* transcript has a role also in the homeostasis of adult organs.

2. Primary cilia in the Ofd1 deficient models

To evaluate the effect of *Ofd1* inactivation on cilia formation in renal cells, we performed staining with an anti-acetylated tubulin antibody that labels the axoneme of primary cilia. At P0 and P7 in sections from *Ofd1*$^{fl/y}$;*cre*^{Ksp} mutant mice immunofluorescence analysis showed that cilia were present in all tubules of *Ksp* mutant kidneys, indicating that cilia form at precystic stages (arrowheads in **Figure 17 B** and **C**). At P14, when cysts can be detected, no cilia protruding from cells lining the renal cysts (Cy) were detected in both female and male mutants (**Figure 17 H** and **I**), whereas cilia were present in non-cystic distal tubules from the same animals (arrowheads in **Figure 17 H** and **I**). To confirm this observation, we performed SEM analysis on WT and mutant animals (one female and two male mutants). Five different slices were analyzed for each animal for a total of approximately 100 cells observed for WT and female mutant and >200 for the male mutants. This study revealed that at P0 and P7, the majority of the cells examined in all animals (>95%), regardless of the genotype, showed the presence of cilia (arrows in **Figure 17 D – F**). Conversely, at P14, cilia were absent from the dilated tubules of mutant kidneys (**Figure 17 M** and **N**), whereas ciliated structures could be detected in WT kidney (arrow in **Figure 17 L**). SEM analysis was performed in close collaboration with Pascal Dollé (Institut de Génétique et de Biologie Moléculaire

et Cellulaire, BP 10142, 67404 Illkirch Cedex, France). To verify whether ciliated cells expressed the Cre recombinase at precystic stages, we performed immunofluorescence analysis with an anti-acetylated tubulin antibody and an antibody recognizing the Cre protein. Our results indicate that at precystic stages, cells expressing the Cre recombinase displayed primary cilia (Zullo, Iaconis et al. 2010). The same experiments were performed on renal sections from IND mice and compared to WT. As in the *Ksp* model, at P8 (precystic stage) cilia are similarly stained with anti-acetylated tubulin in mutants and controls (**Figure 18 A** and **B**). In addition, at P18 (cystic stage) we observed that only cells that underline the cysts lack the primary cilium (Cy in **Figure 18 D**), while in non-dilated tubules cilia are present (arrows in **Figure 18 D**). Since 80% of renal cells from IND mutants don't express Ofd1 (as described above in Figure 15 A), our results suggest that primary cilia do form in Ofd1-depleted cells in precystic stages. In addition, we performed SEM analysis on kidney sections and measured the length of the primary cilium. We counted 100 cilia on slices from two different IND mutants and two controls and compared both the mean size of cilia and the cilia length distribution (**Figure 18 E** and **F**). This analysis performed in close collaboration with Dr. Caroline Miller and Dr. Vincent Gattone (Electron Microscopy Center; Indiana University School of Medicine) revealed that the length of cilia is comparable between mutants and controls. The data obtained so far in both the *Ksp* and the IND models indicate that cilia initially formed in the absence of Ofd1 and were then subsequently lost after cyst formation although further analysis will be necessary to asses the ultra-structure and the functionality of this organelle.

3. Study of the mTOR pathway in OFD1 deficient models

3.1. The mTOR pathway in murine models of OFDI

Several lines of evidence link the mTOR pathway to cystic kidney disease (Shillingford, Murcia et al. 2006; Boletta 2009) and see also introduction. To test a possible alteration of this pathway in *Ksp* mutants, we initially performed immunofluorescence experiments using an antibody against the phospho-S6 ribosomal protein (P-S6), which is considered a read-out of the mTOR pathway. This study revealed a diffuse activation of S6 in mutant kidneys, which was more evident in the cells surrounding the cysts, thus suggesting an abnormal activation of the

mTOR pathway (**Figure 19 A–G**). Interestingly, deregulation of the mTOR pathway was also observed in non-dilated tubules, suggesting that the upregulation of this pathway precedes cyst formation (arrowheads in **Figure 19 D** and **G**). Moreover, it should also be noted that not all cysts display upregulation of the mTOR pathway (asterisks in **Figure 19 D** and **F**). As a control, we performed immunofluorescence analysis using both an antibody recognizing the Cre protein and the antibody against P-S6. Our study demonstrated that the majority of the cells positive for P-S6 also express the Cre recombinase in mutant animals. This result further strengthens the link between the upregulation of the mTOR pathway and the absence of *Ofd1*. We then looked at both the phosphorylation state and the expression levels of S6 by western blotting analysis. This study revealed an increase in the amount of P-S6 in *Ksp* mutant kidneys from both male and female mutant animals (**Figure 19 H**, top panel), whereas no changes in the total amount of S6 protein were detected (**Figure 19 H**, bottom panel). We also analyzed some components of the pathway upstream of S6. We looked at the basal level and phosphorylation statuses of Akt, mTOR and p70S6 kinase, but no differences were observed in kidneys from *Ksp* mutants compared to controls (**Figure 20**). Moreover, we also analyzed the phosphorylation status of S6 in kidneys at P8 and at this stage the levels of P-S6 were comparable between mutants and WT. To further evaluate the role of mTOR signaling in cystogenesis, mutant mice and control littermates were treated with rapamycin, a specific inhibitor of the mTOR pathway (Sabers, Martin et al. 1995), starting from P14, when the renal cysts appear in our conditional knock-out model. After 10 days of treatment, animals were sacrificed at P24 and analyzed. Histological analysis of rapamycin-treated mutant mice showed a clear reduction in the number and size of cysts compared to non-treated mutant animals (**Figure 21 A** and **B**). Haematoxylin-eosin analysis revealed a normal structure of kidneys in control mice treated with rapamycin (**Figure 21 C**). We also calculated the cystic index and showed that it is significantly reduced in rapamycin-treated mutant mice, confirming that the rapamycin treatment does indeed slow cysts progression (**Figure 21 D**). Taken together, these results suggest that cystogenesis in our mouse model is mTOR-dependent (Zullo, Iaconis et al. 2010).

As described above, the levels of *Ofd1* inactivation in the *Ksp* model are rather low (about 30%). We were wondering if low differences in phosphorylation and basal levels of proteins were lost for a dilution effect. We thus decided to characterize the IND model in which as described before we obtained inactivation of the *Ofd1* transcript in 80% of renal cells (**Figure 15 A**). First, we confirmed the alteration of the mTOR pathway by

immunofluorescence (**Figure 22 A** and **B**) and by Western Blot (**Figure 22 C**) with an antibody against P-S6. In this model we observed that the levels of P-S6 are higher in IND mice compared to controls and we were able to see differences starting from P10 (central line in **Figure 22 C**), the stage in which cysts start to appear. Then we looked upstream to S6 both at the basal level and phosphorylation status of Akt, mTOR and p70S6 kinase, Interestingly, we found that levels of P-Akt are higher in IND mutants compared to controls (**Figure 22 D**). In particular, the alteration was observed using an antibody that recognizes Akt phosphorylated at Ser473. This site is a target of a positive feedback mediated by the mTORC2 complex. The phosphorylation levels of the other components of the pathway between Akt and S6, namely mTOR and p70S6 kinase, were comparable between mutants and controls as well as the phosphorylation levels of Akt at Thr308, which is a target site of upstream components of the mTOR pathway (**Figure 23**). Taken together these results suggested us that Ofd1 is likely to act as a downstream regulator in the mTOR pathway. In order to evaluate the involvement of the mTOR pathway in other affected organs we performed western blot analysis with the antibody against P-S6 on protein extracts from the liver of a P20 IND mutant. The levels of P-S6 in the liver of IND mice were comparable to those observed in WT animals (**Figure 24**), suggesting that the deregulation of the mTOR pathway does not occur in all organs and is possibly linked to renal cystogenesis.

3.2. The mTOR pathway in "in vitro" OFDI deficient systems

To further address the nature of the upregulation of this pathway, we transfected Madin–Darby canine kidney cells (MDCK) and human embryonic kidney cells (HEK293) with siRNAs designed against respectively the canine and human *OFD1* transcript and measured P-S6 levels. Interestingly, the phosphorylated form of the S6 protein was increased in both *OFD1* siRNA-treated cells as early as 48 h after transfection, when the levels of the *OFD1* transcript decrease by 60% and 80% in MDCK and HEK293 cells, respectively (**Figure 25**). These results suggest that the upregulation of mTOR is not a secondary event and is directly linked to the *OFD1* inactivation.

4. OFD1 and the protein synthesis

4.1. OFD1 is a component of the preinitiation complex of translation (PIC)

To identify hypothetical partners of the OFD1 protein, HEK293 cells stably expressing the 3XflagOFD1 protein were generated. After plating, cells were lysed and tagged OFD1 with its interactors was isolated by affinity purification. The proteins isolated were digested by trypsin and the extracted peptide fragments were analyzed by a mass spectrometer (**Figure 26**). These experiments were performed in close collaboration with Professor Piero Pucci (CEINGE - Biotecnologie Avanzate, Naples). In the output, a number of ribosomal proteins and other proteins involved in the regulation of protein synthesis were listed. Because of the involvement of the mTOR pathway in driving protein synthesis (Ma and Blenis 2009; Van Der Kelen, Beyaert et al. 2009), I focused my attention on this group of hypothetical partners of OFD1. Among them, there were three different subunits of the eIF3 complex namely eIF3 β, ε and δ. First we confirmed the interaction between OFD1 and two different subunits (η and δ) of eIF3 by co-immunoprecipitation (co-IP) experiments. HEK293 cells were transiently transfected with a construct expressing 3XFlagOFD1 and immunoprecipitation experiments were performed using an antibody that specifically binds the subunit η of the eIF3 complex. The precipitate was then analyzed by Western blot with an antibody against the 3Xflag peptide and as shown in **Figure 27 A** the presence of a band corresponding to the OFD1 protein was detected. We then decided to confirm the interaction between endogenous proteins in HEK293 cells. For this experiment the immunoprecipitation was performed first with an antibody against eiF3η and a band corresponding to OFD1 was detected by western Blotting analysis (**Figure 27 B**). Then Co-IP experiments were performed with an antibody against OFD1 and subsequent Western Blot analysis performed with the specific antibodies revealed the presence of both the eiF3η and eIF3δ subunits of the eIF3 complex (**Figura 27 C)**. All together these results indicate that OFD1 physically interacts with the eIF3 complex.

However, we also wondered about the subcellular compartment in which such an interaction could occur. Data from the literature indicate that the eIF3 complex is distributed in the cytoplasm, even if a nuclear localization for subunit eIF3e was described (Watkins and Norbury 2004). We thus performed immunofluorescence experiments. Interestingly, using an antibody against eIF3δ we observed that this subunit colocalizes with OFD1 at the centrosome in HEK293 cells stably overexpressing GFP-OFD1 (**Figure 28**). We tested by immunofluorescence in

HEK293 cells also an additional component of the PIC, namely eIF4E. Also in this case we could determine colocalization of eIF4E with different centrosomal markers, such as centrin and γ-tubulin (**Figure 28**). In addition colocalization of eIF4E with OFD1 in HEK293 overexpressing GFP-OFD1 was also demonstrated (**Figure 28**). We also quantified by confocal microscopy the levels of colocalization. Our results indicate a low percentage of colocalization (15%) between eIF4E and γ-tubulin, while eIF4E was shown to perfectly colocalize with GFP-OFD1 (**Figure 29**). Previous data demonstrated that OFD1 localizes at the mother centriole ((Singla, Romaguera-Ros et al. 2010) and our unpublished data). Our results suggest that also eIF4E localizes at the mother centriole. Interestingly, in HEK293 treated with siRNA against *OFD1*, eIF4E seems to accumulate at the centrosome (**Figure 30** panel **A**), suggesting that OFD1 could control the recruitment of the components of the PIC.

4.2. OFD1 regulates protein synthesis in the kidney

At this point we reasoned that OFD1 could regulate protein synthesis in the kidney and that this could represent a possible link with the deregulation of the mTOR pathway observed in models with *Ofd1* kidney inactivation. To test this hypothesis we looked at the amount of P-S6 bound to the eIF3 complex in silenced HEK293 cells compared to WT by co-immunoprecipitation. Surprisingly, the levels of P-S6 bound to eIF3η are higher in *OFD1*-siRNA treated cells compared to control cells (**Figure 31**). Finally, to better characterize the involvement of OFD1 in the formation of the translation machinery we decided to extract polysomes from both HEK293 cells and kidneys from IND and WT mice. These experiments were performed in collaboration with my external supervisor, Dr. Mario Pende (Inserm U845, Université Paris Descartes). Polysomes are a cluster of ribosomes, bound to an mRNA molecule. Many ribosomes read one mRNA simultaneously, progressing along the mRNA to synthesize the same protein. Discrimination between actively translated and translationally silent mRNAs in the cell can be efficiently carried out using sucrose-gradient fractionation (polysome gradients), since this technique allows separation of free ribonucleoprotein particles (ribosome-free mRNA) from mRNAs bound to an increasing number of ribosomes (polysome-bound mRNA). The mTOR pathway was associated with an increase of polysomes due to its role in translation and polysomal fractionation is a popular method used to study general translation in the cells. Actively translated polysome-bound mRNAs and protein involved in the regulation of

translation were separated from messenger free ribonucleoproteins using sucrose gradient fractionation (**Figure 32 A**). We extracted polysomes at two different stages: a precystic stage (P8) and a cystic stage (P20). Polysomal profile was similar between IND and WT mice at P8, while a significant difference was observed at P20 (**Figure 32 B**). After polysomes fractionation we first demonstrated that polysomal fractions were not contaminate by cytoplasm. Indeed western blot analysis with an antibody against GAPDH revealed that this protein was absent in polysomal fractions from kidneys at the different stages analyzed (**Figure 33 A**), while, on the contrary and as expected, eIF3η was present (**Figure 33 B** lanes 2 and 3). OFD1 was also present both in polysomal kidney extracts and cellular extracts (**Figure 33 C**) and more interestingly, we showed a physical interaction between OFD1 and eIF3η in kidney fractions (**Figure 33 B** lane 4). In addition, we also observed by immunofluorescence that eIF4E seems to accumulate, in a precystic stage, at the centrosome in kidney sections from IND mice compared to WT (**Figure 30** panel **B**). These results suggest a role for OFD1 in the regulation of the PIC at the stage of P8 when no differences, by looking at the polysomal profile, could be detected in the general translation.

We decided to test whether OFD1 could have a direct role in the translation. First, in collaboration with the Bioinformatic core at TIGEM, we looked for known RNA binding region in the OFD1 protein using two different bioinformatic tools: BindN (http://bioinfo.ggc.org/bindn/) and RNABindR (http://bindr.gdcb.iastate.edu/RNABindR/). This analysis did not reveal significative binding region although more experiments will be required to address this point. We then proceeded with different approaches in the *in vitro* and *in vivo* available systems. We transfected HEK293 cells with a bicistronic reporter plasmid allowing both cap-dependent expression of renilla luciferase and expression of HCV IRES dependent firefly luciferase (cap-independent) (Holz, Ballif et al. 2005; Csibi, Cornille et al. 2010). Firefly luciferase was used as an internal reporter to normalize the transfection, while renilla luciferase levels in the cells depend from cap-dependent/PIC driven translation efficiency. We observed that *OFD1*-silenced HEK293 cells had higher levels of renilla luciferase activity compared to control cells (**Figure 34**). To exclude the possibility that the accumulation of renilla was due to impairment of degradation we treated cells with cycloheximide, a potent inhibitor of translation and analysed the cells after 5 hours. After treatment the rate of degradation of the renilla was comparable between silenced and control cells, suggesting that normal degradation occurred and that the accumulation of renilla was

due to upregulation of translation (**Figure 34**). To confirm *in vivo* the impairment of translation we isolated total and polysomal RNA from kidneys from WT and IND mice (two for each genotype) and performed microarray experiments. We first compared the results obtained from polysomal and total RNA and eliminated the genes in common. This step allowed us to get read off the transcripts with an altered level of translation due to transcription impairment. This analysis indicated the presence of over 130 transcripts, which were differentially expressed between WT and IND mice. We then tried to cluster genes by gene ontology analysis using the Database for Annotation, Visualization and Integrated Discovery (DAVID) bioinformatic tool. Unfortunately no clusters could be identified.

4.3. Is GH involved in the deregulation of the mTOR pathway observed in Ofd1 depleted models?

We carried out an extensive analysis of the differentially expressed gene identified by microarray analysis taking advantage of the available scientific literature. This effort allowed us to identify few transcripts of potential biological interest. Among these we focused our attention on the Growth hormone (GH). First and interestingly, western blot analysis on kidney lysates confirmed the higher amount of GH in IND mutants compared to WT animals at the precystic stage (**Figure 35**).

GH has been recently demonstrated to be involved in the uptake of aminoacids (AA) and consequently in the activation of the mTOR pathway (Hayashi and Proud 2007). An extensive amount of published data indicates that, after starvation, the mTOR pathway is completely switched off and is reactivated by adding AA and/or nutrients (Proud 2002). It was demonstrated that stimulation of the cells only with AA mediates this response through a non-canonical pathway that does not involve the PI3K/Akt cascade (Gulati, Gaspers et al. 2008). Instead, upon addition of nutrients without AA the mTORC1 complex is activated by PI3K/Akt cascade. The reactivation of the mTOR pathway by nutrients and AA together occurs through the two different pathways simultaneously. Therefore, we decided to verify whether the mTOR pathway activation in our system is AA-dependent. To address this point both HEK293 *OFD1*-silenced and control cells were grown over-night with serum-deprived medium containing sodium pyruvate and AA. After 16 hours, cells were starved for 2 hours with HBSS saline solution in order to deprive cells of all kind of nutrients including AA. Cells were then re-stimulated for 30 minutes either

with AA (without nutrients) or dialyzed FBS (nutrients without AA) or complete FBS (nutrients plus AA). Treated cells were lysated and protein extracts were used to evaluate the levels of P-S6 by western blot analysis. Interestingly, our analysis showed that *OFD1*-silenced cells were more sensitive to AA and complete FBS re-stimulation compared to control cells, while re-stimulation with dialyzed FBS gave similar results in silenced and control cells (**Figure 36**). On the basis of these results we concluded that *OFD1*-depleted cells show an increased sensitivity to AA. These results were consistent with the normal phosphorylation levels described for Akt in our systems, indeed AA stimuli activates mTOR pathway response through a non-canonical pathway that does not involve the PI3K/Akt cascade. Finally we hypothesize that the increased sensitivity to AA could be due to the increased amount of GH observed in OFD1 depleted models. This observation pave the way to new possible functional approaches and may offer new links between deregulation of the mTOR pathway and renal cystic disease. However, additional experiments are necessary to elucidate the connections between these phenomena.

5. Cell cycle and renal cysts development in OFD1 deficient murine models

Based on the involvement of mTOR in cell proliferation we performed staining with the anti-PCNA antibody that recognize proliferating cells in late G1, S and early G2 phases, in WT and *Ksp* mutant kidneys at P21. We observed a marked increase of proliferating cells in mutant kidneys compared to WT (**Figure 37**). We confirmed the same results on renal sections from IND and control mice at P18. Note that, at P10 also WT sections were positive because the kidney is still proliferating and growing (**Figure 38**). We confirmed the increased cell proliferation with BrdU (Bromodeoxyuridine) staining that marks cells in S phase. We injected both WT and IND mice at P18 with BrdU and collected kidneys after 6 hours. Sections were stained with an anti-BrdU antibody and we observed an increased number of cells positive at the staining in sections from IND mutants compared to controls (**Figure 39**). However, PH3 (phospho-hystone 3) staining revealed a slight increase of mitotic cells in IND mice at P18 compared to WT, while no differences were observed at P8 and P10 (**Figure 40**). We also performed immunohistochemistry (ICH) and immunofluorescence experiments with an antibody against Ki67 that marks all proliferating cells and we did not observe differences between IND and WT in all stages analyzed

(**Figure 41**). These results suggest that *Ofd1*-depleted cells undergo a delay in cell progression and enter in a quiescent phase.

6. Analysis of the pathways commonly involved in renal cystic disease.

Different pathways have been involved in renal cysts development as discussed in the paragraph 3.2 of the Introduction. To address the possible involvement of the JACK-STAT pathway and/or Wnt pathway in the pathogenesis of the renal cystic phenotype observed in the IND model, we analyzed by western blot the levels of p21, p27 (redouts of the JACK-STAT pathway) and βcatenin (as a marker of the Wnt caconical pathway) proteins in lysates from kidneys of both WT and IND mice at P20. Our analysis did not reveal any differences in the total amount of these proteins (**Figure 42**). These preliminary results seem to exclude a role for both the JACK-STAT and the Wnt pathways. However further experiments will be necessary to complete exclude this possibility.

7. Autophagy and renal cyst in OFD1 deficient models

As discussed above, the mTOR pathway is one of the key regulators of autophagy. To understand if this process is deregulated in OFD1-deficient models we looked at different markers of autophagy both in *in vitro* and *in vivo* systems. First we looked at LC3 by Western Blot, interestingly, we found that the levels of both LC3I and II are higher in OFD1-silenced-MDCK cells and kidney from the IND model at P8 compared to controls, while no differences were visible in the protein lysates obtained from null $Ofd1^{\Delta 4\text{-}5}$ male embryos at E10.5 and protein lysates from kidneys obtained from the IND animals at P20 (**Figure 43**). There results, although very preliminary, suggest that an alteration of the autophagy process may occur specifically in the renal system and in a precystic stage. This is an early finding and it is quite difficult at this point to predict whether there is a link between autophagy and cyst development and further experiments are necessary to unravel and fully understand this observation.

DISCUSSION

My PhD project focused on the elucidation of the role of the *Ofd1* transcript in the renal cystic disease observed in Oral-facial-digital type I syndrome. In order to do so I generated and characterized murine conditional models and in *Ofd1*-depleted cellular systems. These tools allowed me to apply *in vivo* and *in vitro* approaches and to get a variety of results, which will be discussed in the following sections:

1. Timing of renal cystic disease in OFDI syndrome

Ofd1 conditional inactivation at early stages of development allowed the generation of a null model in which female mutants die at the perinatal stage and male mutants die by the stage of E12. We demonstrated that $Ofd1^{\Delta 4\text{-}5/+}$ heterozygous females develop glomerular cysts as early as E14.5 (Ferrante, Zullo et al. 2006). To date, we never observed cysts of tubular origin in $Ofd1^{\Delta 4\text{-}5}$ mutant females. OFDI patients display a prevalence of glomerulocystic kidney disease with a minor population of cysts from distal tubules (Feather, Winyard et al. 1997). It is conceivable that glomeruli are more sensitive to *Ofd1* deficiency leading to the early appearance of glomerular cysts in $Ofd1^{\Delta 4\text{-}5}$ females and to the predominance of cysts of glomerular origin in OFDI patients. Unfortunately, due to the perinatal female lethality we cannot analyze $Ofd1^{\Delta 4\text{-}5}$ females at more advanced stages to verify whether tubular cysts will develop at later stages in this model. However, in the conditional models used in this study cysts started to develop from the distal portion of the nephron. Concerning the *Ksp* mutants, the *Cre* is expressed starting from E15.5 in the medullary portion of the kidney and, accordingly, cysts originated from distal tubules. In these mutants, we also observed at later stages glomerular cysts and it is well established that the *Ksp* transcript is not expressed in glomerular structures (Shao, Somlo et al. 2002). The same observation has been reported for the $KspCre;Hnf1\beta^{flox/flox}$ mutants (Gresh, Fischer et al. 2004), while no glomerular cysts were observed in the $Pkd1^{flox/-}$*:Ksp-Cre* animals (Shibazaki, Yu et al. 2008). These results suggest that the glomerular cysts in these models may be the product of secondary cystogenetic events, which appear to take place only when specific transcripts (*Hnf1β* and *Ofd1*) are inactivated. On the other hand, in the IND model, in which we inactivated *Ofd1* ubiquitously at birth, tubular cysts do form starting from P10. One possibility could be that after birth tubules are more sensitive to molecular signals than glomeruli because at P0 glomeruli are already formed

while tubules, and consequently the entire kidney, is still growing in size until P12-P14. This growth is due to elongation of distal portions of the nephron and branching of tubules. However, in the IND model, we observed glomerular cysts at P25 when the gene is inactivated at P0 and at 11 months when the gene is inactivated at P60, suggesting also a direct role of Ofd1 in cysts formation in the glomeruli. In addition, it was reported that also the zebrafish *Ofd1*-deficient model has glomeruli alteration supporting a direct role of the protein in glomeruli development (Ferrante, Romio et al. 2009).

These results allow us to draw two conclusions: 1) the *Ofd1* transcript is important from the early stages of renal development and 2) *Ofd1* inactivation can lead to cystic dilation of both tubular and glomerular structures.

Different animal models for renal cystic disease have been generated, although with great variability in the stage and site of occurrence of renal cysts. These differences are partly due to the use of different cre lines, different genetic backgrounds of the murine models and to the specific role, site and timing of expression, of the genes to be inactivated. However, recent data showed that inactivation of *Pkd1* in mice before postnatal day 12 resulted in severe PKD, while inactivation at postnatal day 14 and later resulted in slow-onset cystic kidney disease (Piontek, Menezes et al. 2007). These data identify a crucial 2-day interval (from P12 to P14) in renal maturation. As a consequence, inducible inactivation of *Pkd1* in the mouse at different time points resulted in a very different disease progression (Lantinga-van Leeuwen, Leonhard et al. 2007; Piontek, Menezes et al. 2007) and this seems to occur also in the Ofd1 IND model. Based on these observations, we cannot exclude a specific role of the *Ofd1* transcript in renal development around P10-P14, when we observe the first dilatation of tubules in the *Ksp* and IND models. Taken together, our data suggest that *Ofd1* is important in all segments of the nephron and the availability of different murine models will be critical to evaluate the role of *Ofd1* in the formation of cysts in the different structures.

2. The ciliary disfuntion and renal cystic disease in OFDI syndrome

The list of ciliary proteins involved in polycystic kidney disease continues to grow, as well as the number of animal models in which the presence of renal cysts is associated to cilia dysfunction (Hildebrandt and Otto 2005). Despite this observation, there are also a few reports of animal models in which inactivation of ciliary proteins

results in cystic kidneys and primary cilia can still be observed inside the cysts although no data is available on the functionality of these cilia (Phillips, Miller et al. 2004; Mokrzan, Lewis et al. 2007). Therefore, although the connection between primary cilium and renal cystic disease is evident, there is no clear demonstration of a direct, causal relationship between ciliary dysfunction and cyst formation. It is important to keep in mind that most cystoproteins are not exclusively localized to the cilia. For example, polycystin-1, nephrocystin and inversin, which are the proteins encoded by the genes responsible for ADPKD, NPHP1, and NPHP2, respectively, have also been detected in other cellular structures (Benzing, Gerke et al. 2001; Donaldson, Dise et al. 2002; Nurnberger, Bacallao et al. 2002; Boletta and Germino 2003) and are involved in cell-cell and cell-matrix interactions. We recently reported that OFD1 is not exclusively localized to the centrosome and basal body, but is present also in the nucleus (Giorgio, Alfieri et al. 2007). Impairment of the function of OFD1 in either of these subcellular compartments could independently result in altered tubular morphology leading to renal cysts formation. One challenge that remains to be addressed is to separate the cilia-specific function and properties of the various proteins from other functions/roles that they might have in the cell. The studies of the different murine models carrying inactivation of the Ift88 protein (also known as Tg737 or polaris) are particularly informative in this regard. Ift88 is a ciliary protein that is crucial for intraflagellar transport and cilium assembly (Taulman, Haycraft et al. 2001; Yoder, Tousson et al. 2002). Mice lacking Ift88 die at mid-gestation, display absence of nodal cilia, and exhibit neural tube and situs inversus (Murcia, Richards et al. 2000). Mice homozygous for a hypomorphic allele named *orpk* survive to birth and have cystic kidney disease associated to the presence of stunted and malformed cilia (Pazour, Dickert et al. 2000; Lehman, Michaud et al. 2008). Unexpectedly, transgenic overexpression of Ift88 in a null TgN737 background results in mice with normal nodal function and renal cystic disease with cilia of normal length and morphology, thus indicating a partial rescue of the functions associated to cilia (Brown and Murcia 2003; Watnick and Germino 2003). Altogether these results suggest that in these models ciliary dysfunction does not fully explain renal cystogenesis. In addition, it is also known that non-ciliary proteins give rise to renal cystic disease when mutated. In particular Bicaudal C is a conserved RNA-binding protein that is mutated in two murine models for renal cystic disease, the *jcpk* and *bpk* models (Cogswell, Price et al. 2003). However, recent findings link the activity of this RNA-binding protein with the orientation of cilia via Wnt signaling (Maisonneuve, Guilleret et al. 2009). Another example is the FLCN protein, also known as folliculin.

Mutations in the *BHD/FLCN* gene cause the Birt–Hogg–Dube' syndrome characterized by renal cystic disease and increased risk for renal neoplasia. The gene product localizes to the cytoplasm and the nucleus and seems to be involved in the regulation of the mTOR pathway (Chen, Futami et al. 2008; Hasumi, Baba et al. 2008; Hasumi, Baba et al. 2009).

We have now demonstrated that, in renal epithelial cells devoid of *Ofd1,* primary cilia are present prior to the formation of renal cysts and their length is comparable to controls both in *Ksp* and IND mice. Cilia are then lost after cysts development. Interestingly the same observation was reported for a conditional mouse model with a *Kif3A* kidney specific inactivation (Lin, Hiesberger et al. 2003). To date, we do not know whether these cilia function normally and further experiments are needed to address this question. Our data confirm the association between primary cilia and renal cystic disease, and we propose that in our model the development of renal cysts might not be a direct consequence of the loss of cilia. Unfortunately, no data are available concerning the presence of cilia in precystic stages in other models for PKD and it is thus difficult to assess whether this hypothesis can be generally applied or it is specific to the renal cystic disease resulting from *Ofd1* inactivation.

3. The role of the mTOR pathway in the pathogenesis of the renal cystic disease observed in OFD1 deficient models

3.1. Deregulation of the mTOR pathway and renal cystic disease: a common theme?

The characterization of the in vivo model with Ofd1 inactivation we have generated allowed us to demonstrate an upregulation of the phospho-S6 molecule both in dilated and non-dilated tubules in the kidneys of *Ksp* and IND mutants. A possible role of the mTOR pathway in renal cystic disease is supported by reports indicating that rapamycin, an inhibitor of mTOR, slows down cyst progression in different animal models, suggesting that the mTOR pathway is a converging point in the cystogenesis (Tao, Kim et al. 2005; Shillingford, Murcia et al. 2006; Wahl, Serra et al. 2006; Zafar, Belibi et al. 2009). Promising and preliminary data in patients affected by ADPKD demonstrated that rapamycin had an effect in reducing the size of renal cysts. Patients affected by ADPKD

frequently receive a renal transplant without removal of the affected cystic kidneys. These patients are usually treated with rapamycin, used as an immunosuppressant, after renal transplantation. Interestingly, Shillingford et al showed a decrease of the volumes of affected kidneys in these patients thus providing evidences for possible new therapeutic approaches for PDKs (Shillingford, Murcia et al. 2006).

Different clinical trials have been planned in patients affected by ADPKD to test possible treatment with rapamycin and its analogues (http://clinicaltrials.gov/). Studies performed on patients suggest that short-term administration of these drugs is safe and tolerate (Serra, Kistler et al. 2007; Serra, Kistler et al. 2009). However, more recent findings showed that long-term treatment of patients results in frequent drug-specific adverse events and did not slow the decline in progressive renal impairment (Walz, Budde et al. 2010). More studies are however needed to understand the possible role of molecules affecting the mTOR pathway in the amelioration of renal cystic disease.

It is still not clear if the upregulation of the mTOR pathway is the cause of cyst development. Different studies, including our report, have shown that not all renal cysts, in ADPKD patients as well as in mouse mutants, show upregulation of the mTOR pathway, suggesting that this pathway could be involved in cyst expansion rather than cyst formation (Boletta 2009). However, the involvement of this pathway in cystogenesis is adequately reported in the literature and a deep and complete knowledge of the molecular mechanisms underlying deregulation of the mTOR pathway in renal cystic disease will be needed to understand the potential benefit of mTOR-related treatments.

The mTOR pathway has also been implicated in tuberous sclerosis (TSC), a tumor suppressor gene syndrome associated with renal cystic disease ((Zhou, Brugarolas et al. 2009) and introduction). In addition, it was recently demonstrated that knockdown of one of the *TSC1* zebrafish homologs leads to renal cystic disease with upregulation of the mTOR pathway in the cells that line renal cysts, and to the presence of longer cilia in the otic vesicle and pronephric ducts from morphants (DiBella, Park et al. 2009). Moreover, mouse embryonic fibroblasts from $Tsc1^{-/-}$ and $Tsc2^{-/-}$ mutants show an increased number of cilia, which is not rescued by treatment with rapamycin, suggesting that the enhanced cilia formation is mTOR-independent (Hartman, Liu et al. 2009). These data underline the link between the mTOR pathway, cilia and renal cysts, even if they do not clarify the role of cilia in the mTOR-dependent mechanisms leading to cyst pathogenesis. In our model we show, for the first time,

that the upregulation of mTOR pathway is evident also in non-dilated tubules where cilia appear to be normally present. In addition, as discussed above, there is accumulating evidence that ciliary proteins have other functions in the cells and that renal cysts can also be linked to non ciliary-proteins. These observations suggest that the activation of mTOR can occur before cyst development and that this event could determine tubules dilation. The persistent activation of the pathway in a portion of the cysts might contribute to the increasing in size of the cysts (Boletta 2009). However, in renal tubules bending of cilia due to fluid flow has been shown to down-regulate mTOR signaling (Boehlke, Kotsis et al. 2010). These data suggest that the absence of cilia observed in a number of renal cystic diseases determines failure to sense urine flow and the upregulation of the mTOR pathway as a consequence. Different data are published that link mTOR, cilia and cysts and further analysis are necessary to understand the connections. Nevertheless, the alteration of the mTOR pathway seems to be a common theme in renal cystic disease and this observation let us to hypothesize the existence of different mechanisms that may converge on the regulation of the mTOR pathway in the different models. Interestingly, we also observed that the levels of P-S6 are not altered in other affected organs obtained from IND mice, such as the liver. These findings underline the importance of this pathway in kidney development and suggest that the alteration of the mTOR pathway may be strictly linked to renal cysts formation. Moreover, these results support the idea that the genes mutated in renal cystic disease, could control the activation of this pathway preferentially in the kidney.

Renal cystic disease is often associated with cysts in other organs, such as pancreas, ovary and liver as in the case of OFD type I syndrome. Until now, nothing is known about the involvement of the mTOR pathway in the cystogenesis of pancreas or ovary. Recent findings showed that Everolimus and other rapamycin analogs reduce liver size but do not ameliorate liver dysfunction, suggesting that the mTOR pathway is not directly linked to cystogenesis in this organ (Gevers and Drenth 2011).

3.2. The role of OFD1 in the translational machinery and cell cycle control

Our study contributed new data on the possible involvement of the OFD1 protein in the regulation of the mTOR pathway trough its involvement in the formation of the PIC. We hypothesize that this role is tightly linked to the centrosomal function of OFD1 and that the deregulation of the cell cycle and the ciliary dysfunction are direct consequence of the impairment of this basic function. We demonstrate that OFD1 protein colocalizes with

different component of the PIC at the centrosome and physically interacts with two subunits of the eIF3 complex both in *in vitro* and *in vivo* models. In addition in a precystic stage, OFD1 is present in polysomal fractions extracted from kidneys and regulates translation of specific targets. The polysomal profile is comparable between mutants and controls, suggesting that general translation is not affected, but microarray analysis on polysomal fractions indicate the presence of over one hundred mRNAs differentially expressed between WT and mutants. Among the possible targets we focused our attention on the GH protein. GH has an important role in the activation of the mTOR pathway through the uptake of AA that seems to be impaired in OFD1-silenced HEK293 cells. The higher level of P-S6 in our systems could be explained by the increased levels of GH associated to increased sensibility to AA. We proposed that OFD1 would act by controlling the formation of the PIC and the regulation of the translation of specific targets such as GH at the centrosome. **Figure 44** illustrates our hypothesis. This mechanism could explain the higher levels of P-S6, the normal phosphorylation levels of protein upstream P-S6 and the cell cycle alteration observed at P20 in the IND model. The higher amounts of GH do not allow downregulation of the mTOR pathway in Ofd1 deficient models compared to controls. The persistent activation of the pathway brings to the alteration of the general translation as showed in the IND model at P20. The upregulation of the mTOR pathway activates the translation of proteins involved in cell cycle regulation. In support to our hypothesis markers of cell cycle are altered only after cysts formation in oura and other in vivo models of renal cystic disease, suggesting that the alteration of the cell cycle is a consequence rather than the cause of cysts formation. In addition, we observed at P20 a slight increase of mitotic cells positive to PH3 and only few cells marked with Ki67. These latter cells should be more numerous considering the number of cells positive for S phase markers. These results suggest that cells probably slow down in cell progression and enter in a quiescent phase. However, at P20 we observed the iper phosphorylation of Akt at Ser473. It is interesting to note that this site is a target of mTORC2, the other complex in which mTOR is involved. This finding suggests a possible activation of the mTORC2 complex. The mTORC2 complex is an important regulator of the cytoskeleton and at this point we cannot exclude that different biological process in conjunction with the alteration of translation could concur to cystogenesis in our models.

3.3. Autophagy in OFD1 deficient models

The mTOR pathway controls the first steps of autophagy induction and membrane recruitment and is one of the main inhibitors of this complex biological process. No experimental evidences have been reported to date on the involvement of autophagy in the development of renal cystic disease. However, because of the frequent deregulation of the mTOR pathway observed in models of renal cystic diseases, we looked at markers of autophagy in *in vivo* and *in vitro* OFD1-deficient models. The levels of both LC3I and II are higher in silenced-MDCK cells and kidney at P8 compared to controls. There results suggest that an alteration of the autophagy process occurs in a precystic stage in kidneys from IND mice. Interestingly, both forms of LC3 accumulate, suggesting that this accumulation precede autophagosome formation. It is known that LC3I was degraded in LC3II by lysosomal enzimes. So when autophagy is blocked LC3II accumulates as a consequence of autophagic body accumulation after the fusion of autophagosome with lysosome. As described before, we observed in our models an impairment of the translation of specific targets. Among the targets, there is the Vps39 protein, involved in the fusion of autophagosome and lysosome. Interestingly this protein resulted to be downregulated in the list of differentially expressed polysomal RNA we obtained after the microarray experiments on polymal fractions. We have not confirmed yet the downregulation of this protein. It is tempting to speculate that the downregulation of Vps39 determines the block of the autophagic process at step 4 (figure 9) when the autophagosome is formed and LC3 is recruited but not digested. We cannot exclude that the activation of the mTOR pathway is a consequence of the activation of autophagy and that autophagy could play a role in cysts development. However, in an advanced cystic stage, at P20, we found that LC3I and II levels are comparable between IND and WT. Because of the complex regulation of the autophagy it could be that compensatory effects determine the normal level of autophagic markers after an initial disequilibrium possibly due to an alteration of the translation of specific component of the process of autophagic body formation. This is a fascinating line of research which will be further pursued in Prof. Franco' laboratory.

CONCLUSION

The Oral-Facial-Digital type I syndrome (OFDI; MIM 311200) is a rare syndromic form of inherited renal cystic disease and belongs to the growing number of disorders ascribed to dysfunction of primary cilia. With the purpose of studying the role of the *Ofd1* transcript in renal cystic disease, we generated two conditional *Ofd1* deficient mouse models (*Ksp* and IND), which resulted in viable mice characterized by renal cystic disease and progressive impairment of renal function. The study of these models allowed us to demonstrate that primary cilia initially form and then disappear after the development of cysts, suggesting that the dysfunction of primary cilia is a consequence rather than the primary cause of renal cystic disease and probably have a role in renal cysts enlargement. Using a variety of different approaches we showed that deregulation of the mTOR pathway is associated to renal cystic disease in our conditional models. Interestingly, deregulation of the mTOR pathway seemed to specifically occur in the kidneys. This finding suggest that the mTOR pathway could have a specific role in renal cystogenesis and underline the importance of this pathway in kidney development. The use of both *in vitro* and *in vivo* systems allowed us to demonstrate that OFD1 has a role in the formation of the pre-initiation complex of translation (PIC) and in the regulation of translation. All together our results shed light on the pathogenetic mechanisms underlying OFD type I syndrome and propose new possible links between renal cystic disease and deregulation of the mTOR pathway.

FUTURE PERSPECTIVE

We have demonstrated that OFD1 regulates the formation of the PIC at the centrosome and that OFD1 inactivation results in an impairment of translation. However, further analysis will be necessary to elucidate the molecular mechanisms underlying this event. We hypothesize that OFD1 prevents the binding of eIF4E to the PIC at the centrosome. We showed that eIF4E accumulates at the centrosome in the absence of OFD1, however we have not yet demonstrated that the binding of eIF4E to the eIF3 complex is stronger in *Ofd1*-depleted systems. In addition, we cannot exclude the possibility that OFD1 regulates the recruitment of the mRNAs at the centrosome. Preliminary bioinformatic analysis did not predict any RNA binding domain in the OFD1 protein sequence, however experimental evidences will be necessary to exclude this possibility.

We have also found that the translation of a number of mRNAs is impaired in IND mice at a precystic stage and so far we focused our attention on GH as a possible target. However, we identified more than 130 differentially expressed mRNAs. The next step will be to understand which molecular pathways could be deregulated by each of these transcripts, which translation is impaired in *Ofd*1-depleted systems. Bioinformatic analysis did not suggest a common biological function for these transcripts, so it is possible that more than one biological process is controlled by OFD1. Interestingly, among the putative targets there is the Vps39 protein. This protein is involved in the fusion of autophagosomes to lysosomes during the autophagic process. Very preliminary data suggest an impairment of autophagy in Ofd1-inactivated models and it will be interesting to investigate the possible involvement of this important biological process in the pathogenesis of renal cystic disease.

Moreover, we hypothesize that the impairment of translation at the centrosome is the first event that leads to cystogenesis and that the alteration in the synthesis of different proteins cause as a consequence the deregulation of different pathways. To test this hypothesis we will treat mice with drugs that inhibit specifically the machinery of translation and we will assess whether this treatment improves the renal cystic phenotype.

Finally, our data indicate for the first time a role in translation for a protein important for ciliary function, namely OFD1. It will be important to address if this is something specific to OFD1 or if it is a novel common function of ciliary proteins. On the same line it will be also interesting to study possible links between the different steps involved in ciliogenesis and this new role of the OFD1 protein. Eventually it will also be important to link impairment of translation to renal cystic disease and/or the other pathological features observed in ciliopathies.

ACKNOWLEDGMENTS

I would like to thank Peter Igarashi for the Ksp-cre line, Pascal Dollé and Nadia Messaddeq for the SEM analysis on Ksp mutants and Alessandra Cantone and G.Battista Capasso for physiological studies. In addition, for the Mass Spectrometry analysis and study of the interaction between OFD1 and eIF3η: Prof. Piero Pucci and his staff, in particular Dr. Maria Monti and Dr. Marianna Cozzolino. Marinella Pirozzi (TIGEM) and Salvatore Arbucci (IGB – CNR Naples) for their kind help in microscopy analysis. I would like to thank also Dr.Mario Pende and his

staff for the analysis of polysomes and helpful discussions. Finally, Prof. Brunella Franco and her group for scientific and human support.

REFERENCES

Azim, H., H. A. Azim, Jr., et al. (2010). "Targeting mTOR in cancer: renal cell is just a beginning." Target Oncol **5**(4): 269-280.

Badano, J. L., N. Mitsuma, et al. (2006). "The Ciliopathies: An Emerging Class of Human Genetic Disorders." Annu Rev Genomics Hum Genet **7**: 125-148.

Becker, J. U., A. Opazo Saez, et al. (2010). "The mTOR pathway is activated in human autosomal-recessive polycystic kidney disease." Kidney Blood Press Res **33**(2): 129-138.

Beevers, C. S., F. Li, et al. (2006). "Curcumin inhibits the mammalian target of rapamycin-mediated signaling pathways in cancer cells." Int J Cancer **119**(4): 757-764.

Benzing, T., P. Gerke, et al. (2001). "Nephrocystin interacts with Pyk2, p130(Cas), and tensin and triggers phosphorylation of Pyk2." Proc Natl Acad Sci U S A **98**(17): 9784-9789.

Benzing, T., M. Simons, et al. (2007). "Wnt signaling in polycystic kidney disease." J Am Soc Nephrol **18**(5): 1389-1398.

Bettencourt-Dias, M., F. Hildebrandt, et al. (2011). "Centrosomes and cilia in human disease." Trends Genet **27**(8): 307-315.

Bhunia, A. K., K. Piontek, et al. (2002). "PKD1 induces p21(waf1) and regulation of the cell cycle via direct activation of the JAK-STAT signaling pathway in a process requiring PKD2." Cell **109**(2): 157-168.

Boehlke, C., F. Kotsis, et al. (2010). "Primary cilia regulate mTORC1 activity and cell size through Lkb1." Nat Cell Biol **12**(11): 1115-1122.

Boletta, A. (2009). "Emerging evidence of a link between the polycystins and the mTOR pathways." Pathogenetics **2**(1): 6.

Boletta, A. and G. G. Germino (2003). "Role of polycystins in renal tubulogenesis." Trends Cell Biol **13**(9): 484-492.

Bonnet, C. S., M. Aldred, et al. (2009). "Defects in cell polarity underlie TSC and ADPKD-associated cystogenesis." Hum Mol Genet **18**(12): 2166-2176.

Brook-Carter, P. T., B. Peral, et al. (1994). "Deletion of the TSC2 and PKD1 genes associated with severe infantile polycystic kidney disease--a contiguous gene syndrome." Nat Genet **8**(4): 328-332.

Brown, N. E. and N. S. Murcia (2003). "Delayed cystogenesis and increased ciliogenesis associated with the re-expression of polaris in Tg737 mutant mice." Kidney Int **63**(4): 1220-1229.

Browne, G. J. and C. G. Proud (2002). "Regulation of peptide-chain elongation in mammalian cells." Eur J Biochem **269**(22): 5360-5368.

Burkhard, P., J. Stetefeld, et al. (2001). "Coiled coils: a highly versatile protein folding motif." Trends Cell Biol **11**(2): 82-88.

Calvet, J. P. and J. J. Grantham (2001). "The genetics and physiology of polycystic kidney disease." Semin Nephrol **21**(2): 107-123.

Chang, M. Y. and A. C. Ong (2011). "Mechanism-Based Therapeutics for Autosomal Dominant Polycystic Kidney Disease: Recent Progress and Future Prospects." Nephron Clin Pract **120**(1): c25-c35.

Chapin, H. C. and M. J. Caplan (2010). "The cell biology of polycystic kidney disease." J Cell Biol **191**(4): 701-710.

Chauvet, V., X. Tian, et al. (2004). "Mechanical stimuli induce cleavage and nuclear translocation of the polycystin-1 C terminus." J Clin Invest **114**(10): 1433-1443.

Chen, J., K. Futami, et al. (2008). "Deficiency of FLCN in mouse kidney led to development of polycystic kidneys and renal neoplasia." PLoS ONE **3**(10): e3581.

Cogswell, C., S. J. Price, et al. (2003). "Positional cloning of jcpk/bpk locus of the mouse." Mamm Genome **14**(4): 242-249.

Connacher, A. A., C. C. Forsyth, et al. (1987). "Orofaciodigital syndrome type I associated with polycystic kidneys and agenesis of the corpus callosum." J Med Genet **24**(2): 116-118.

Corbit, K. C., A. E. Shyer, et al. (2008). "Kif3a constrains beta-catenin-dependent Wnt signalling through dual ciliary and non-ciliary mechanisms." Nat Cell Biol **10**(1): 70-76.

Csibi, A., K. Cornille, et al. (2010). "The translation regulatory subunit eIF3f controls the kinase-dependent mTOR signaling required for muscle differentiation and hypertrophy in mouse." PLoS One **5**(2): e8994.

D'Angelo, A. and B. Franco (2009). "The dynamic cilium in human diseases." Pathogenetics **2**(1): 3.

D'Angelo, A. and B. Franco (2011). "The primary cilium in different tissues-lessons from patients and animal models." Pediatr Nephrol **26**(5): 655-662.

Davenport, J. R. and B. K. Yoder (2005). "An incredible decade for the primary cilium: a look at a once-forgotten organelle." Am J Physiol Renal Physiol **289**(6): F1159-1169.

de Conciliis, L., A. Marchitiello, et al. (1998). "Characterization of Cxorf5 (71-7A), a novel human cDNA mapping to Xp22 and encoding a protein containing coiled-coil alpha-helical domains." Genomics **51**(2): 243-250.

Deltas, C. and G. Papagregoriou (2010). "Cystic diseases of the kidney: molecular biology and genetics." Arch Pathol Lab Med **134**(4): 569-582.

Dennis, P. B., A. Jaeschke, et al. (2001). "Mammalian TOR: a homeostatic ATP sensor." Science **294**(5544): 1102-1105.

Dere, R., P. D. Wilson, et al. (2010). "Carboxy terminal tail of polycystin-1 regulates localization of TSC2 to repress mTOR." PLoS One **5**(2): e9239.

DiBella, L. M., A. Park, et al. (2009). "Zebrafish Tsc1 reveals functional interactions between the cilium and the TOR pathway." Hum Mol Genet **18**(4): 595-606.

Distefano, G., M. Boca, et al. (2009). "Polycystin-1 regulates extracellular signal-regulated kinase-dependent phosphorylation of tuberin to control cell size through mTOR and its downstream effectors S6K and 4EBP1." Mol Cell Biol **29**(9): 2359-2371.

Doege, T. C., H. C. Thuline, et al. (1964). "Studies of a Family with the Oral-Facial-Digital Syndrome." N Engl J Med **271**: 1073-1078.

Donaldson, J. C., R. S. Dise, et al. (2002). "Nephrocystin-conserved domains involved in targeting to epithelial cell-cell junctions, interaction with filamins, and establishing cell polarity." J Biol Chem **277**(32): 29028-29035.

Donnai, D., L. Kerzin-Storrar, et al. (1987). "Familial orofaciodigital syndrome type I presenting as adult polycystic kidney disease." J Med Genet **24**(2): 84-87.

Emes, R. D. and C. P. Ponting (2001). "A new sequence motif linking lissencephaly, Treacher Collins and oral-facial-digital type 1 syndromes, microtubule dynamics and cell migration." Hum Mol Genet **10**(24): 2813-2820.

Espeillac, C., C. Mitchell, et al. (2011). "S6 kinase 1 is required for rapamycin-sensitive liver proliferation after mouse hepatectomy." The Journal of clinical investigation **121**(7): 2821-2832.

Feather, S. A., P. J. Winyard, et al. (1997). "Oral-facial-digital syndrome type 1 is another dominant polycystic kidney disease: clinical, radiological and histopathological features of a new kindred." Nephrol Dial Transplant **12**(7): 1354-1361.

Feistel, K. and M. Blum (2006). "Three types of cilia including a novel 9+4 axoneme on the notochordal plate of the rabbit embryo." Dev Dyn **235**(12): 3348-3358.

Ferrante, M. I., A. Barra, et al. (2003). "Characterization of the OFD1/Ofd1 genes on the human and mouse sex chromosomes and exclusion of Ofd1 for the Xpl mouse mutant." Genomics **81**(6): 560-569.

Ferrante, M. I., G. Giorgio, et al. (2001). "Identification of the gene for oral-facial-digital type I syndrome." Am J Hum Genet **68**(3): 569-576.

Ferrante, M. I., L. Romio, et al. (2009). "Convergent extension movements and ciliary function are mediated by ofd1, a zebrafish orthologue of the human oral-facial-digital type 1 syndrome gene." Hum Mol Genet **18**(2): 289-303.

Ferrante, M. I., A. Zullo, et al. (2006). "Oral-facial-digital type I protein is required for primary cilia formation and left-right axis specification." Nat Genet **38**(1): 112-117.

Fischer, D. C., U. Jacoby, et al. (2009). "Activation of the AKT/mTOR pathway in autosomal recessive polycystic kidney disease (ARPKD)." Nephrol Dial Transplant **24**(6): 1819-1827.

Fischer, E., E. Legue, et al. (2006). "Defective planar cell polarity in polycystic kidney disease." Nat Genet **38**(1): 21-23.

Fliegauf, M., J. Horvath, et al. (2006). "Nephrocystin specifically localizes to the transition zone of renal and respiratory cilia and photoreceptor connecting cilia." J Am Soc Nephrol **17**(9): 2424-2433.

Foster, K. G. and D. C. Fingar (2010). "Mammalian target of rapamycin (mTOR): conducting the cellular signaling symphony." The Journal of biological chemistry **285**(19): 14071-14077.

Frank, J. (2003). "Toward an understanding of the structural basis of translation." Genome Biol **4**(12): 237.

Frias, M. A., C. C. Thoreen, et al. (2006). "mSin1 is necessary for Akt/PKB phosphorylation, and its isoforms define three distinct mTORC2s." Curr Biol **16**(18): 1865-1870.

Gedeon, A. K., C. Oley, et al. (1999). "Gene localization for oral-facial-digital syndrome type 1 (OFD1:MIM 311200) proximal to DXS85." Am J Med Genet **82**(4): 352-354.

Gevers, T. J. and J. P. Drenth (2011). "Somatostatin analogues for treatment of polycystic liver disease." Current opinion in gastroenterology **27**(3): 294-300.

Gibson, W. T., J. H. Veldhuis, et al. (2011). "Control of the mitotic cleavage plane by local epithelial topology." Cell **144**(3): 427-438.

Giorgio, G., M. Alfieri, et al. (2007). "Functional characterization of the OFD1 protein reveals a nuclear localization and physical interaction with subunits of a chromatin remodeling Complex." Mol Biol Cell **18**(11): 4397-4404.

Goetz, S. C. and K. V. Anderson (2010). "The primary cilium: a signalling centre during vertebrate development." Nat Rev Genet **11**(5): 331-344.

Gorlin, R. J. (2001). "Asymmetry." Am J Med Genet **101**(4): 290-291.

Gorlin, R. J. and J. Psaume (1962). "Orodigitofacial dysostosis--a new syndrome. A study of 22 cases." J Pediatr **61**: 520-530.

Gresh, L., E. Fischer, et al. (2004). "A transcriptional network in polycystic kidney disease." The EMBO journal **23**(7): 1657-1668.

Guertin, D. A. and D. M. Sabatini (2005). "An expanding role for mTOR in cancer." Trends Mol Med **11**(8): 353-361.

Gulati, P., L. D. Gaspers, et al. (2008). "Amino acids activate mTOR complex 1 via Ca2+/CaM signaling to hVps34." Cell metabolism **7**(5): 456-465.

Gurrieri, F., B. Franco, et al. (2007). "Oral-facial-digital syndromes: review and diagnostic guidelines." Am J Med Genet A **143**(24): 3314-3323.

Hartman, T. R., D. Liu, et al. (2009). "The tuberous sclerosis proteins regulate formation of the primary cilium via a rapamycin-insensitive and polycystin 1-independent pathway." Hum Mol Genet **18**(1): 151-163.

Hasumi, H., M. Baba, et al. (2008). "Identification and characterization of a novel folliculin-interacting protein FNIP2." Gene **415**(1-2): 60-67.

Hasumi, Y., M. Baba, et al. (2009). "Homozygous loss of BHD causes early embryonic lethality and kidney tumor development with activation of mTORC1 and mTORC2." Proc Natl Acad Sci U S A **106**(44): 18722-18727.

Hayashi, A. A. and C. G. Proud (2007). "The rapid activation of protein synthesis by growth hormone requires signaling through mTOR." American journal of physiology. Endocrinology and metabolism **292**(6): E1647-1655.

Hayashi, S. and A. P. McMahon (2002). "Efficient recombination in diverse tissues by a tamoxifen-inducible form of Cre: a tool for temporally regulated gene activation/inactivation in the mouse." Developmental biology **244**(2): 305-318.

He, C. and D. J. Klionsky (2009). "Regulation mechanisms and signaling pathways of autophagy." Annu Rev Genet **43**: 67-93.

Hiesberger, T., Y. Bai, et al. (2004). "Mutation of hepatocyte nuclear factor-1beta inhibits Pkhd1 gene expression and produces renal cysts in mice." J Clin Invest **113**(6): 814-825.

Hildebrandt, F. and E. Otto (2005). "Cilia and centrosomes: a unifying pathogenic concept for cystic kidney disease?" Nat Rev Genet **6**(12): 928-940.

Hirokawa, N., Y. Tanaka, et al. (2009). "Left-right determination: involvement of molecular motor KIF3, cilia, and nodal flow." Cold Spring Harb Perspect Biol **1**(1): a000802.

Holz, M. K., B. A. Ballif, et al. (2005). "mTOR and S6K1 mediate assembly of the translation preinitiation complex through dynamic protein interchange and ordered phosphorylation events." Cell **123**(4): 569-580.

Horsley, V. and G. K. Pavlath (2002). "NFAT: ubiquitous regulator of cell differentiation and adaptation." J Cell Biol **156**(5): 771-774.

Hurd, T. W. and F. Hildebrandt (2011). "Mechanisms of nephronophthisis and related ciliopathies." Nephron Exp Nephrol **118**(1): e9-14.

Ibraghimov-Beskrovnaya, O. (2007). "Targeting dysregulated cell cycle and apoptosis for polycystic kidney disease therapy." Cell Cycle **6**(7): 776-779.

Ichimura, Y. and M. Komatsu (2011). "Pathophysiological role of autophagy: lesson from autophagy-deficient mouse models." Exp Anim **60**(4): 329-345.

Inoki, K., Y. Li, et al. (2002). "TSC2 is phosphorylated and inhibited by Akt and suppresses mTOR signalling." Nat Cell Biol **4**(9): 648-657.

Kim, D. H., D. D. Sarbassov, et al. (2002). "mTOR interacts with raptor to form a nutrient-sensitive complex that signals to the cell growth machinery." Cell **110**(2): 163-175.

Kim, D. H., D. D. Sarbassov, et al. (2003). "GbetaL, a positive regulator of the rapamycin-sensitive pathway required for the nutrient-sensitive interaction between raptor and mTOR." Mol Cell **11**(4): 895-904.

Kim, J., J. E. Lee, et al. (2010). "Functional genomic screen for modulators of ciliogenesis and cilium length." Nature **464**(7291): 1048-1051.

Kruger, M., C. Beger, et al. (2001). "Involvement of proteasome alpha-subunit PSMA7 in hepatitis C virus internal ribosome entry site-mediated translation." Molecular and cellular biology **21**(24): 8357-8364.

Lakso, M., B. Sauer, et al. (1992). "Targeted oncogene activation by site-specific recombination in transgenic mice." Proc Natl Acad Sci U S A **89**(14): 6232-6236.

Lal, M., X. Song, et al. (2008). "Polycystin-1 C-terminal tail associates with beta-catenin and inhibits canonical Wnt signaling." Hum Mol Genet **17**(20): 3105-3117.

Lancaster, M. A. and J. G. Gleeson (2009). "The primary cilium as a cellular signaling center: lessons from disease." Curr Opin Genet Dev **19**(3): 220-229.

Lantinga-van Leeuwen, I. S., W. N. Leonhard, et al. (2007). "Kidney-specific inactivation of the Pkd1 gene induces rapid cyst formation in developing kidneys and a slow onset of disease in adult mice." Human molecular genetics **16**(24): 3188-3196.

Lee, K., L. Battini, et al. (2011). "Cilium, centrosome and cell cycle regulation in polycystic kidney disease." Biochim Biophys Acta **1812**(10): 1263-1271.

Lehman, J. M., E. J. Michaud, et al. (2008). "The Oak Ridge Polycystic Kidney mouse: modeling ciliopathies of mice and men." Dev Dyn **237**(8): 1960-1971.

Lieberthal, W. and J. S. Levine (2009). "The role of the mammalian target of rapamycin (mTOR) in renal disease." J Am Soc Nephrol **20**(12): 2493-2502.

Lin, F., T. Hiesberger, et al. (2003). "Kidney-specific inactivation of the KIF3A subunit of kinesin-II inhibits renal ciliogenesis and produces polycystic kidney disease." Proc Natl Acad Sci U S A **100**(9): 5286-5291.

Ma, L., Z. Chen, et al. (2005). "Phosphorylation and functional inactivation of TSC2 by Erk implications for tuberous sclerosis and cancer pathogenesis." Cell **121**(2): 179-193.

Ma, X. M. and J. Blenis (2009). "Molecular mechanisms of mTOR-mediated translational control." Nat Rev Mol Cell Biol **10**(5): 307-318.

Macca, M. and B. Franco (2009). "The molecular basis of oral-facial-digital syndrome, type 1." Am J Med Genet C Semin Med Genet **151C**(4): 318-325.

Maisonneuve, C., I. Guilleret, et al. (2009). "Bicaudal C, a novel regulator of Dvl signaling abutting RNA-processing bodies, controls cilia orientation and leftward flow." Development **136**(17): 3019-3030.

Maiuri, M. C., E. Zalckvar, et al. (2007). "Self-eating and self-killing: crosstalk between autophagy and apoptosis." Nat Rev Mol Cell Biol **8**(9): 741-752.

Masyuk, T. V., B. N. Radtke, et al. (2011). "Inhibition of Cdc25A Suppresses Hepato-renal Cystogenesis in Rodent Models of Polycystic Kidney and Liver Disease." Gastroenterology.

Mokrzan, E. M., J. S. Lewis, et al. (2007). "Differences in renal tubule primary cilia length in a mouse model of Bardet-Biedl syndrome." Nephron Exp Nephrol **106**(3): e88-96.

Morleo, M. and B. Franco (2008). "Dosage compensation of the mammalian X chromosome influences the phenotypic variability of X-linked dominant male-lethal disorders." J Med Genet **45**(7): 401-408.

Murcia, N. S., W. G. Richards, et al. (2000). "The Oak Ridge Polycystic Kidney (orpk) disease gene is required for left-right axis determination." Development **127**(11): 2347-2355.

Nagy, A. (2000). "Cre recombinase: the universal reagent for genome tailoring." Genesis **26**(2): 99-109.

Nauli, S. M., F. J. Alenghat, et al. (2003). "Polycystins 1 and 2 mediate mechanosensation in the primary cilium of kidney cells." Nat Genet **33**(2): 129-137.

Nigg, E. A. and T. Stearns (2011). "The centrosome cycle: Centriole biogenesis, duplication and inherent asymmetries." Nat Cell Biol **13**(10): 1154-1160.

Nonaka, S., Y. Tanaka, et al. (1998). "Randomization of left-right asymmetry due to loss of nodal cilia generating leftward flow of extraembryonic fluid in mice lacking KIF3B motor protein." Cell **95**(6): 829-837.

Nurnberger, J., R. L. Bacallao, et al. (2002). "Inversin forms a complex with catenins and N-cadherin in polarized epithelial cells." Mol Biol Cell **13**(9): 3096-3106.

Odent, S., B. Le Marec, et al. (1998). "Central nervous system malformations and early end-stage renal disease in oro-facio-digital syndrome type I: a review." Am J Med Genet **75**(4): 389-394.

Okumura, Y., N. Sugiyama, et al. (2009). "ERK regulates renal cell proliferation and renal cyst expansion in inv mutant mice." Acta Histochem Cytochem **42**(2): 39-45.

Papillon, L. and J. Psaume (1954). "[Hereditary abnormality of the buccal mucosa: abnormal bands and frenula]." Revue Stomatol **55**(4): 209-227.

Parnell, S. C., B. S. Magenheimer, et al. (2002). "Polycystin-1 activation of c-Jun N-terminal kinase and AP-1 is mediated by heterotrimeric G proteins." J Biol Chem **277**(22): 19566-19572.

Patel, V., L. Li, et al. (2008). "Acute kidney injury and aberrant planar cell polarity induce cyst formation in mice lacking renal cilia." Hum Mol Genet **17**(11): 1578-1590.

Pazour, G. J., B. L. Dickert, et al. (2000). "Chlamydomonas IFT88 and its mouse homologue, polycystic kidney disease gene tg737, are required for assembly of cilia and flagella." J Cell Biol **151**(3): 709-718.

Pearson, R. D., X. Liu, et al. (2009). "puma: a Bioconductor package for propagating uncertainty in microarray analysis." BMC bioinformatics **10**: 211.

Phillips, C. L., K. J. Miller, et al. (2004). "Renal cysts of inv/inv mice resemble early infantile nephronophthisis." J Am Soc Nephrol **15**(7): 1744-1755.

Piontek, K., L. F. Menezes, et al. (2007). "A critical developmental switch defines the kinetics of kidney cyst formation after loss of Pkd1." Nat Med **13**(12): 1490-1495.

Potter, C. J., H. Huang, et al. (2001). "Drosophila Tsc1 functions with Tsc2 to antagonize insulin signaling in regulating cell growth, cell proliferation, and organ size." Cell **105**(3): 357-368.

Potter, C. J., L. G. Pedraza, et al. (2003). "The tuberous sclerosis complex (TSC) pathway and mechanism of size control." Biochem Soc Trans **31**(Pt 3): 584-586.

Praetorius, H. A. and K. R. Spring (2005). "A physiological view of the primary cilium." Annu Rev Physiol **67**: 515-529.

Prattichizzo, C., M. Macca, et al. (2008). "Mutational spectrum of the oral-facial-digital type I syndrome: a study on a large collection of patients." Hum Mutat **29**(10): 1237-1246.

Proud, C. G. (2002). "Regulation of mammalian translation factors by nutrients." European journal of biochemistry / FEBS **269**(22): 5338-5349.

Quarmby, L. M. and J. D. Parker (2005). "Cilia and the cell cycle?" J Cell Biol **169**(5): 707-710.

Rajawat, Y. S. and I. Bossis (2008). "Autophagy in aging and in neurodegenerative disorders." Hormones (Athens) **7**(1): 46-61.

Rakkolainen, A., S. Ala-Mello, et al. (2002). "Four novel mutations in the OFD1 (Cxorf5) gene in Finnish patients with oral-facial-digital syndrome 1." J Med Genet **39**(4): 292-296.

Rattray, M., X. Liu, et al. (2006). "Propagating uncertainty in microarray data analysis." Briefings in bioinformatics **7**(1): 37-47.

Raught, B., F. Peiretti, et al. (2004). "Phosphorylation of eucaryotic translation initiation factor 4B Ser422 is modulated by S6 kinases." EMBO J **23**(8): 1761-1769.

Riley, B. E., S. E. Kaiser, et al. (2010). "Ubiquitin accumulation in autophagy-deficient mice is dependent on the Nrf2-mediated stress response pathway: a potential role for protein aggregation in autophagic substrate selection." J Cell Biol **191**(3): 537-552.

Romio, L., V. Wright, et al. (2003). "OFD1, the gene mutated in oral-facial-digital syndrome type 1, is expressed in the metanephros and in human embryonic renal mesenchymal cells." J Am Soc Nephrol **14**(3): 680-689.

Sabers, C. J., M. M. Martin, et al. (1995). "Isolation of a protein target of the FKBP12-rapamycin complex in mammalian cells." J Biol Chem **270**(2): 815-822.

Salinas, C. F., G. S. Pai, et al. (1991). "Variability of expression of the orofaciodigital syndrome type I in black females: six cases." Am J Med Genet **38**(4): 574-582.

Sarbassov, D. D., S. M. Ali, et al. (2004). "Rictor, a novel binding partner of mTOR, defines a rapamycin-insensitive and raptor-independent pathway that regulates the cytoskeleton." Curr Biol **14**(14): 1296-1302.

Sarbassov, D. D., D. A. Guertin, et al. (2005). "Phosphorylation and regulation of Akt/PKB by the rictor-mTOR complex." Science **307**(5712): 1098-1101.

Satir, P. and S. T. Christensen (2007). "Overview of structure and function of mammalian cilia." Annu Rev Physiol **69**: 377-400.

Satir, P., L. B. Pedersen, et al. (2010). "The primary cilium at a glance." J Cell Sci **123**(Pt 4): 499-503.

Schalm, S. S., D. C. Fingar, et al. (2003). "TOS motif-mediated raptor binding regulates 4E-BP1 multisite phosphorylation and function." Curr Biol **13**(10): 797-806.

Scolari, F., B. Valzorio, et al. (1997). "Oral-facial-digital syndrome type I: an unusual cause of hereditary cystic kidney disease." Nephrol Dial Transplant **12**(6): 1247-1250.

Seeley, E. S. and M. V. Nachury (2010). "The perennial organelle: assembly and disassembly of the primary cilium." J Cell Sci **123**(Pt 4): 511-518.

Serra, A. L., A. D. Kistler, et al. (2009). "Safety and tolerability of sirolimus treatment in patients with autosomal dominant polycystic kidney disease." Nephrology, dialysis, transplantation : official publication of the European Dialysis and Transplant Association - European Renal Association **24**(11): 3334-3342.

Serra, A. L., A. D. Kistler, et al. (2007). "Clinical proof-of-concept trial to assess the therapeutic effect of sirolimus in patients with autosomal dominant polycystic kidney disease: SUISSE ADPKD study." BMC Nephrol **8**: 13.

Shahbazian, D., P. P. Roux, et al. (2006). "The mTOR/PI3K and MAPK pathways converge on eIF4B to control its phosphorylation and activity." EMBO J **25**(12): 2781-2791.

Shao, X., S. Somlo, et al. (2002). "Epithelial-specific Cre/lox recombination in the developing kidney and genitourinary tract." J Am Soc Nephrol **13**(7): 1837-1846.

Shaulian, E. and M. Karin (2002). "AP-1 as a regulator of cell life and death." Nat Cell Biol **4**(5): E131-136.

Shibazaki, S., Z. Yu, et al. (2008). "Cyst formation and activation of the extracellular regulated kinase pathway after kidney specific inactivation of Pkd1." Human molecular genetics **17**(11): 1505-1516.

Shillingford, J. M., N. S. Murcia, et al. (2006). "The mTOR pathway is regulated by polycystin-1, and its inhibition reverses renal cystogenesis in polycystic kidney disease." Proc Natl Acad Sci U S A **103**(14): 5466-5471.

Shillingford, J. M., K. B. Piontek, et al. (2010). "Rapamycin ameliorates PKD resulting from conditional inactivation of Pkd1." J Am Soc Nephrol **21**(3): 489-497.

Simons, M., J. Gloy, et al. (2005). "Inversin, the gene product mutated in nephronophthisis type II, functions as a molecular switch between Wnt signaling pathways." Nat Genet **37**(5): 537-543.

Singla, V., M. Romaguera-Ros, et al. (2010). "Ofd1, a human disease gene, regulates the length and distal structure of centrioles." Dev Cell **18**(3): 410-424.

Sonenberg, N. and A. Pause (2006). "Signal transduction. Protein synthesis and oncogenesis meet again." Science **314**(5798): 428-429.

Stapleton, F. B., J. Bernstein, et al. (1982). "Cystic kidneys in a patient with oral-facial-digital syndrome type I." Am J Kidney Dis **1**(5): 288-293.

Stolc, V., M. P. Samanta, et al. (2005). "Genome-wide transcriptional analysis of flagellar regeneration in Chlamydomonas reinhardtii identifies orthologs of ciliary disease genes." Proc Natl Acad Sci U S A **102**(10): 3703-3707.

Tao, Y., J. Kim, et al. (2005). "Rapamycin markedly slows disease progression in a rat model of polycystic kidney disease." J Am Soc Nephrol **16**(1): 46-51.

Taulman, P. D., C. J. Haycraft, et al. (2001). "Polaris, a protein involved in left-right axis patterning, localizes to basal bodies and cilia." Mol Biol Cell **12**(3): 589-599.

Terryn, S., A. Ho, et al. (2011). "Fluid transport and cystogenesis in autosomal dominant polycystic kidney disease." Biochim Biophys Acta **1812**(10): 1314-1321.

Thauvin-Robinet, C., M. Cossee, et al. (2006). "Clinical, molecular, and genotype-phenotype correlation studies from 25 cases of oral-facial-digital syndrome type 1: a French and Belgian collaborative study." J Med Genet **43**(1): 54-61.

Thornton, S., N. Anand, et al. (2003). "Not just for housekeeping: protein initiation and elongation factors in cell growth and tumorigenesis." J Mol Med (Berl) **81**(9): 536-548.

Tokunaga, C., K. Yoshino, et al. (2004). "mTOR integrates amino acid- and energy-sensing pathways." Biochem Biophys Res Commun **313**(2): 443-446.

Toprak, O., A. Uzum, et al. (2006). "Oral-facial-digital syndrome type 1, Caroli's disease and cystic renal disease." Nephrology, dialysis, transplantation : official publication of the European Dialysis and Transplant Association - European Renal Association **21**(6): 1705-1709.

Toriello, H. V. (1993). "Oral-facial-digital syndromes, 1992." Clin Dysmorphol **2**(2): 95-105.

Van Der Kelen, K., R. Beyaert, et al. (2009). "Translational control of eukaryotic gene expression." Crit Rev Biochem Mol Biol **44**(4): 143-168.

Wahl, P. R., A. L. Serra, et al. (2006). "Inhibition of mTOR with sirolimus slows disease progression in Han:SPRD rats with autosomal dominant polycystic kidney disease (ADPKD)." Nephrol Dial Transplant **21**(3): 598-604.

Wahrman, J., M. Berant, et al. (1966). "The oral-facial-digital syndrome: a male-lethal condition in a boy with 47/xxy chromosomes." Pediatrics **37**(5): 812-821.

Walz, G., K. Budde, et al. (2010). "Everolimus in patients with autosomal dominant polycystic kidney disease." The New England journal of medicine **363**(9): 830-840.

Ward, C. J., D. Yuan, et al. (2003). "Cellular and subcellular localization of the ARPKD protein; fibrocystin is expressed on primary cilia." Hum Mol Genet **12**(20): 2703-2710.

Waters, A. M. and P. L. Beales (2011). "Ciliopathies: an expanding disease spectrum." Pediatr Nephrol **26**(7): 1039-1056.

Watkins, S. J. and C. J. Norbury (2004). "Cell cycle-related variation in subcellular localization of eIF3e/INT6 in human fibroblasts." Cell proliferation **37**(2): 149-160.

Watnick, T. and G. Germino (2003). "From cilia to cyst." Nat Genet **34**(4): 355-356.

Wettke-Schafer, R. and G. Kantner (1983). "X-linked dominant inherited diseases with lethality in hemizygous males." Hum Genet **64**(1): 1-23.

Wilson, P. D. (2004). "Polycystic kidney disease: new understanding in the pathogenesis." Int J Biochem Cell Biol **36**(10): 1868-1873.

Wilson, P. D. (2008). "Mouse models of polycystic kidney disease." Curr Top Dev Biol **84**: 311-350.

Winyard, P. and D. Jenkins (2011). "Putative roles of cilia in polycystic kidney disease." Biochim Biophys Acta **1812**(10): 1256-1262.

Wu, M., A. Arcaro, et al. (2009). "Pulse mTOR inhibitor treatment effectively controls cyst growth but leads to severe parenchymal and glomerular hypertrophy in rat polycystic kidney disease." Am J Physiol Renal Physiol **297**(6): F1597-1605.

Yoder, B. K. (2007). "Role of primary cilia in the pathogenesis of polycystic kidney disease." J Am Soc Nephrol **18**(5): 1381-1388.

Yoder, B. K., A. Tousson, et al. (2002). "Polaris, a protein disrupted in orpk mutant mice, is required for assembly of renal cilium." Am J Physiol Renal Physiol **282**(3): F541-552.

Zafar, I., F. A. Belibi, et al. (2009). "Long-term rapamycin therapy in the Han:SPRD rat model of polycystic kidney disease (PKD)." Nephrol Dial Transplant **24**(8): 2349-2353.

Zafar, I., K. Ravichandran, et al. (2010). "Sirolimus attenuates disease progression in an orthologous mouse model of human autosomal dominant polycystic kidney disease." Kidney Int **78**(8): 754-761.

Zhou, J. (2009). "Polycystins and primary cilia: primers for cell cycle progression." Annu Rev Physiol **71**: 83-113.

Zhou, J., J. Brugarolas, et al. (2009). "Loss of Tsc1, but not Pten, in renal tubular cells causes polycystic kidney disease by activating mTORC1." Hum Mol Genet **18**(22): 4428-4441.

Zullo, A., D. Iaconis, et al. (2010). "Kidney-specific inactivation of Ofd1 leads to renal cystic disease associated with upregulation of the mTOR pathway." Human molecular genetics **19**(14): 2792-2803.

FIGURE

TABLE I. The Clinical Spectrum in Oral–Facial–Digital Syndrome Type 1

Clinical features	Published cases with mutations in % (n)
Craniofacial	87.30% (110/126)
Abnormal hair/alopecia	21.5% (29/135)
Milia	29.4% (37/126)
Facial dysmorphism	69.1% (87/126)
Cleft lip/pseudocleft of the upper lip	32.6% (44/135)
Oral	96.8% (122/126)
Tongue anomalies	84.1% (106/126)
Oral frenula	63.7% (86/135)
Alveolar ridge clefting	22.2% (28/126)
Cleft palate/high arched palate	49.6% (67/135)
Teeth abnormalities	43.3% (58/134)
Skeletal	88.1% (111/126)
Forelimb	83.3% (105/126)
Hindlimb	44.4% (56/126)
Brachydactyly	63.7% (86/135)
Clinodactyly	47.4% (64/135)
Syndactyly	49.6% (67/135)
Polydactyly preaxial	19.3% (26/135)
Polydactyly postaxial	3.7% (5/135)
Kidneys	
Cystic kidney disease	37.3% (50/134)
Neurologic	
Central nervous system (CNS) involvement[a]	48.4% (61/126)
Mental retardation (MR)	28.9% (39/135)

The total no. of cases for each category was determined according to the available information. No. 135 includes all patients described in [Ferrante et al., 2001; Rakkolainen et al., 2002; Romio et al., 2003; Morisawa et al., 2004; Thauvin-Robinet et al., 2006, 2009; Prattichizzo et al., 2008]. No. 126 includes the same patients with the exception of those described in [Thauvin-Robinet et al., 2009]. No. 134 include all cases but 1 described in [Thauvin-Robinet et al., 2009] for which no information was available for that specific clinical feature. Index cases as well as affected relatives carrying the mutation were considered.

[a]Includes mental retardation (MR)/selective cognitive impairment and/or CNS malformations.

Table I. The clinical spectrum in OFD type I syndrome from (Macca and Franco 2009)

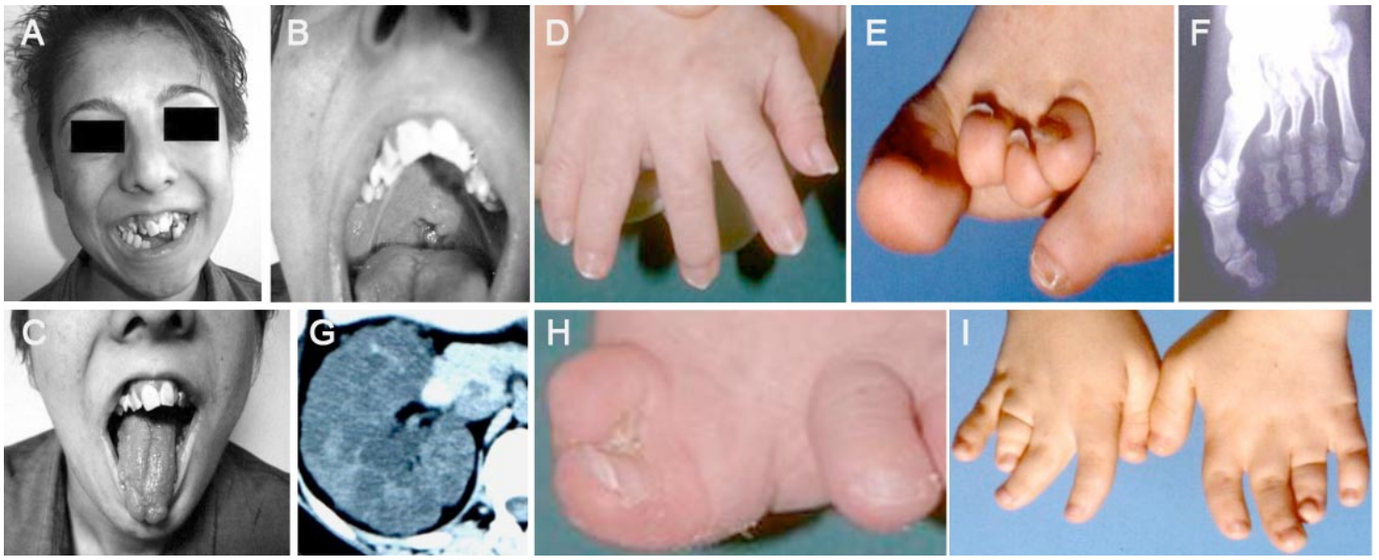

Figure 1. Clinical signs of OFDI syndrome. (A) Peculiar face of the patient and tooth abnormalities, (B) cleft palate, (C) lobulated tongue, (D) clinodactyly, (E and F) Brachydactyly, (G) Cystic kidney, (H) Hallux duplication, (I) Brachydactyly and syndactyly. (modified from (Toprak, Uzum et al. 2006); (Macca and Franco 2009)).

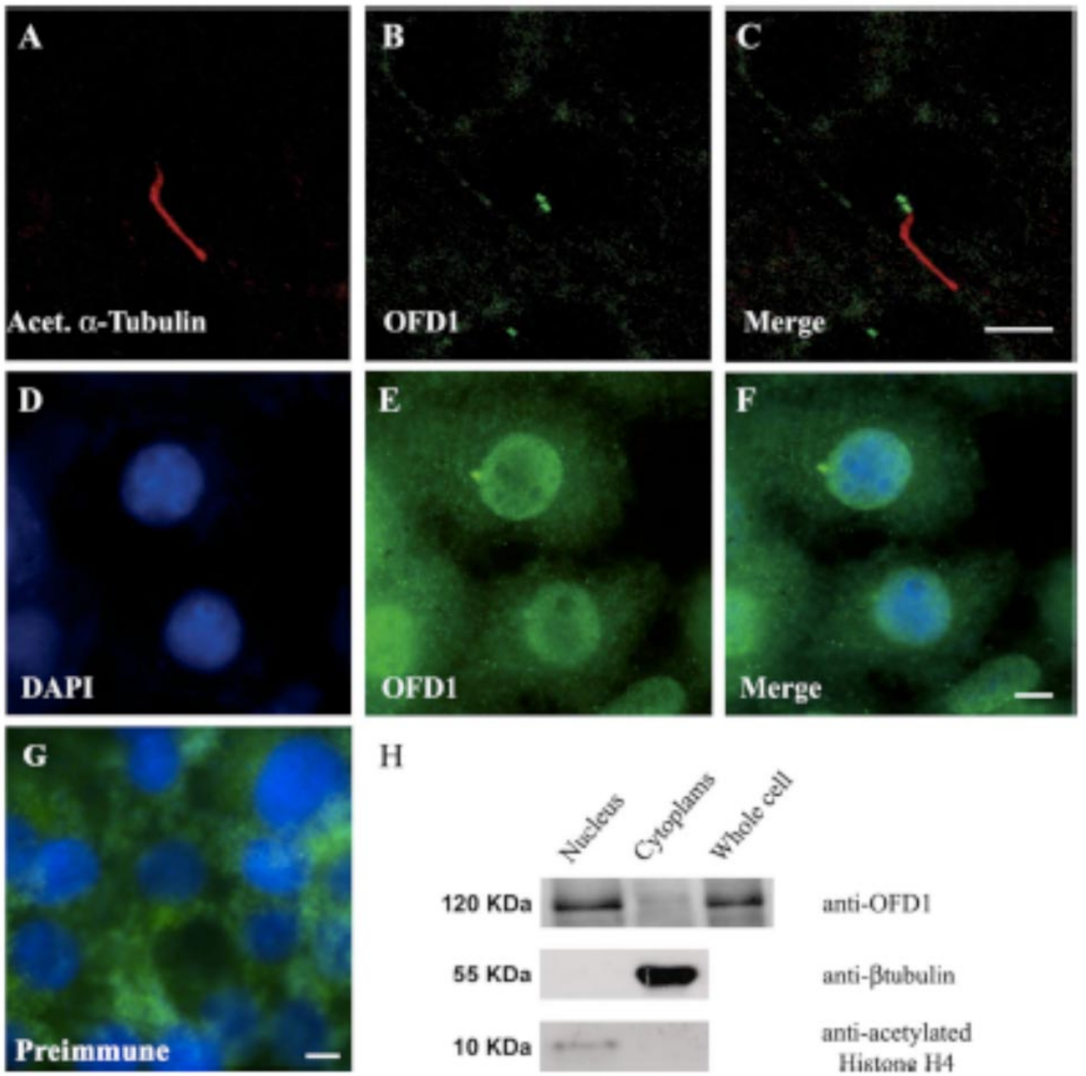

Figure 2. Subcellular localization of the endogenous OFD1 protein. Localization at primary cilium was investigated by confocal microscopy in MDCK cells. (A) Staining with the anti-acetylated-tubulin. (B) Staining with the anti-OFD1 antibody. OFD1 localizes at the basal body of the primary cilium as the merge in C shows. In Cos-7 cells studied by immunofluorescence microscopy, the anti-OFD1 detects also a diffuse signal in the nucleoplasm (E), which disappears when using the preimmune (G). Nuclei are stained with DAPI (D). (H) Nuclear and cytoplasmic fractions from whole Cos-7 cell extracts. Immunoblotting with anti-OFD1 Cter antibody shows that the endogenous OFD1 is present in both cellular compartments. The same amount of protein from the two compartments and from whole cell was loaded. To verify the purity of the extracts, the samples were immunoblotted with anti- βtubulin and anti-acetyl-Hystone H4 (Giorgio, Alfieri et al. 2007).

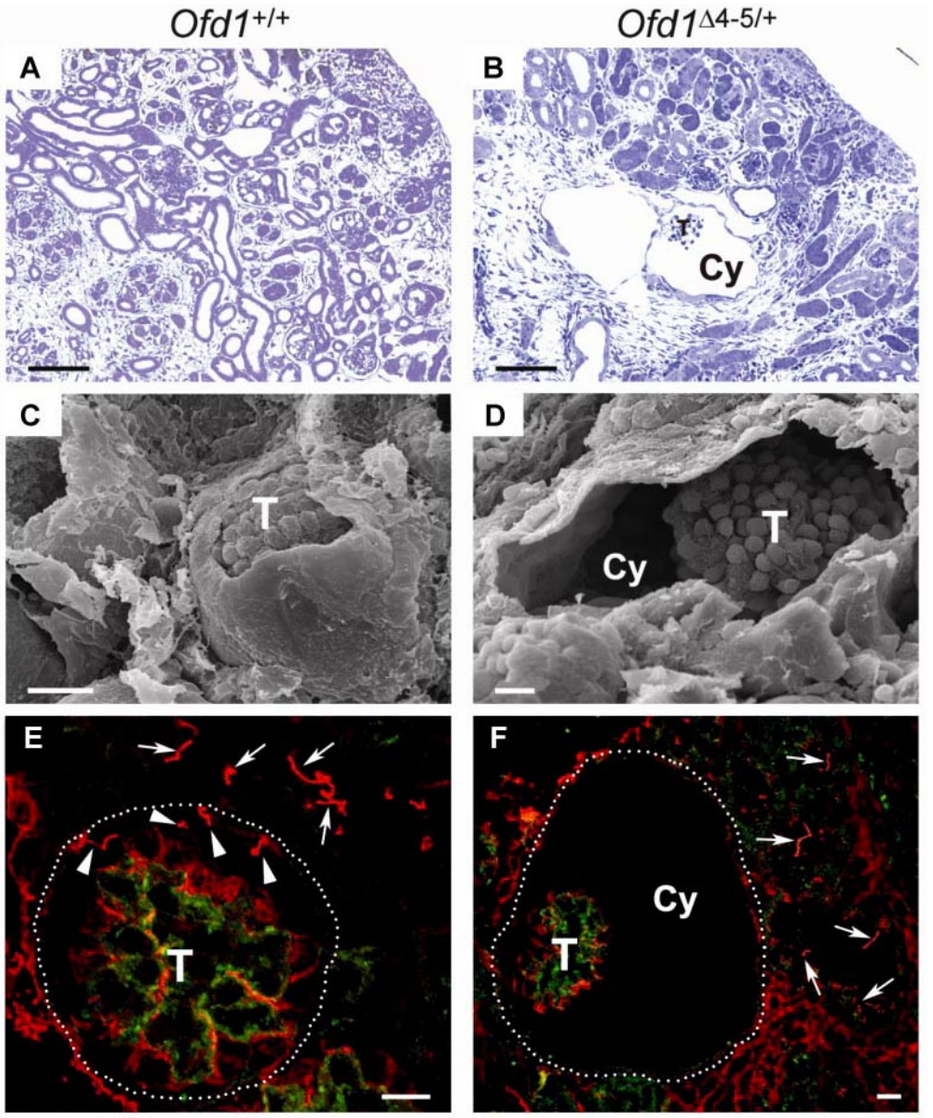

Figure 3. Analysis of the cortical region of the kidneys of wild-type and *Ofd1*$^{\Delta 4/5/+}$ mutant animals at P0. (A and B) Kidney semithin sections of a P0 wild-type mouse (A) and an *Ofd1*$^{\Delta 4/5/+}$ female mouse (B) stained with toluidine blue. In both specimens, the nephrogenic zone is normal; in the mutant, glomerular cysts are observed. Cy, glomerular cyst; T, tuft. Scale bars, 100 mm. (C and D) Scanning electron micrographs show normal glomeruli in a wild-type mouse (C) and a cystic glomerulus in the mutant mouse (D). Scale bars, 10 μm. (E and F) Kidney sections were immunostained with antibody against acetylated tubulin (red) marking ciliary axonemes and with a ZO1 antibody (green) to the tight junctions. Arrowheads indicate primary cilia in the wild-type glomerulus (E), and arrows indicate primary cilia in the tubuli of a wild-type (E) and a mutant (F) mouse. No cilia were observed on the surface of epithelial cells lining the cyst in the mutant mouse (F). Wild-type and cystic glomeruli are outlined with dotted line. Scale bars, 10 μm (Ferrante, Zullo et al. 2006).

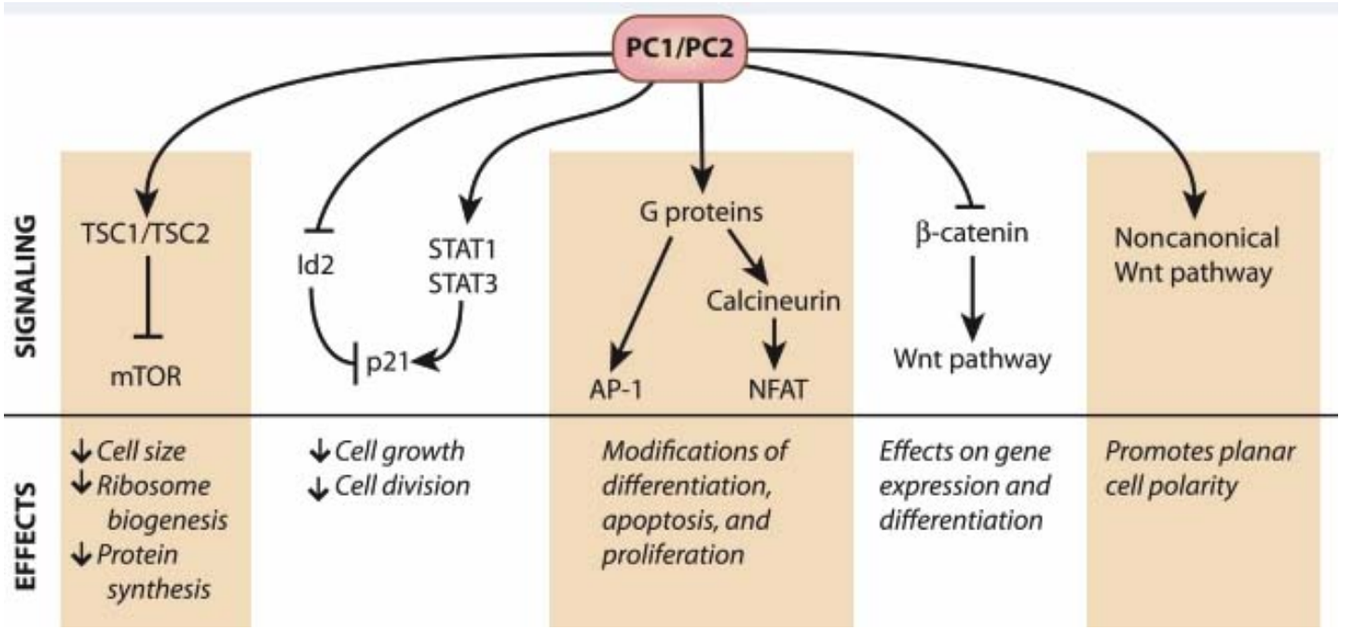

Figure 4. Pc1 and Pc2 affect multiple signaling pathways. Summary of the effects that Pc1 and Pc2 exert on pathways. Multiple direct and indirect interactions allow the polycystin proteins to inhibit or stimulate pathways involved in cellular growth and differentiation (Chapin and Caplan 2010).

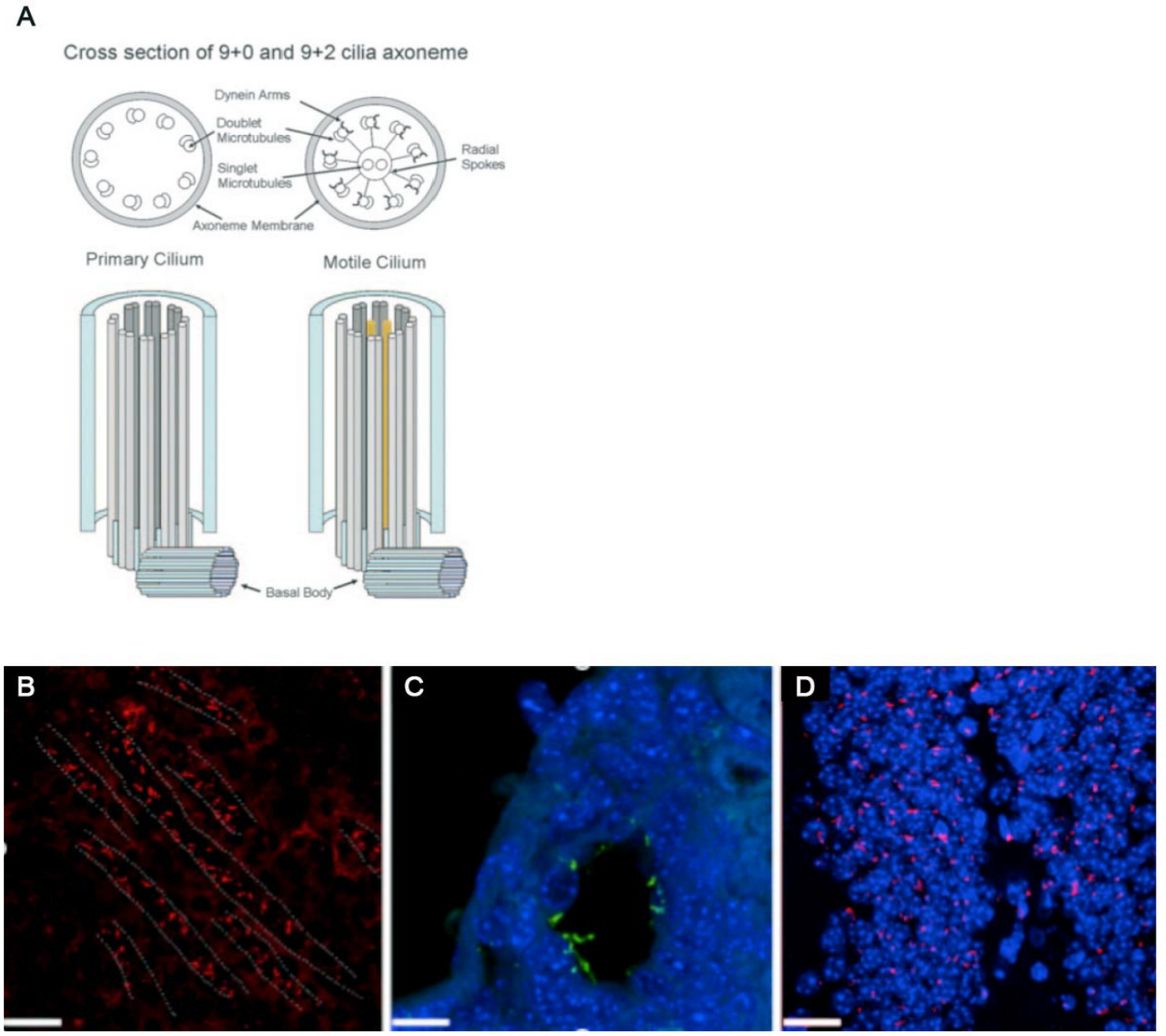

Figure 5. The primary cilium. (A) Motile or immotile (primary) cilia. Structural differences determine the motility of a cilium. Motile cilia (*right*) consist of 9 doublet microtubules surrounding 2 inner singlet microtubules used to conduct force. Primary cilia (*left*) are lacking both singlet microtubules and dynein arms (from Davenport and Yoder, 2005). (B-D) Primary cilia in different tissues. (B) Primary cilia in the renal tubules of a mouse at P7 stained with anti-acetylated α tubulin (red); dashed lines indicate the shape of the tubules. (C) Primary cilia in a bile duct of an adult murine liver (1 month old) stained with anti-acetylated α tubulin (green); nuclei were stained with 4′-6-diamidino-2-phenylindole (DAPI). (D) Primary cilia in the dentate gyrus of an adult murine hippocampus (3 months old) stained with anti-acetylated α tubulin (red); nuclei were stained with DAPI. Scale bars: 10 μm (D'Angelo and Franco 2011).

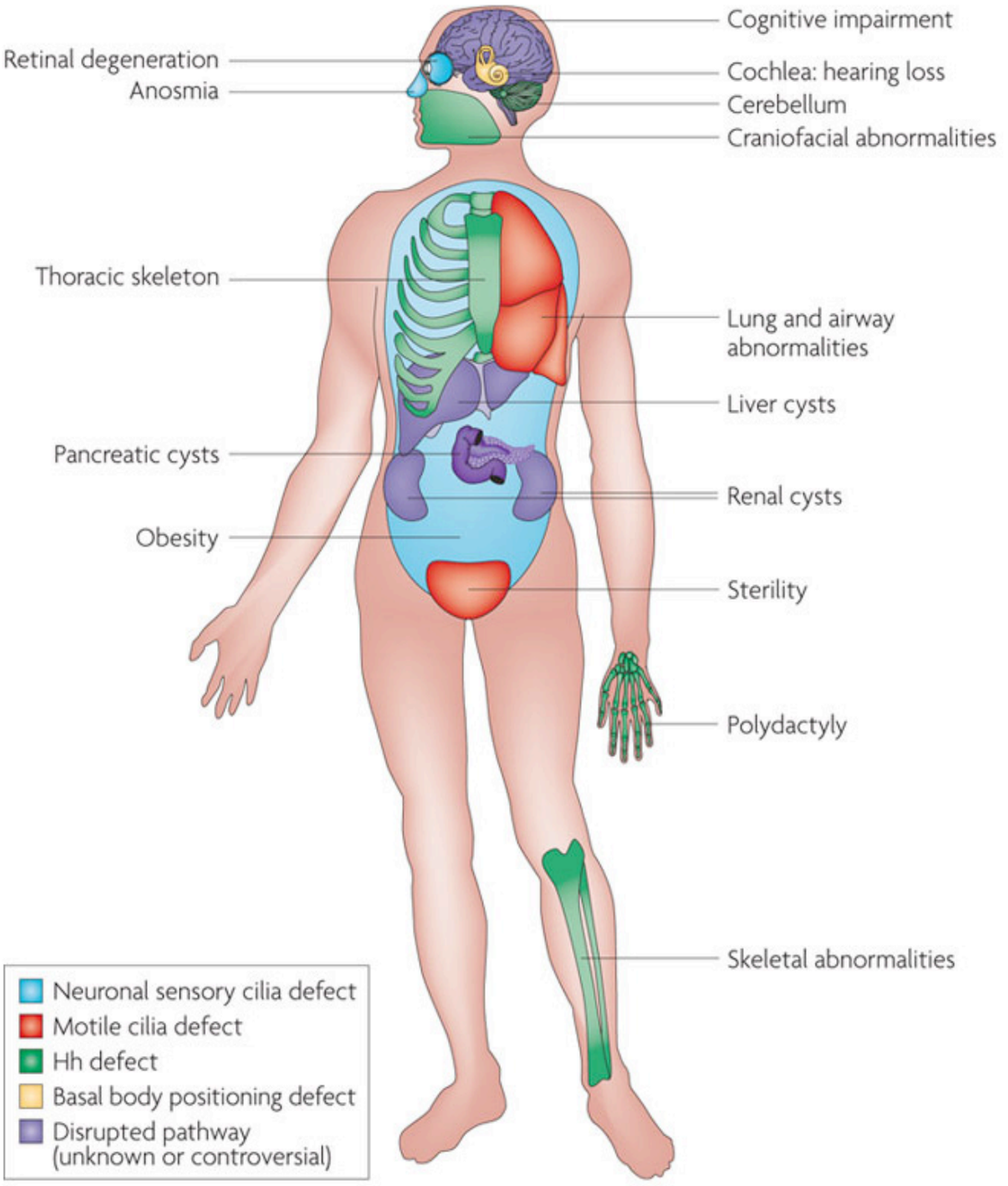

Figure 6. Phenotypic Consequences of ciliary dysfunction. In the figure all the organs and tissues commonly affected in ciliopathies are indicated (Goetz and Anderson 2010).

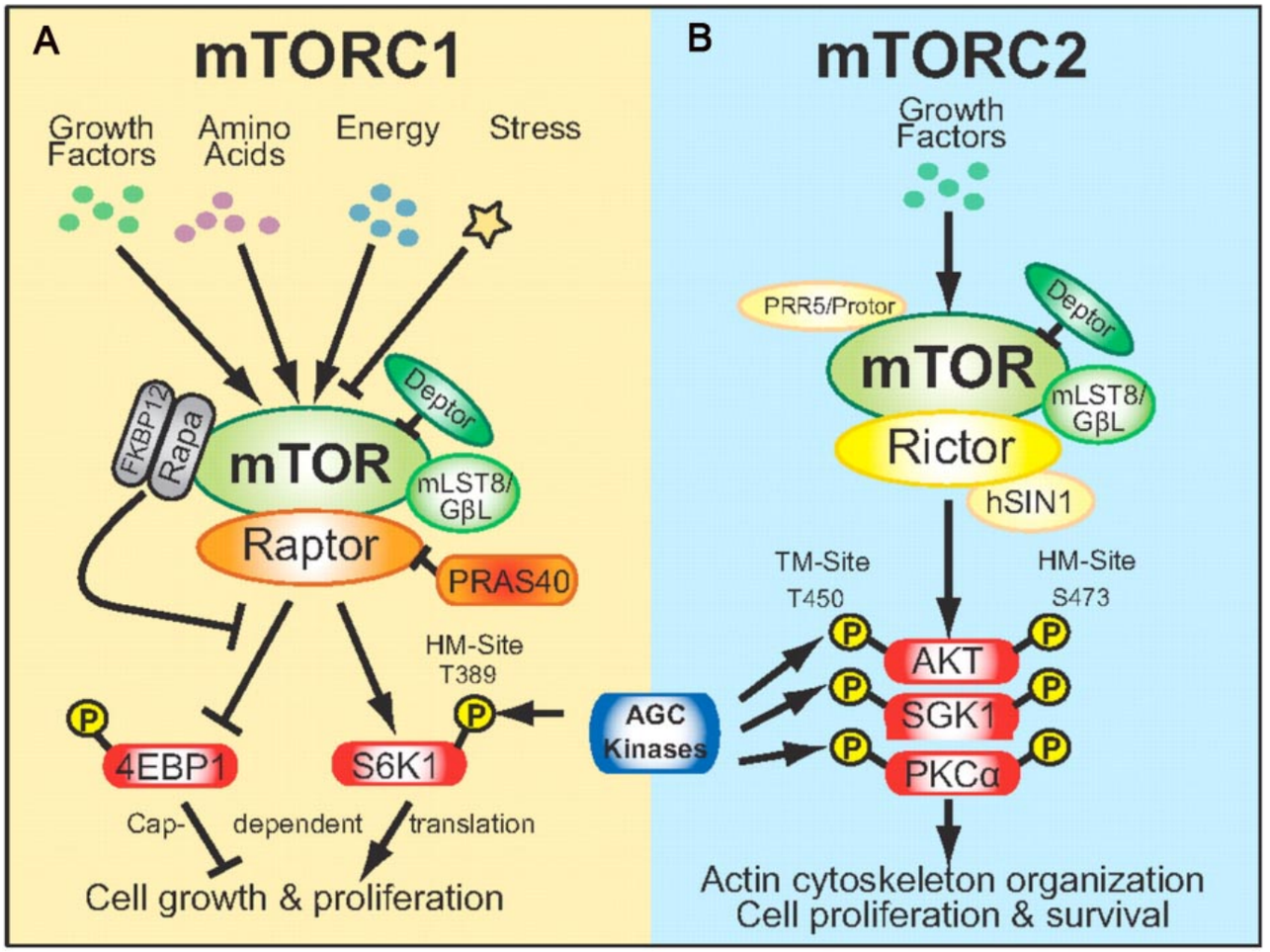

Figure 7. mTORC1 *versus* mTORC2. Distinct rapamycin sensitivities, partner proteins, substrates, and cellular functions distinguish the two known mTOR signaling complexes, mTORC1 (A) and mTORC2 (B) (Foster and Fingar 2010).

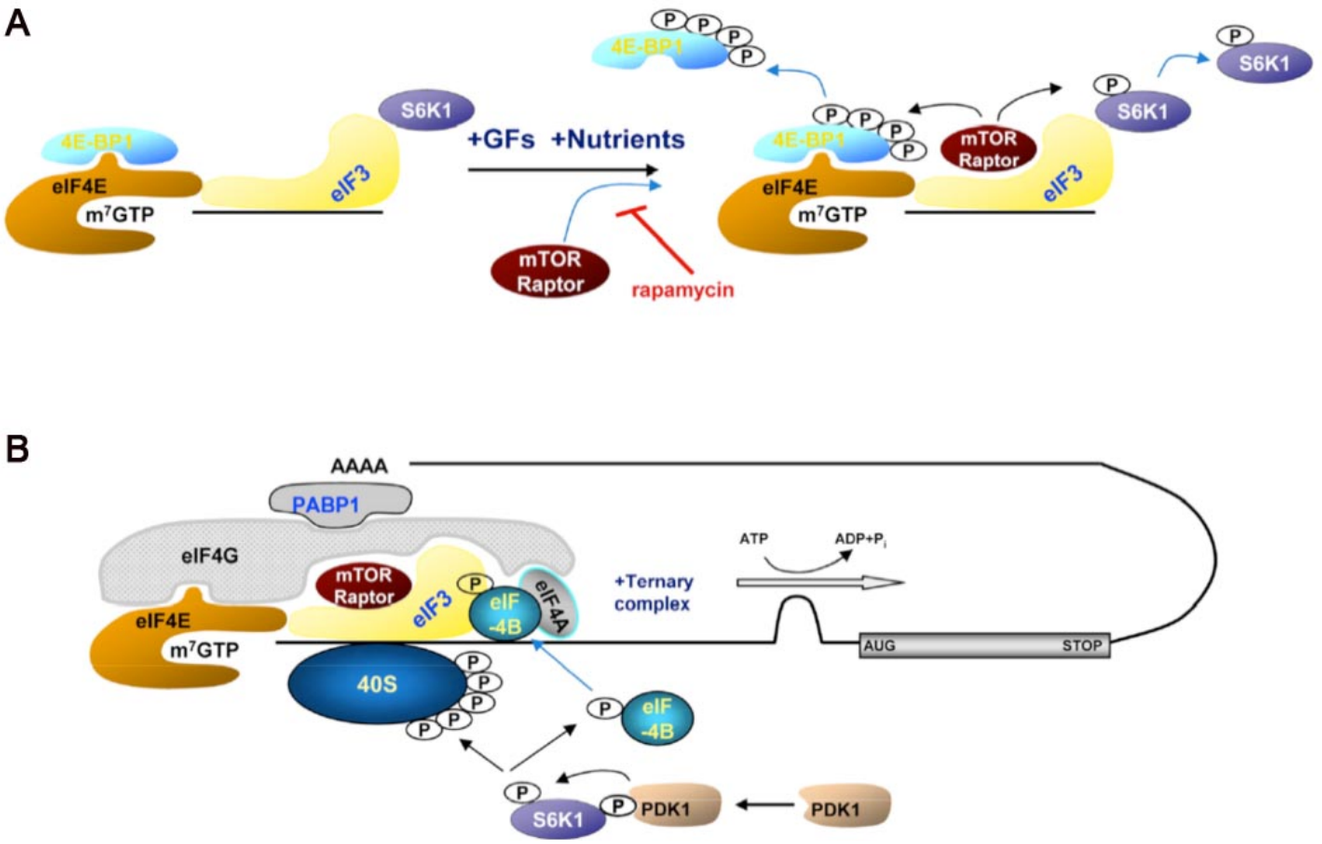

Figure 8. Model of Dynamic Interaction between the eIF3 Complex and mTOR/Raptor, S6K1, and eIF4B. Under basal conditions, S6K1 is associated with the eIF3 complex. Upon mitogen stimulation, an activation complex is formed in which mTOR/raptor is recruited to the eIF3 complex and phosphorylates S6K1 and 4E-BP1. Phosphorylation of S6K1 at T389 leads to its dissociation from the eIF3 complex (A). T389-phosphorylated S6K1 then binds to PDK1, which phosphorylates S6K1 at T229. The fully activated S6K1 then phosphorylates eIF4B and S6 (B). Phosphorylation of eIF4B at S422 promotes its association with the translation preinitiation complex. Concurrently, mTOR/raptor phosphorylates 4E-BP1 (A), which dissociates from the cap complex, allowing recruitment of the eIF4G scaffold to the cap bound eIF4E as part of the eIF4F translation initiation complex (B). This sequence of events leads to preinitiation-complex assembly and initiation of protein translation (Holz, Ballif et al. 2005).

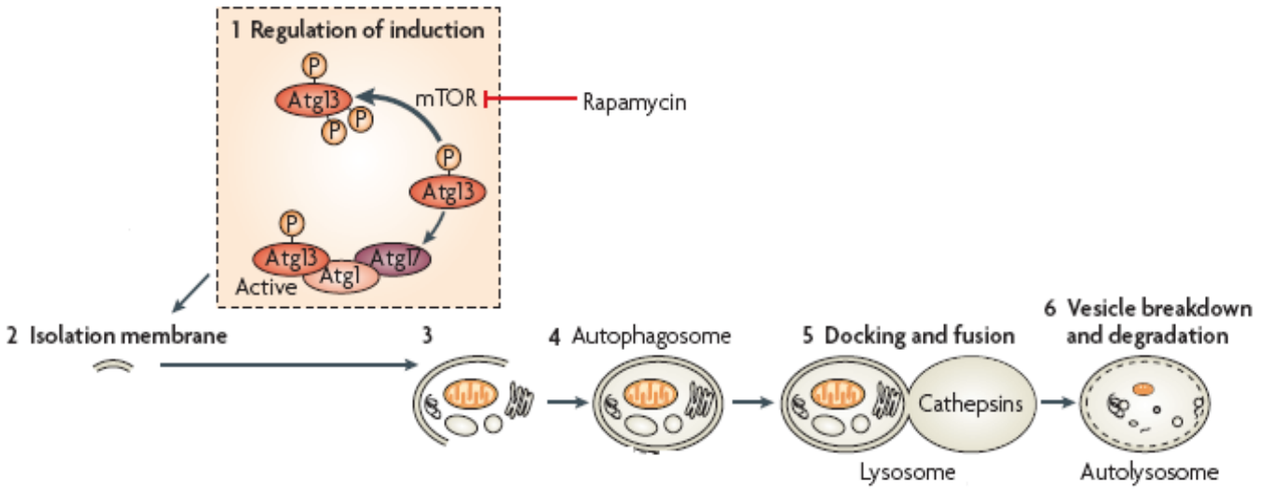

Figure 9. Autophagy process. The mTOR pathway controls the first steps of autophagy induction and membrane recruitment (steps 1 and 2). Membranes elongate to form vescicles (step 3) and extremities fuse to complete the double-membrane structure called autophagosome (step 4). The next critical step is transport and fusion of the autophagosome with the lysosomes (step 5). The last step in the autophagic process is the degradation of the autophagic body content by lysosomal enzymes, which ensures recycling of essential cytoplasmic contents (step 6) (Maiuri, Zalckvar et al. 2007).

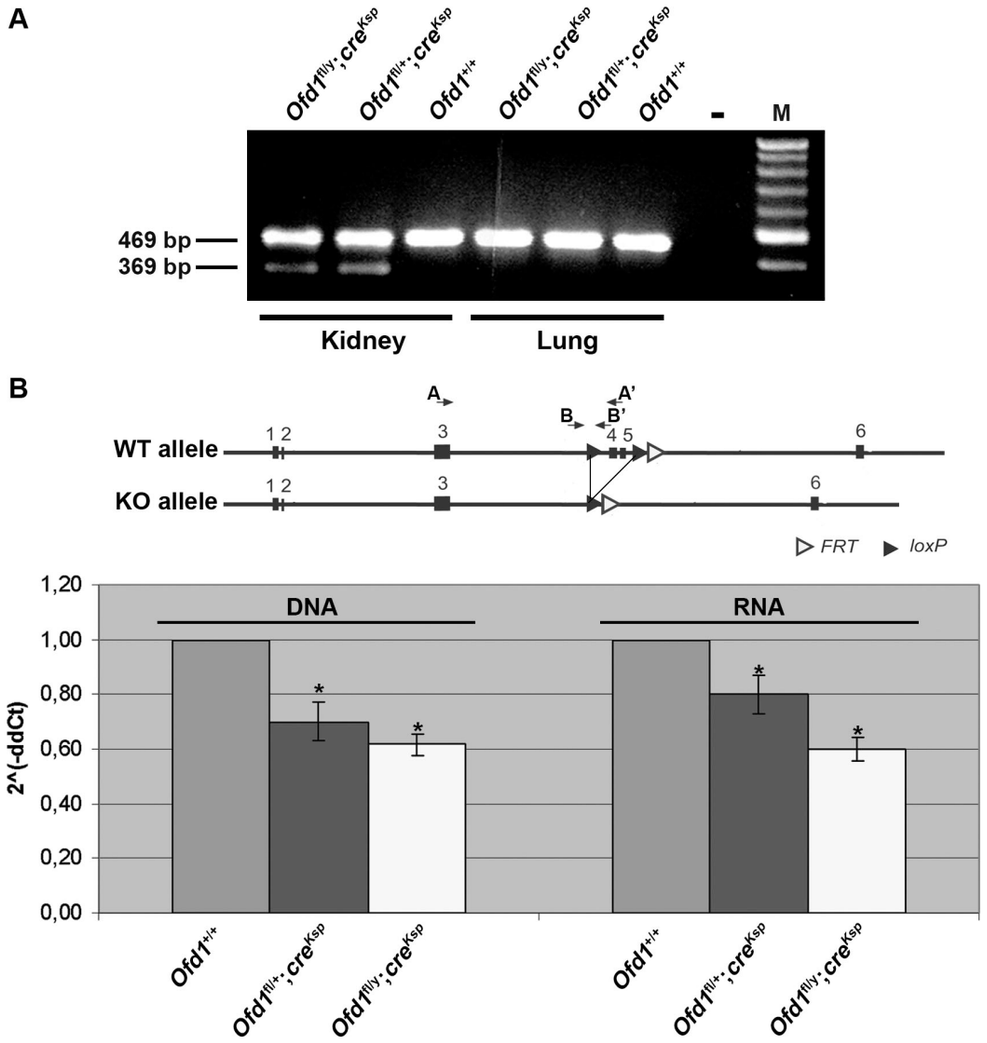

Figure 10. *Ofd1* inactivation in *Ofd1^{fl};cre^{Ksp}* (*Ksp)* mutant animals. (A) RT–PCR analysis showed the presence of the mutant *Ofd1$^{\Delta 4\text{-}5}$* allele (369 bp) only in the kidney of *Ofd1$^{fl/y}$;cre^{Ksp}* and *Ofd1$^{fl/+}$;cre^{Ksp}* mutant animals. The mutated allele is absent in the lung of mutants and in the kidney and lung of WT (*Ofd1$^{+/+}$*) mice. All samples showed the presence of the WT allele (469 bp). No amplification was observed in the negative control. M = marker. (B) Quantitative RT–PCR with primers that specifically amplified the WT Ofd1 allele on genomic DNA (primers A and A′) and on RNA (primers B and B′). The position of the primers is displayed in the upper scheme. The analysis was performed on genomic DNA and RNA from kidneys of conditional mutants (*Ofd1$^{fl/y}$;cre^{Ksp}*, *Ofd1$^{fl/+}$;cre^{Ksp}*) and controls (*Ofd1$^{+/+}$*). Significant differences between mutants and controls and were analyzed by Student's t-test (*p-value*=0.05) are indicated (asterisk). Error bars represent standard error of the mean (Zullo, Iaconis et al. 2010).

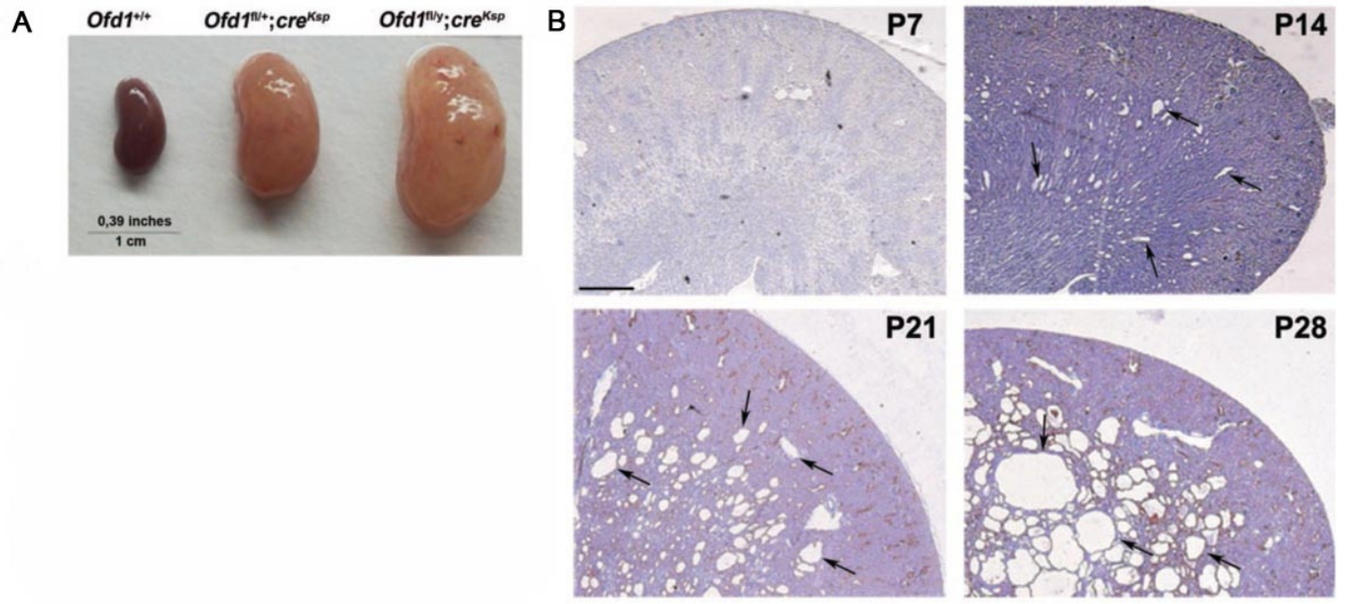

Figure 11. Characterization of *Ofd1^{fl};cre^{Ksp}* (*Ksp)* mutant animals. (A) Gross appearance of kidneys from *Ofd1$^{+/+}$* (left), *Ofd1$^{fl/+}$;cre^{Ksp}* (center) and *Ofd1$^{fl/y}$;cre^{Ksp}* (right) mice at P70. (B) Hematoxylin/eosin staining of kidneys sections from *Ofd1$^{fl/y}$;cre^{Ksp}* mutants at different stages. At P7, no cysts are visible. Dilated tubules appeared at P14 and cysts (black arrows), rapidly increased in size and number. Bar=500 mm (Zullo, Iaconis et al. 2010).

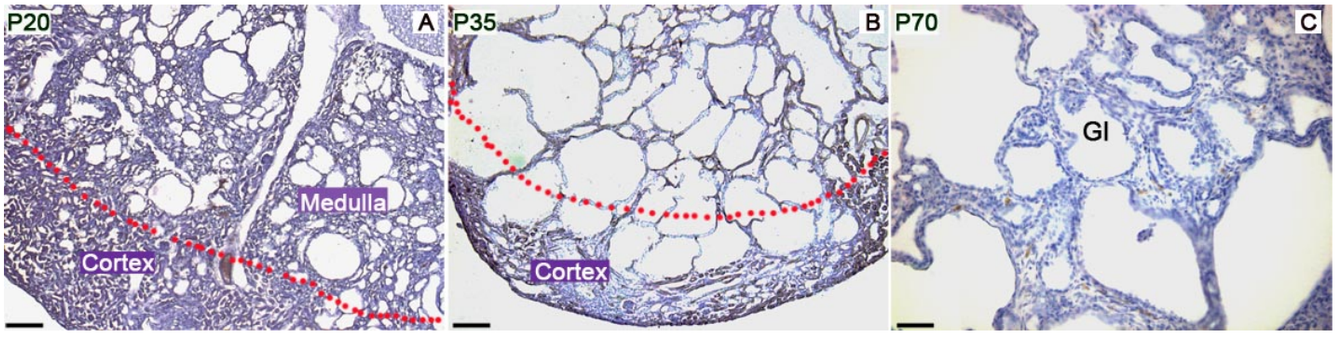

Figure 12. Cysts progression in *Ofd1^{fl};cre^{Ksp}* (*Ksp)* mutants. Hematoxylin/eosin staining of kidney sections from mice at P20 (A) P35 (B) and P70 (C). (A) Cysts were confined to the medulla of the kidney at P20, while no cysts appeared in the cortex. (B) By P35, cysts appear in the kidney cortex and we observed a massive replacement of the renal parenchyma by cysts. (C) Glomerular cysts (Gl) starts to develop in *Ksp* mutants at P70. Bar=50 μm.

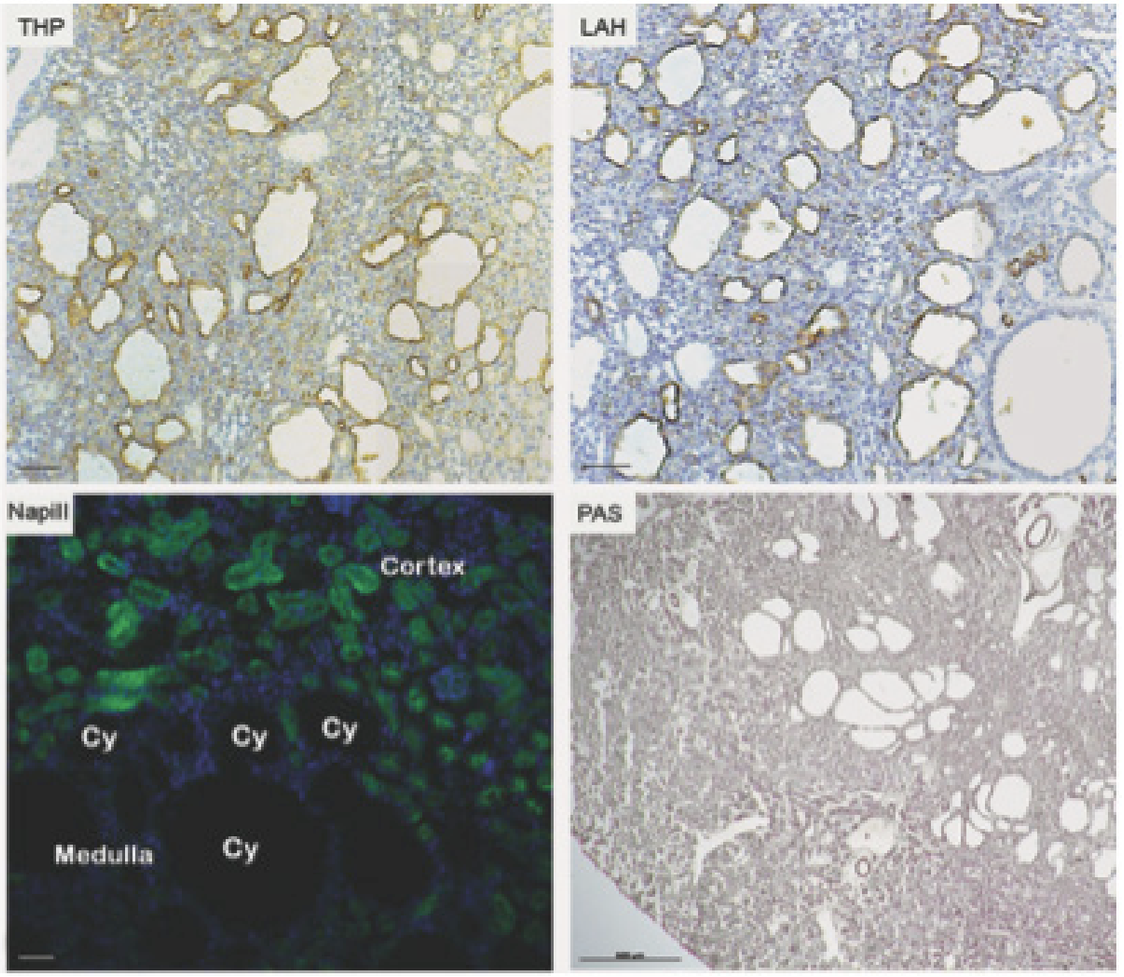

Figure 13. Cysts origin in *Ofd1*$^{fl/y}$;*cre*^{Ksp} (*Ksp*) mutant animals. Kidneys from *Ofd1*$^{fl/y}$;*cre*^{Ksp} mutants at P21 were stained for Tamm–Horsfall protein (THP), Arachis Hypogaea Lectin (LAH) and Na-PiII cotransporter (green, NaPiII). The cysts were positive for THP and LAH, thus indicating a distal tubular origin of cysts. Na-PiII transporter, a marker of proximal tubules, did not label any cysts (Cy) at this stage. Nuclei were counterstained with 4',6-diamidino-2-phenylindole (DAPI, blue). Periodic Acid Schiff staining (PAS) on kidneys from *Ofd1*$^{fl/y}$;*cre*^{Ksp} excluded the presence of fibrosis. Bar=50 μm for THP, LAH, and NapiII panels; Bar=500 μm for PAS staining (Zullo, Iaconis et al. 2010).

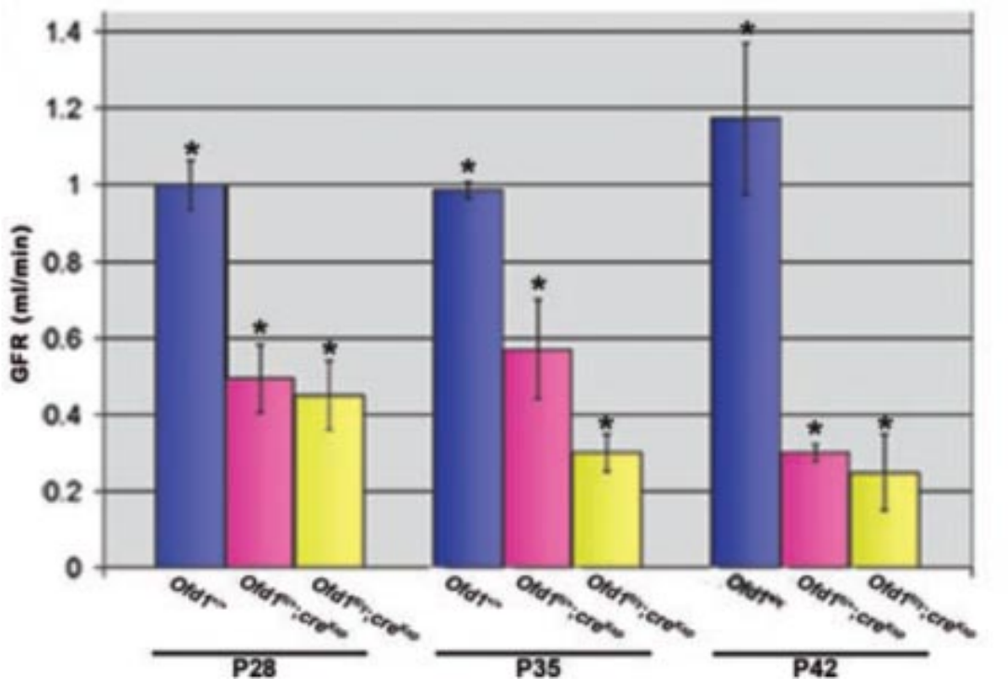

Figure 14. Glomerular filtration Rate (GFR) in *Ofd1^{fl};cre^{Ksp}* (*Ksp*) mutants. GFR at different stages showed a reduced renal function in the kidney from mutant males (*Ofd1$^{fl/y}$;cre^{Ksp}*) and females (*Ofd1$^{fl/+}$;cre^{Ksp}*) compared with control littermates (*Ofd1$^{+/+}$*) Bars = standard error of the mean. Data were analyzed by Student's t-test.*p-value=0.05 (Zullo, Iaconis et al. 2010).

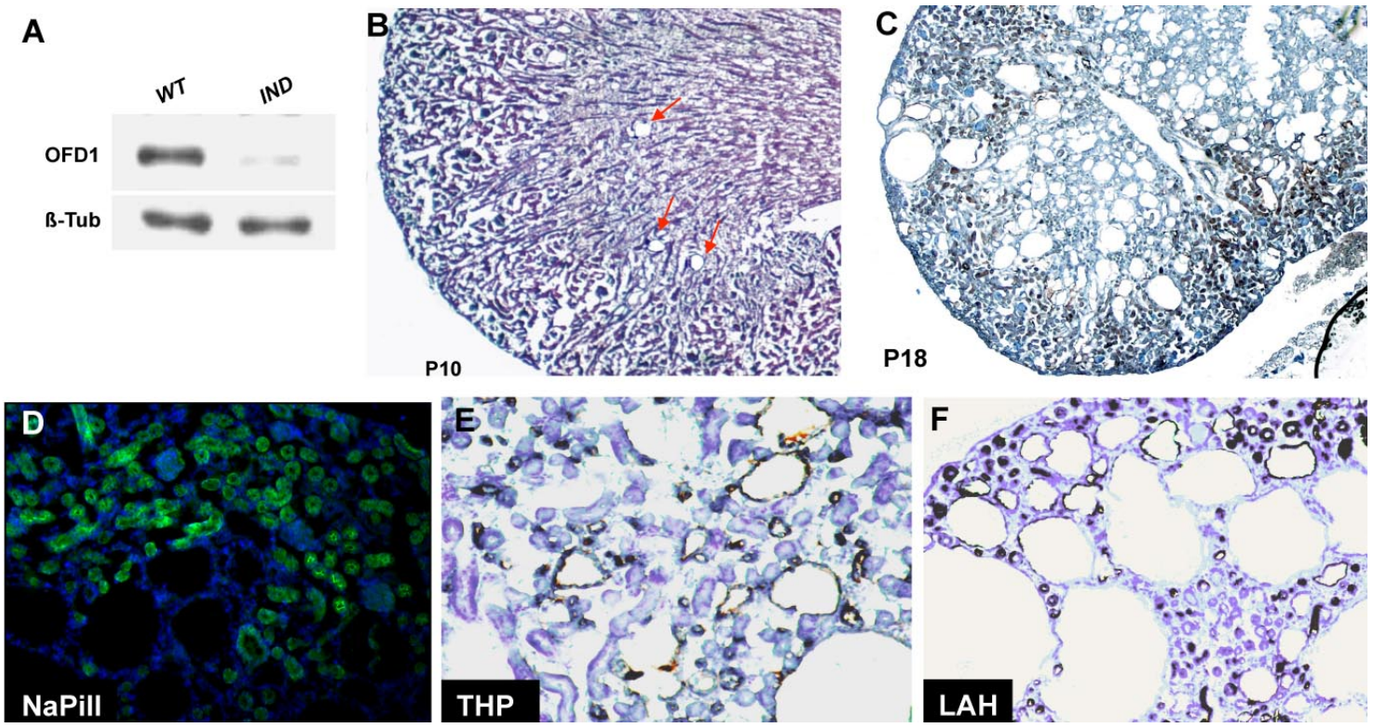

Figure 15. Characterization of the *Ofd1*$^{fl/y}$;*CAGGcre*$^{ER\text{-}TM}$ (IND) mice. (A) WB with an antibody against OFD1 on kidney lysates from controls (WT) and *Ofd1*$^{fl/y}$;*CAGGcre*$^{ER\text{-}TM}$ (IND) mice. (B,C) Hematoxylin/eosin staining of kidneys sections from IND mutants at different stages. (B) At P10, dilated tubules appear (red arrows). (C) Cysts, rapidly increased in size and number, replacing the majority of the parenchyma at P18. (D-F) Kidneys from IND mutants at P18 were stained for Na-PiII cotransporter (D green, NaPiII), Tamm–Horsfall protein (THP) and Arachis Hypogaea Lectin (LAH). The cysts were positive for THP and LAH, thus indicating a distal tubular origin of cysts. Bar=50µm for NapiII, THP and LAH panels; Bar=500 µm for Hematoxylin/eosin staining.

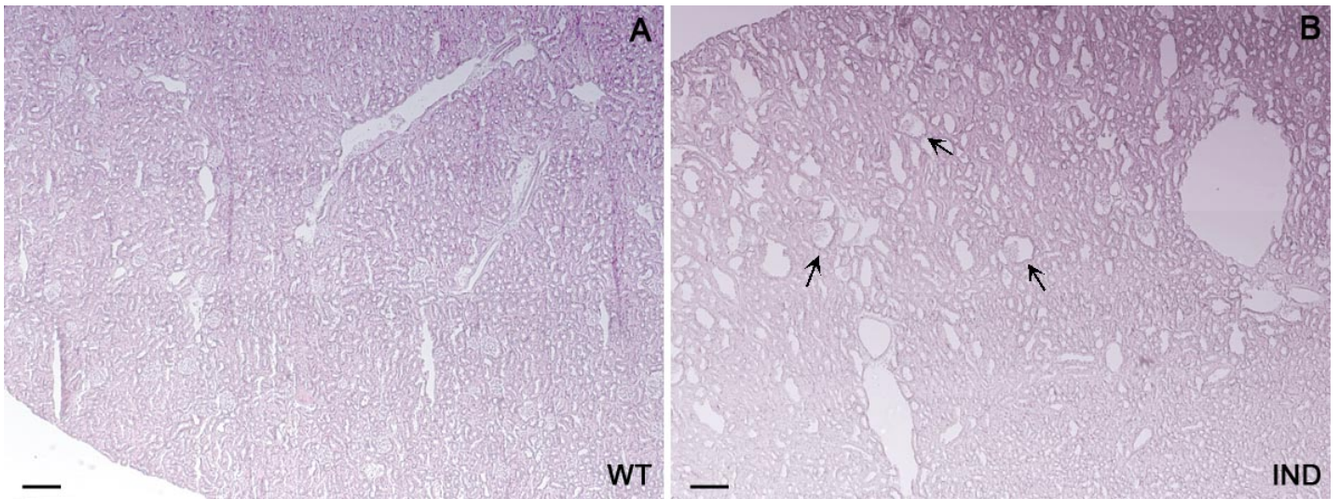

Figure 16. Renal cysts in adult *Ofd1*$^{fl/y}$;*CAGGcre*$^{ER\text{-}TM}$ (IND) mice induced at P60. Hematoxylin/eosin staining of WT (A) and *Ofd1*$^{fl/y}$;*CAGGcre*$^{ER\text{-}TM}$ (IND) (B) adult renal sections at 11 months from mice injected with tamoxifen at P60. (A) WT mice showed a normal parenchyma (B) IND mice developed cysts both in the cortex and in the medullary portion of the kidney. Glomerular cysts were indicated by black arrows. Bar=200μm.

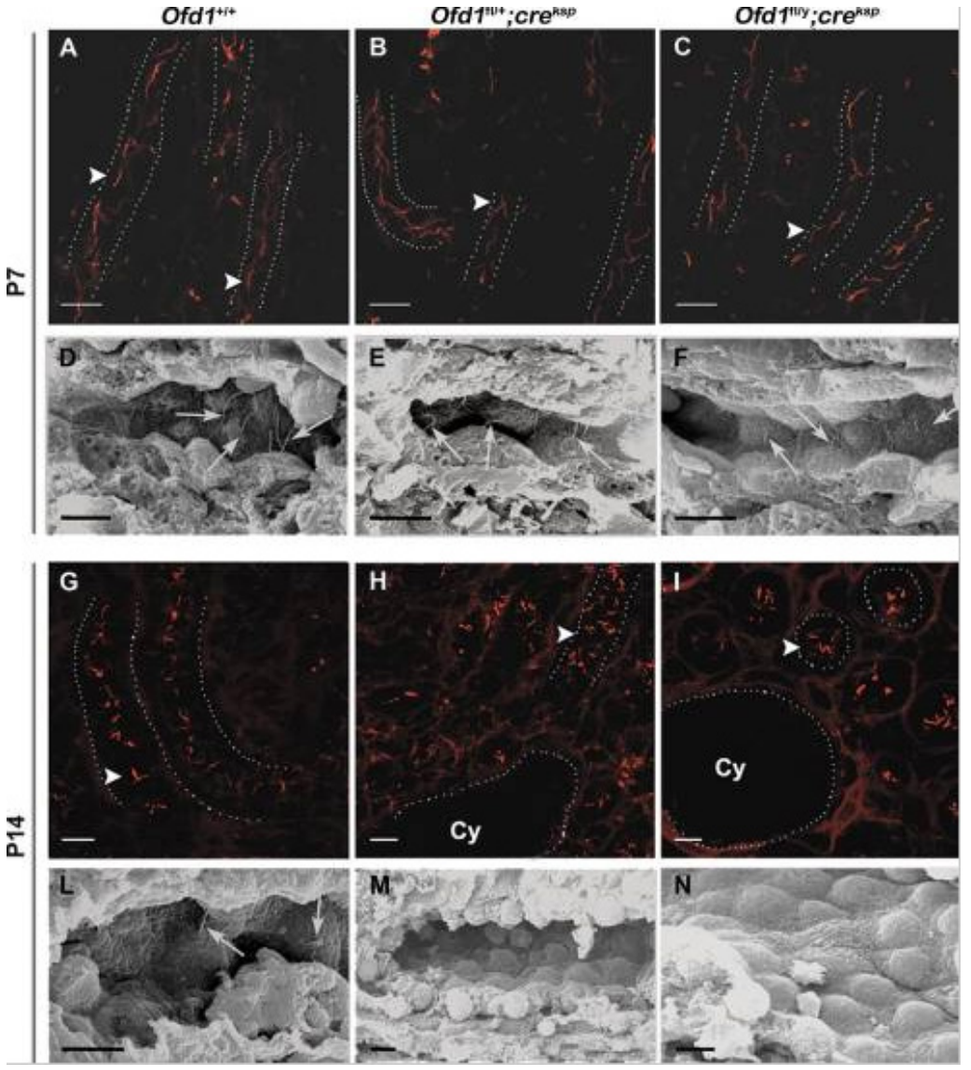

Figure 17. Analysis of primary cilia in renal tubules of *Ofd1*^{fl};*cre*^{Ksp} (*Ksp*) mutant animals. Immunostaining with anti-acetylated tubulin (red) and SEM analysis revealed the presence of cilia in *Ksp (Ofd1*^{fl};*cre*^{Ksp} *)* and WT littermates (*Ofd1*$^{+/+}$) at P7 in the kidney distal tubules [arrowheads in (A–C), arrows in (D–F)]. Immunostaining with anti-acetylated tubulin (red) showed the absence of cilia in the cells lining the cysts (Cy) and the presence of cilia in non-dilated tubules (arrowheads) from *Ofd1*$^{fl/+}$;*cre*^{Ksp} (H) and *Ofd1*$^{fl/y}$;*cre*^{Ksp} (I) mutants at P14. Cilia are normally seen in *Ofd1*$^{+/+}$ control animals (G). SEM analysis confirm the absence of cilia from cells lining cystic dilations in both *Ofd1*$^{fl/+}$;*cre*^{Ksp} (M) and *Ofd1*$^{fl/y}$;*cre*^{Ksp} (N) mutants at P14, whereas cilia are (H) and *Ofd1*$^{fl/y}$;*cre*^{Ksp} (I) mutants at P14, whereas cilia are present in control littermates at the same stage (arrows in L). Bars = 10 μm (A–C, G–I); 5 μm (D–F, L–N). Tubules are outlined with dotted lines (Zullo, Iaconis et al. 2010).

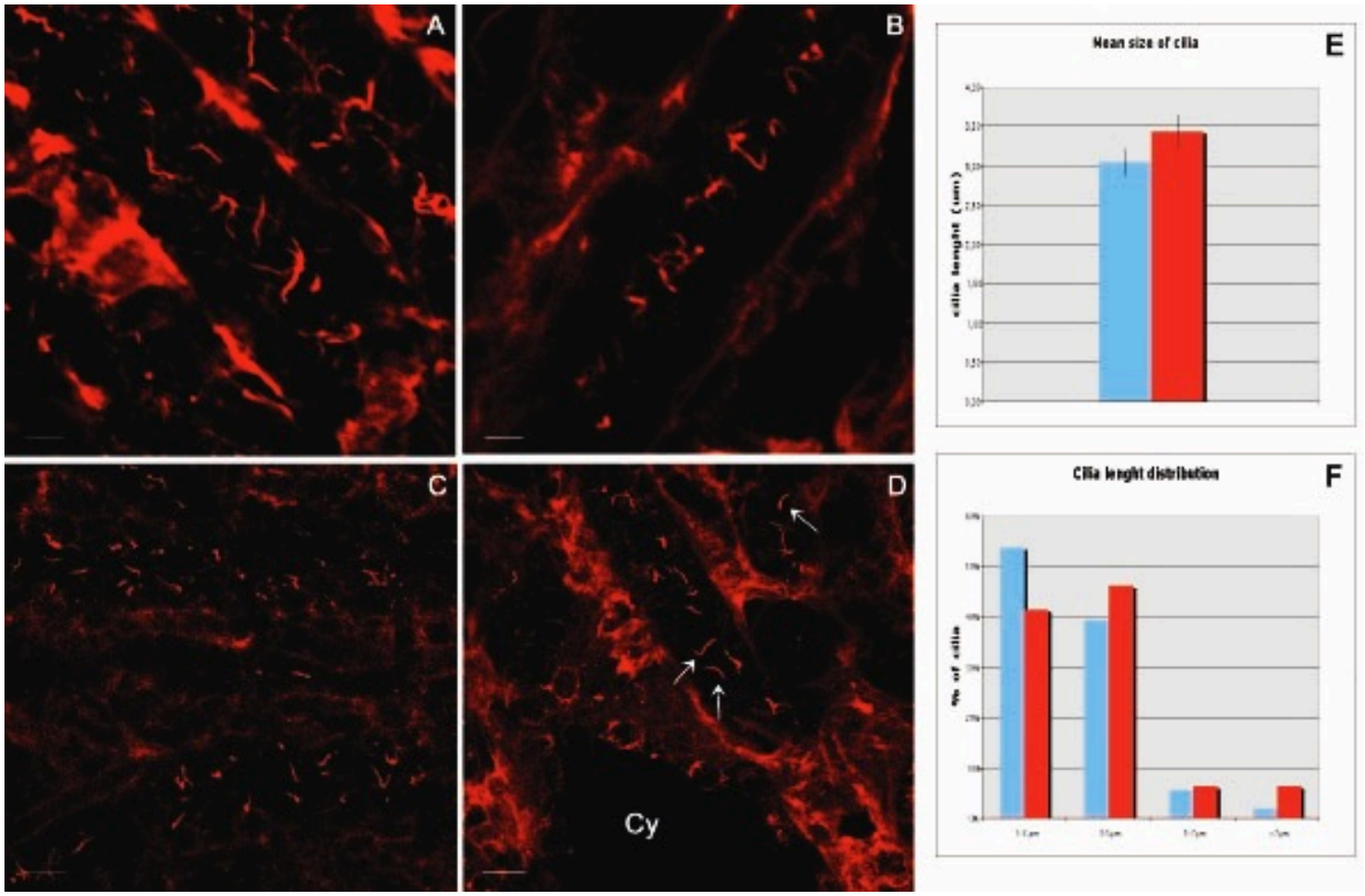

Figure 18. Analysis of primary cilia in renal tubules of *Ofd1*$^{fl/y}$;*CAGGcre*$^{ER\text{-}TM}$ (IND) mutant animals. (A-B) Immunostaining with anti-acetylated tubulin (red) revealed the presence of cilia in WT (A) and *Ofd1*$^{fl/y}$;*CAGGcre*$^{ER\text{-}TM}$ (IND) littermates (B) at P8 in the kidney distal tubules. (C) Cilia are normally stained in WT animals at P18. (D) Immunostaining with anti-acetylated tubulin (red) showed the absence of cilia in the cells lining the cysts (Cy) and the presence of cilia in non-dilated tubules (arrows) from IND mutants at P18. (E) The mean size of cilia and (F) the cilia length distribution are comparable between IND mutants (blue bars) and WT (red bars). Bar=5µm in A and B; Bar=10µm in C and D.

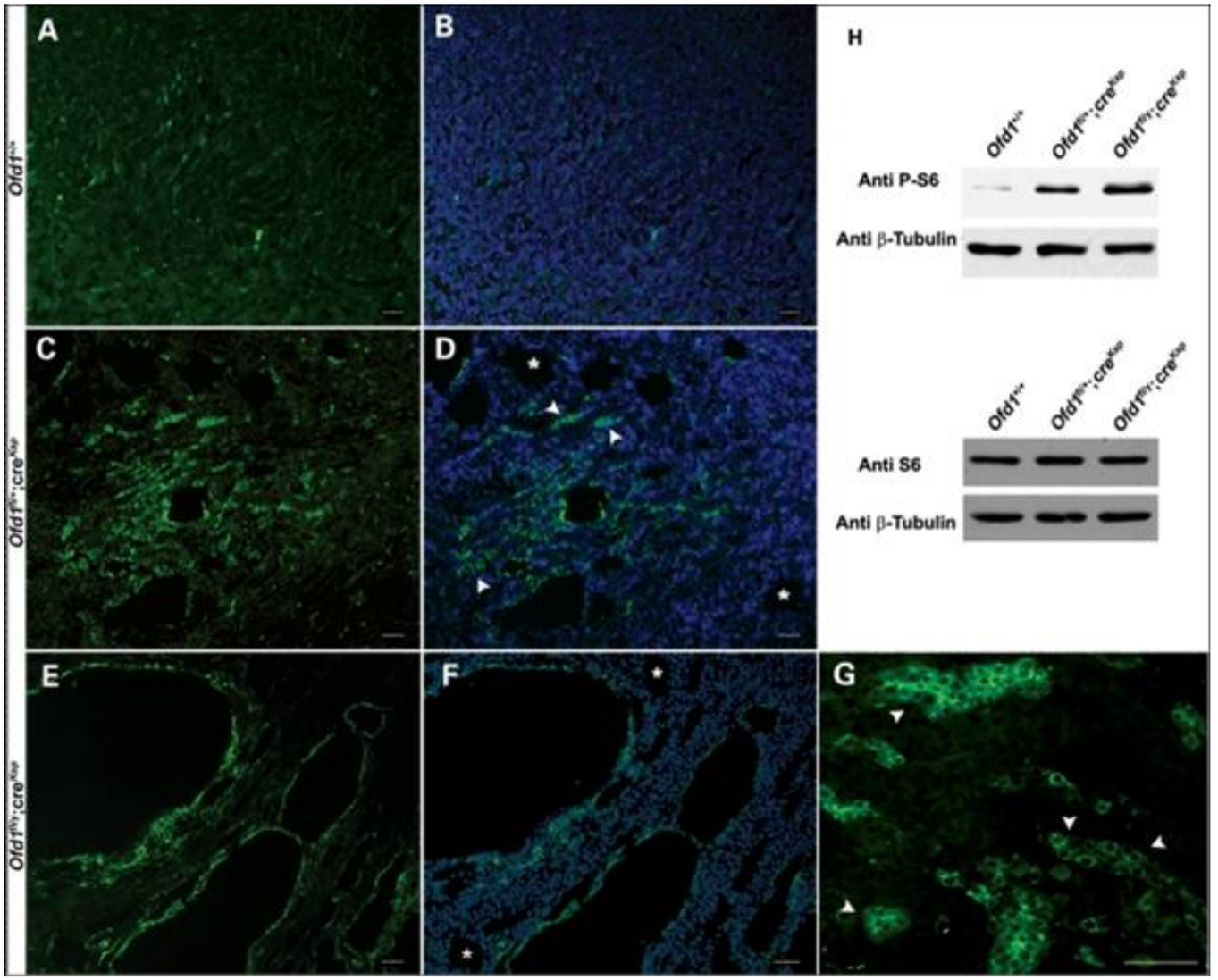

Figure 19. Upregulation of the mTOR pathway in *Ofd1*^{fl};*cre*^{Ksp} (*Ksp)* mutant animals at P21. Immunostaining and western blot analysis with anti-phospho S6 (P-S6). The immunofluorescence revealed an higher level of P-S6 (green) on kidney sections from *Ofd1*$^{fl/+}$;*cre*^{Ksp} (C and D) and *Ofd1*$^{fl/y}$;*cre*^{Ksp} (E–G) mutant animals when compared with *Ofd1*$^{+/+}$ controls (A and B). In (B), (D) and (F), nuclei were counterstained with DAPI (blue). Fews cysts do not display staining with anti P-S6 (asterisks in D and F). Upregulation of P-S6 (arrowheads) is observed also in non-dilated tubules in both *Ofd1*$^{fl/+}$;*cre*^{Ksp} (D) and *Ofd1*$^{fl/y}$;*cre*^{Ksp} (magnification in G) mutant animals. Bars (A–G) = 50 µm. (H) Western blot analysis of total S6 (lower panel) and P-S6 (upper panel) on total protein extracts of kidneys from *Ofd1*$^{+/+}$, *Ofd1*$^{fl/+}$;*cre*^{Ksp} and *Ofd1*$^{fl/y}$;*cre*^{Ksp} animals confirmed the upregulation of the mTOR pathway (Zullo, Iaconis et al. 2010).

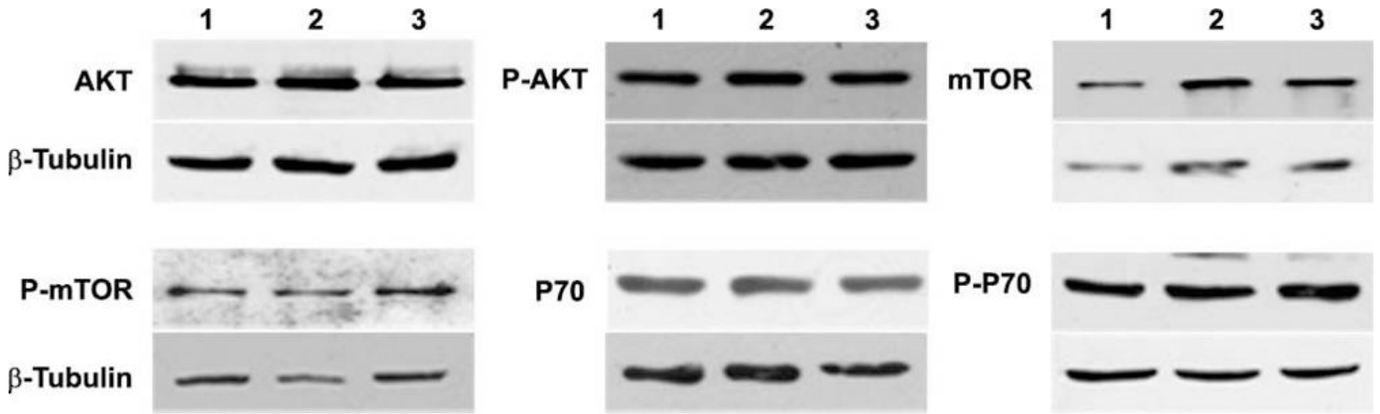

Figure 20. Analysis of the proteins upstream the mTORC1 complex in *Ofd1*^{fl};*cre*^{Ksp} (*Ksp*) mutants. We analyzed both basal and phosphorilation levels of proteins upstream mTOR in kidney lysates from mice at P21. No differences were observed between *Ksp* male mutants (1), female mutants (2) and WT (3) for Akt, mTOR and P70 as well as for the phosphorylated forms P-P70, P-mTOR, P-AKT.

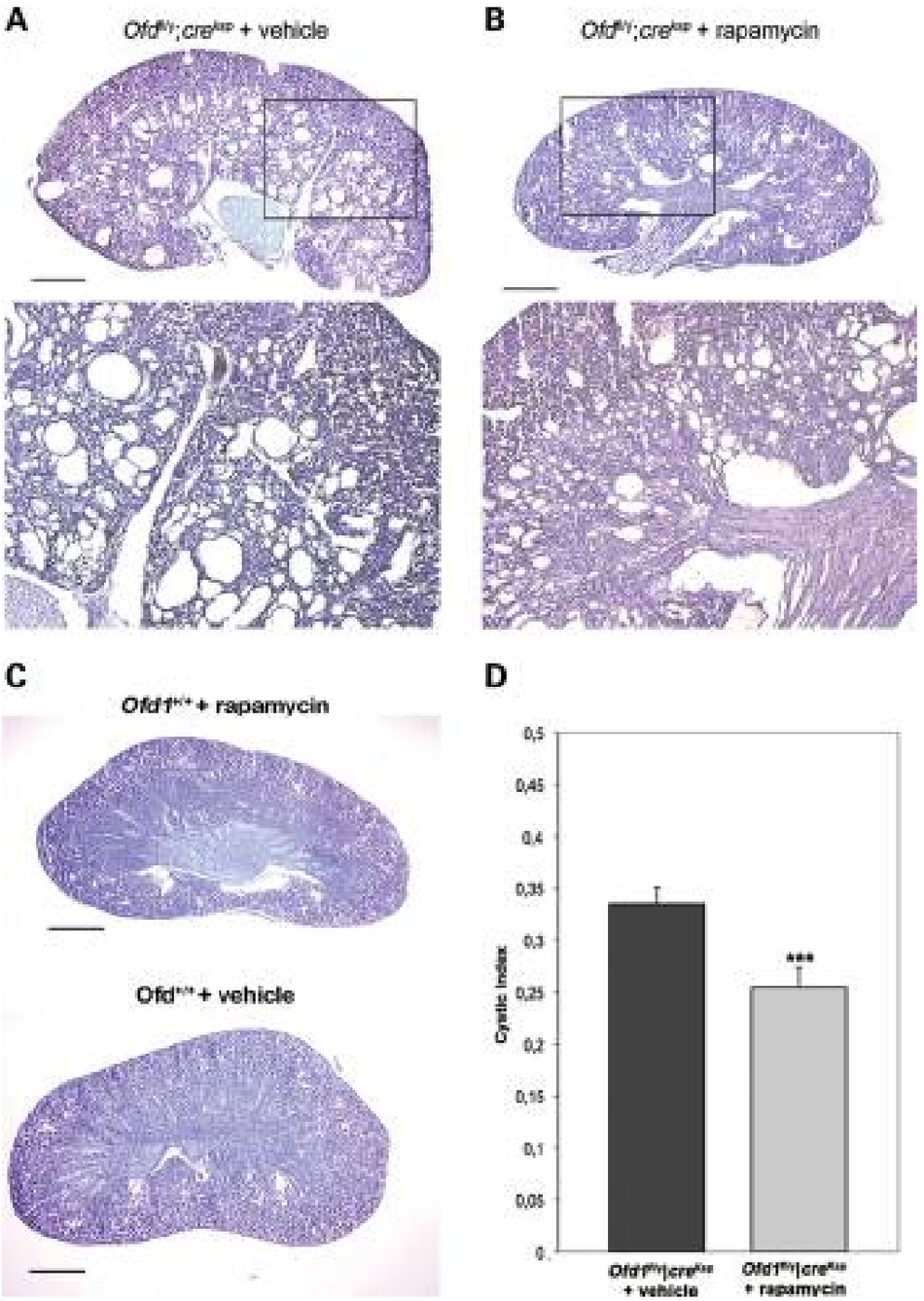

Figure 21. Rapamycin treatment of *Ofd1*$^{fl/y}$;*cre*^{Ksp} (*Ksp*) animals. Rapamycin treatment significantly improves the renal cystic phenotype observed in *Ofd1*$^{fl/y}$;*cre*^{Ksp} (*Ksp*) animals (**B**) when compared to mutant animals treated with vehicle alone (**A**). Bottom panels in A and B represent higher magnification of the boxed images. In **C** kidneys from wild-type littermates treated with rapamycin or vehicle alone are shown as a control. (**D**) Cystic indices were calculated based on representative renal sections from non-treated and treated *Ofd1*$^{fl/y}$;*cre*^{Ksp} mice (*n* = 3 kidneys). Bars in A,B and C= 1,2 mm. Data were analyzed by Student's *t*-test. ***P<0,005 (Zullo, Iaconis et al. 2010).

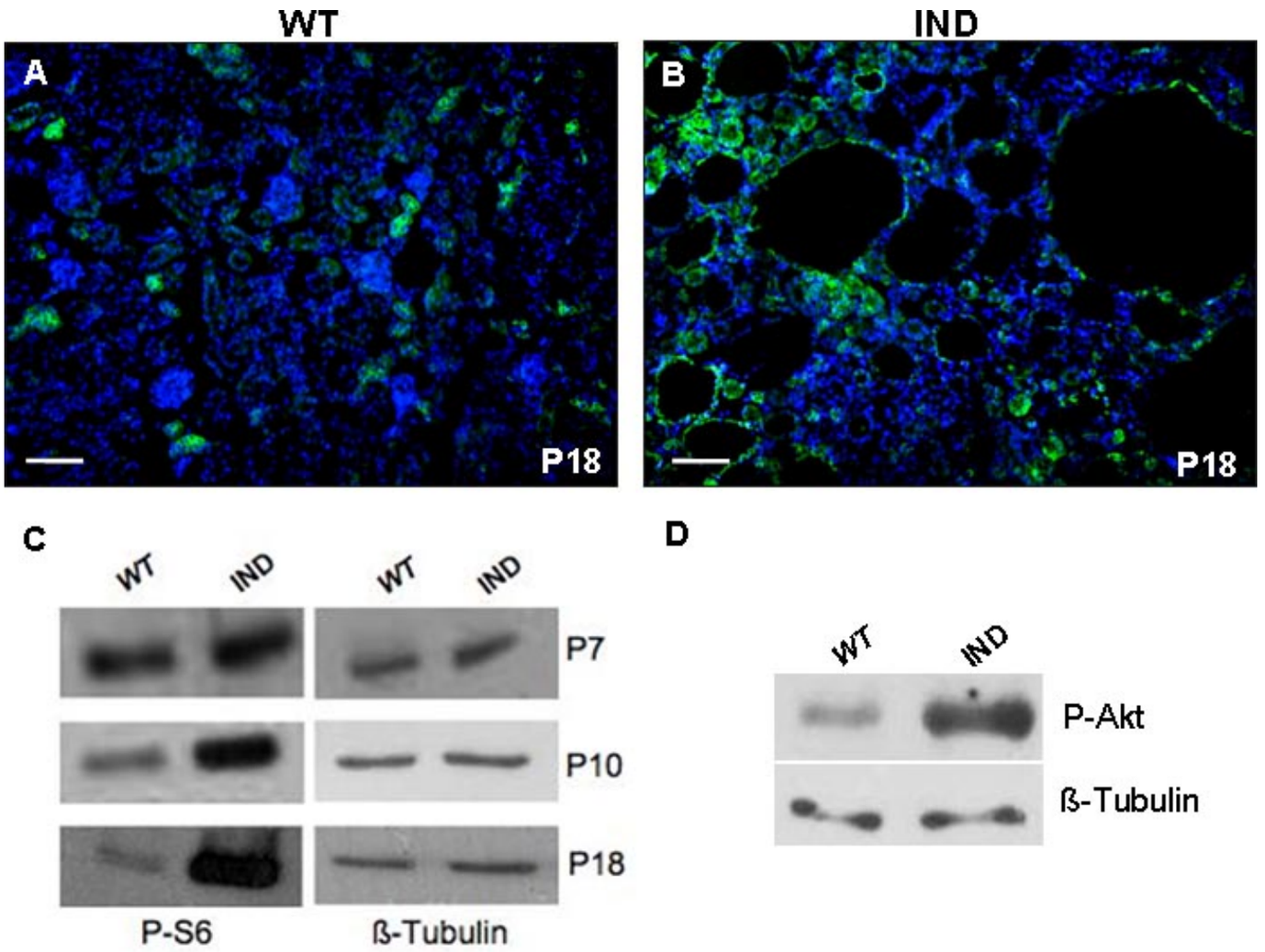

Figure 22. P-S6 and P-Akt analysis in *Ofd1*$^{fl/y}$;*CAGGcre*$^{ER\text{-}TM}$ (IND) mice. (A and B) Immunofluorescence analysis of P-S6 in WT (A) and IND (B) mice at P18 revealed an upregulation of the mTOR pathway in cells lining a number of cysts and non-dilated tubules. (C) Western Blot experiments on renal lysates at different stages showed a higher amount of P-S6 in IND mice starting from P10. (D) Levels of P-Akt (Ser473) were increased in IND mice compared to WT. Bar=50µm.

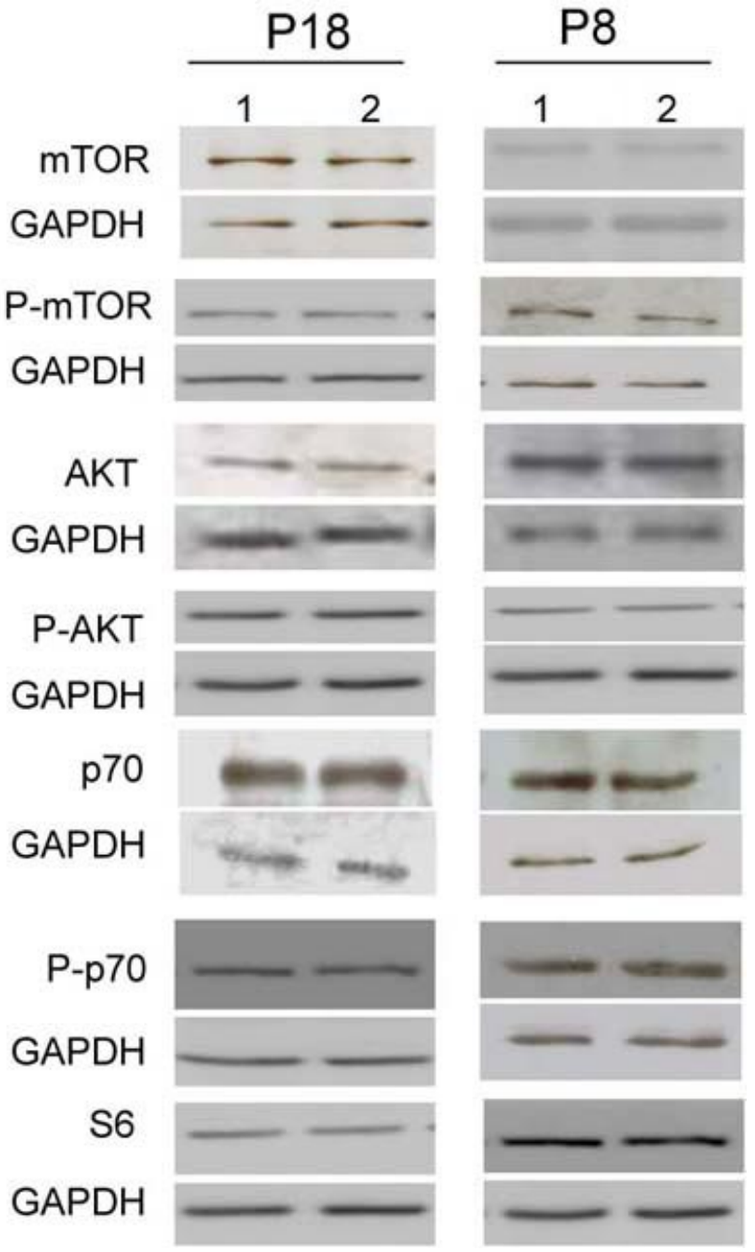

Figure 23. Analysis of the proteins upstream the mTORC1 complex in the *Ofd1*$^{fl/y}$;*CAGGcre*$^{ER\text{-}TM}$ (IND) mutants. We analyzed by western blot different proteins involved in the mTOR pathway in lysates from mutant kidneys at P8 and P18. Both total amount and phosphorylated levels of the proteins analyzed displayed no differences between WT (1) and IND mutants (2) in all stages analyzed. P-Akt in this figure refers to Thr308 phosphorylation site.

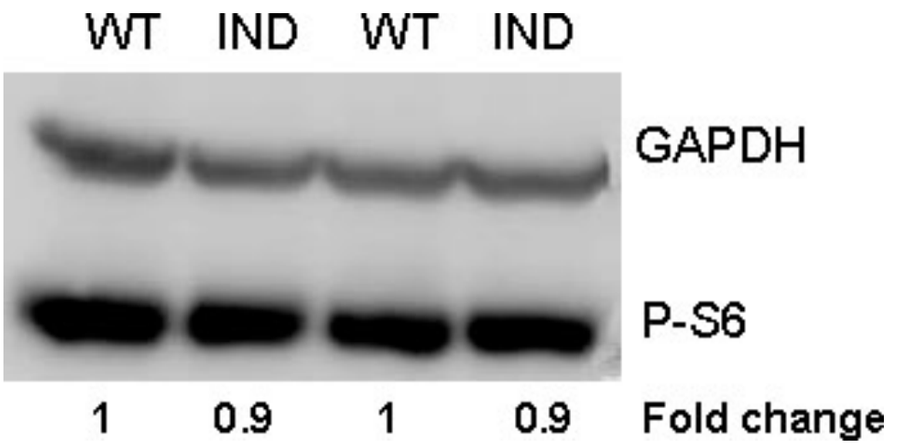

Figure 24. Levels of P-S6 in the liver of *Ofd1*$^{fl/y}$;*CAGGcre*$^{ER\text{-}TM}$ (IND) mutants. Livers from two different IND mutants and WT mice were isolated. Total lysates were analyzed by Western Blot analysis to verify the levels of P-S6. No differences were observed between WT and IND mice. Fold change was calculated using ImageJ.

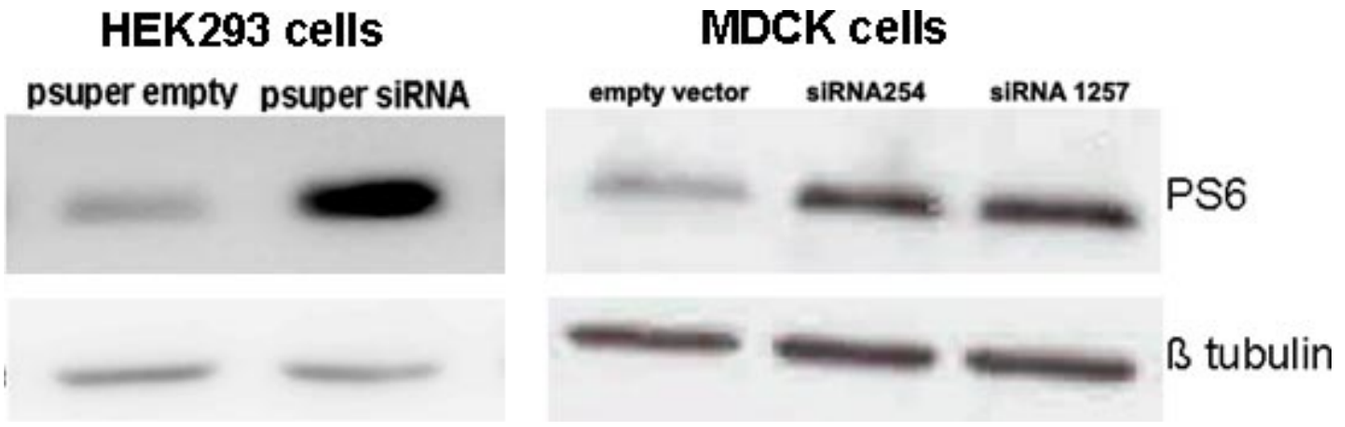

Figure 25. Activation of P-S6 in *Ofd1*-depleted *in vitro* systems. Western blot analysis with anti phospho S6 (PS6) antibody reveals a higher level of activated S6 protein in HEK293 (left panel) and MDCK cells (right panel) transfected with different siRNAs against the *OFD1* transcript compared to cells transfected with the empty vector. Cells were collected 48 hours after transfection.

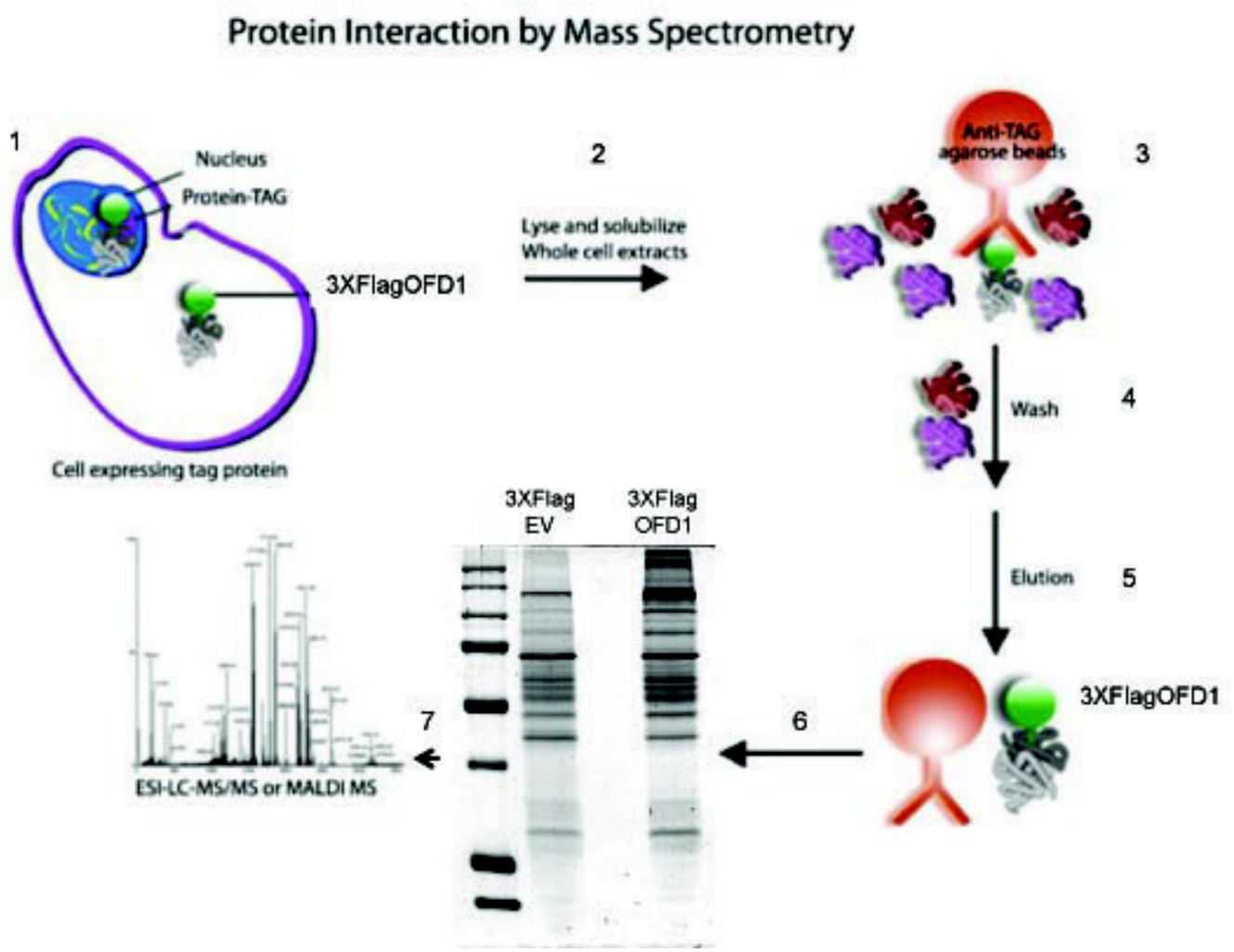

Figure 26. Mass spectrometry analysis to identify putatite OFD1 interactors. Schematic representation of the methodological approach used for mass spectrometry. Cells were transfected with a construct overexpressing the 3XFlagOFD1 protein or with 3XFlag empty vector (EV) (step 1). Cells were lysed (step 2) and the protein with its interactors was immunoprecipitated with an anti-flag resin (step 3). After wash (step 4) the protein complex was eluted in order to obtain the resin-free protein complex (step 5). Proteins were then loaded in an acrylamide gel (step 6) and the bands were cut, digested and analyzed with the mass analyzer (step 7).

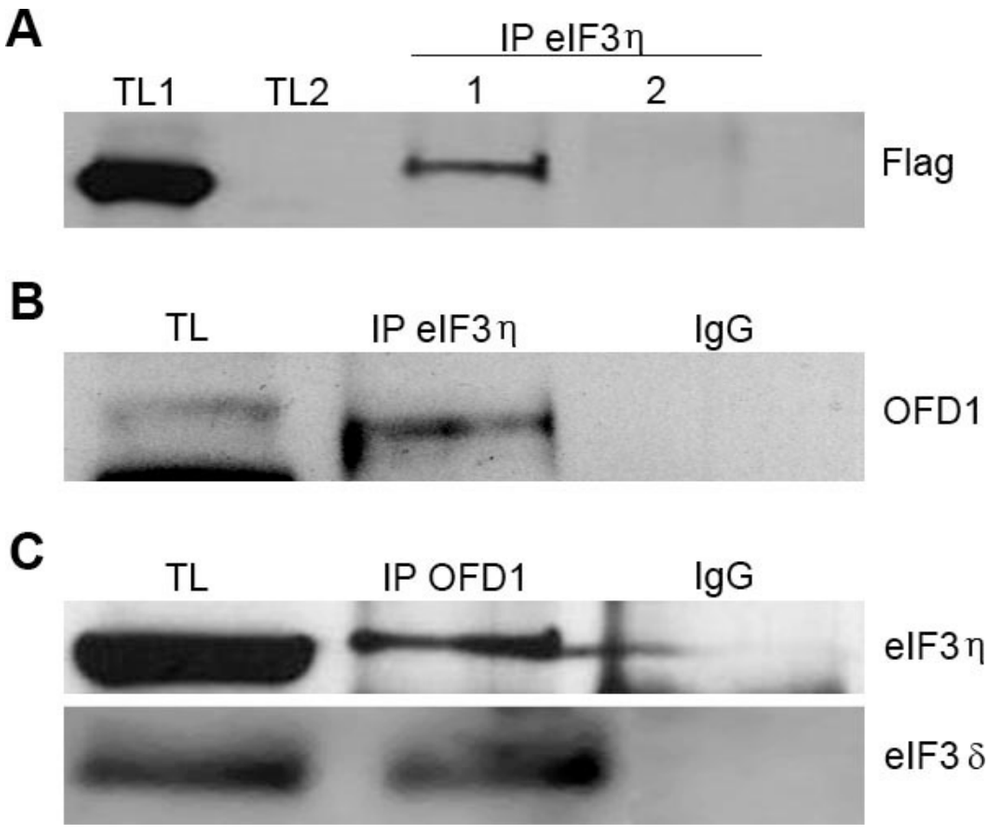

Figure 27. Co-IP experiments confirm that OFD1 interacts with components of the PIC. (A) OFD1 was detected with an anti Flag antibody in total lysate of HEK293 cells overexpressing 3XFlag-OFD1 (TL1), while is absent in total lysate of cells transfected with the empty vector (TL2). Total lysates were immunoprecipitated with an anti eIF3η antibody and OFD1 was detected in Co-IP performed on cells expressing 3XFlag OFD1 (1) while it is absent in Co-IP experiment performed on cells transfected with the empty vector (2). (B and C) Co-IP experiments performed on endogenous proteins confirmed the interactions between OFD1 and the two subunits of the eIF3 complex (eIF3δ and eIF3η). (B) Co-IP was performed with an antibody recognizing eIF3η and OFD1 was detected by Western Blot. (C) Co-IP was performed with an antibody recognizing OFD1 and eIF3η and eIF3δ subunits were detected. IgG were used as control.

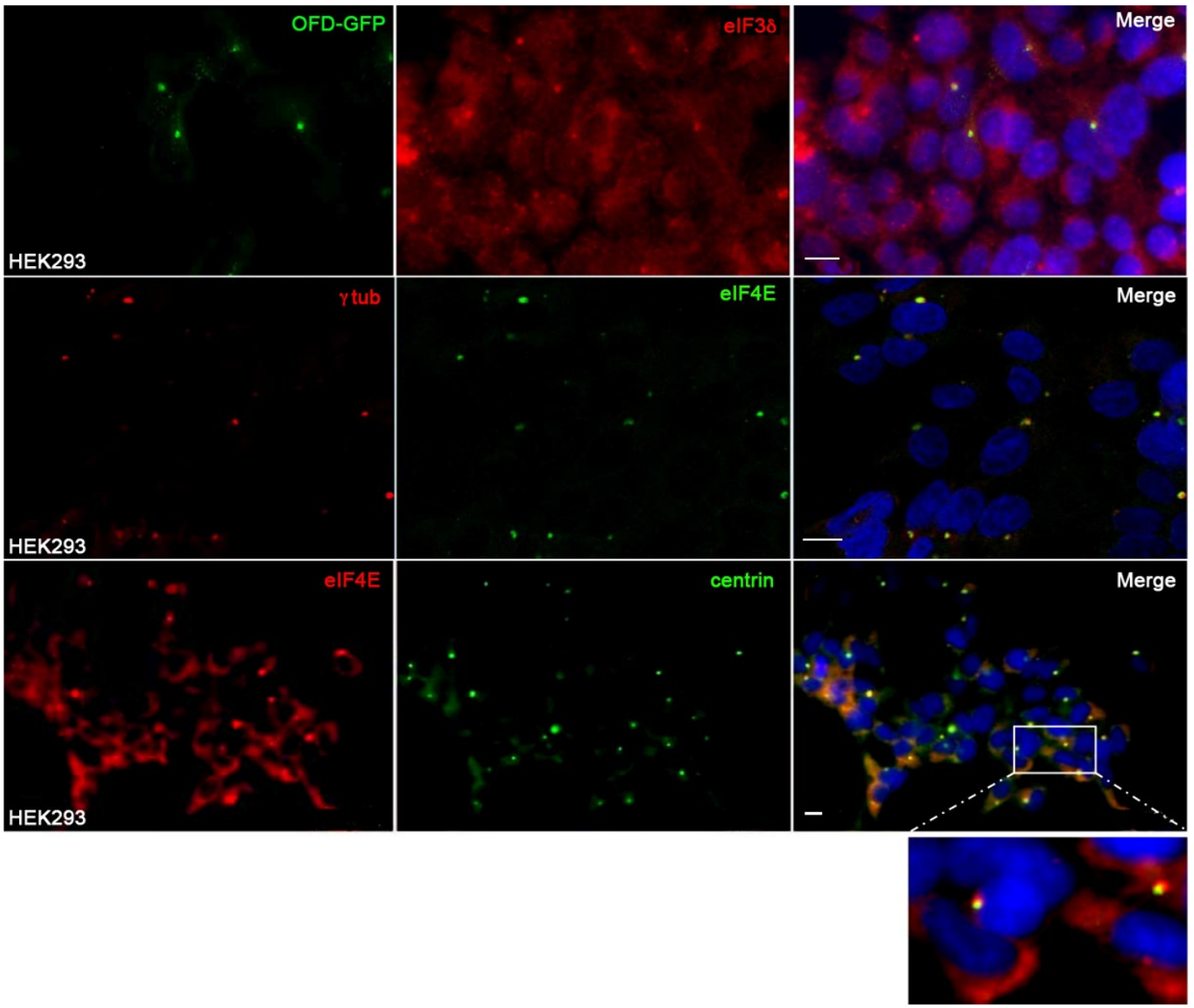

Figure 28. Centrosomal localization of the components of the PIC. Immunofluorescence experiments showed that eIF3δ (red) colocalizes at the centrosome with OFD1-GFP (green) (merge third panel, first row). eIF4E (green) colocalizes with the γ-tubulin (red) as shown by the merge of the two signals (merge third panel, second row). eIF4E (red) colocalize also with centrin (green) as shown by the merge of the two signals (merge third panel, third row). Bar=20μm.

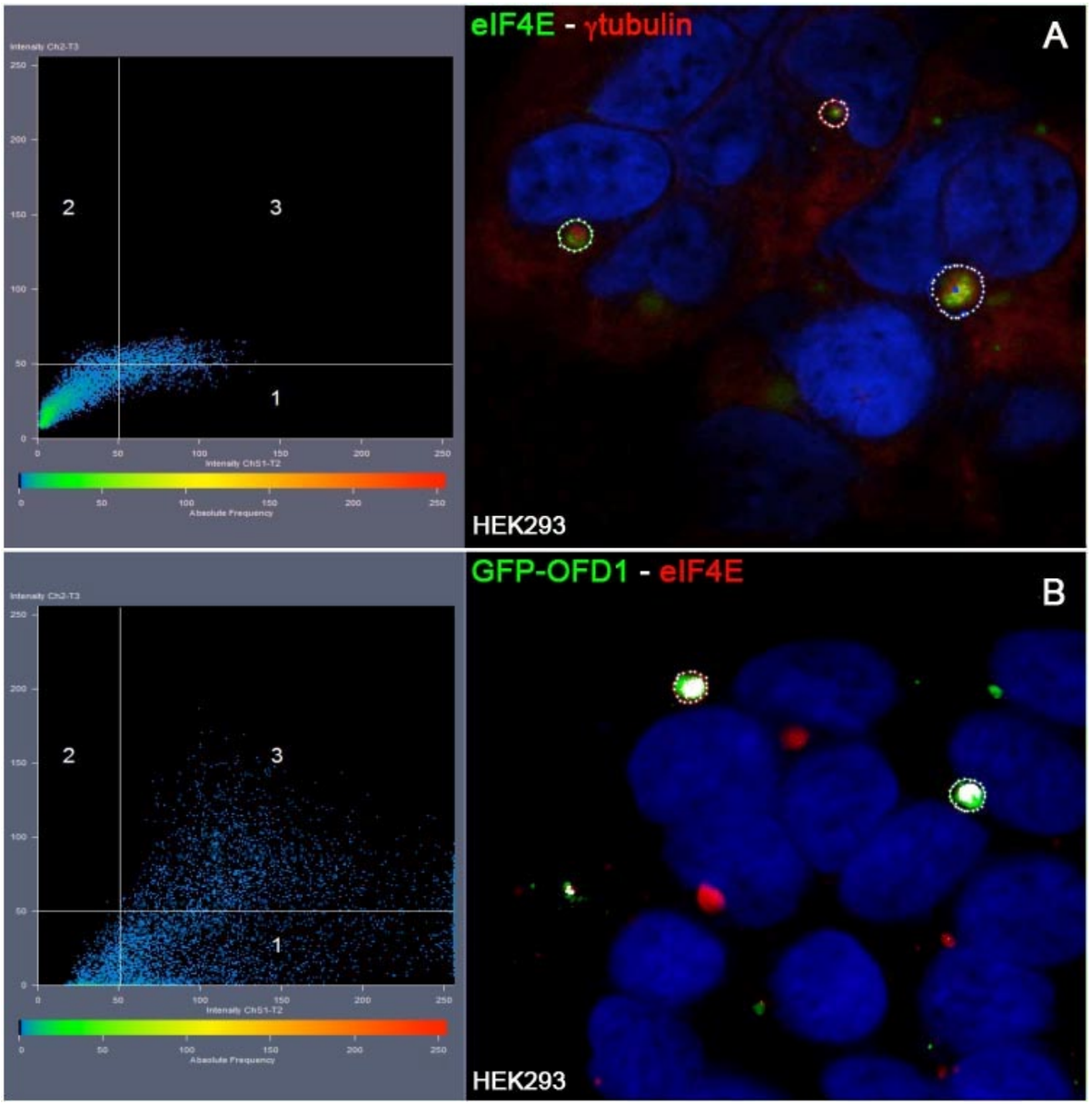

Figure 29. Analysis of the centrosomal localization of eIF4E. Immunofluorescence experiments showed that (A) eIF4E (green) colocalizes partially with the γtubulin (red) (dotted circles in A). (B) The colocalization was almost complete when cells overexpressing GFP-OFD1 (green) were stained with eIF4E (red) (dotted circles in B). (A-B) We quantified the percentage of colocalization with confocal microscopy. The area contained in the dotted circles was selected and the green and red fluorescence was calculated. In both panels the area number 3 shows the number of pixels positive for both (red and green) florescent signals.

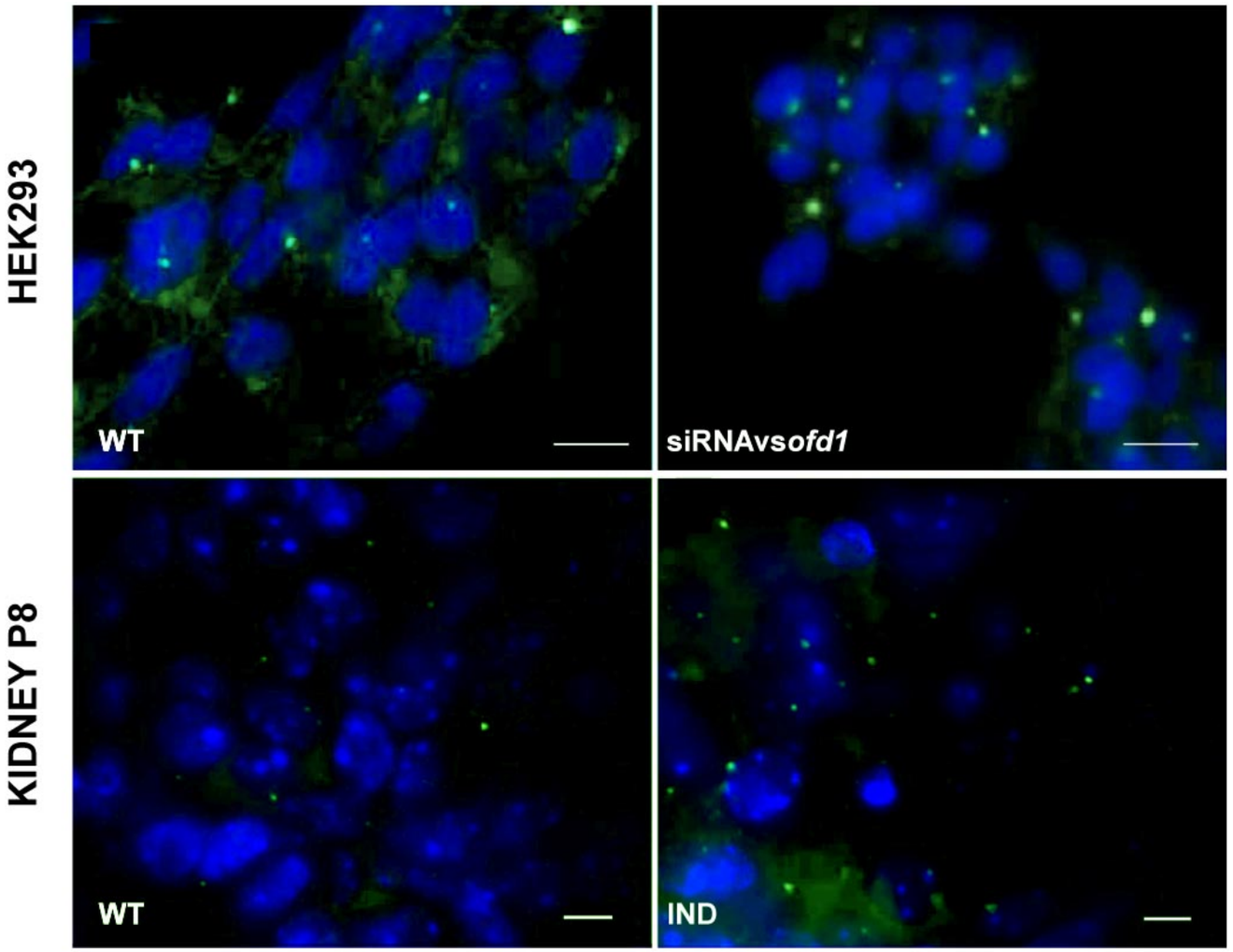

Figure 30. eIF4E accumulates at the centrosome in *Ofd1* deficient models. Staining with an antibody recognizing the eIF4E protein (green) in HEK293 cells (A) and kidney sections from *Ofd1*$^{fl/y}$;*CAGGcre*$^{ER\text{-}TM}$ (IND) mice at P8 (B). Nuclei were stained with DAPI. Bar=20μm in A Bar=10μm in B.

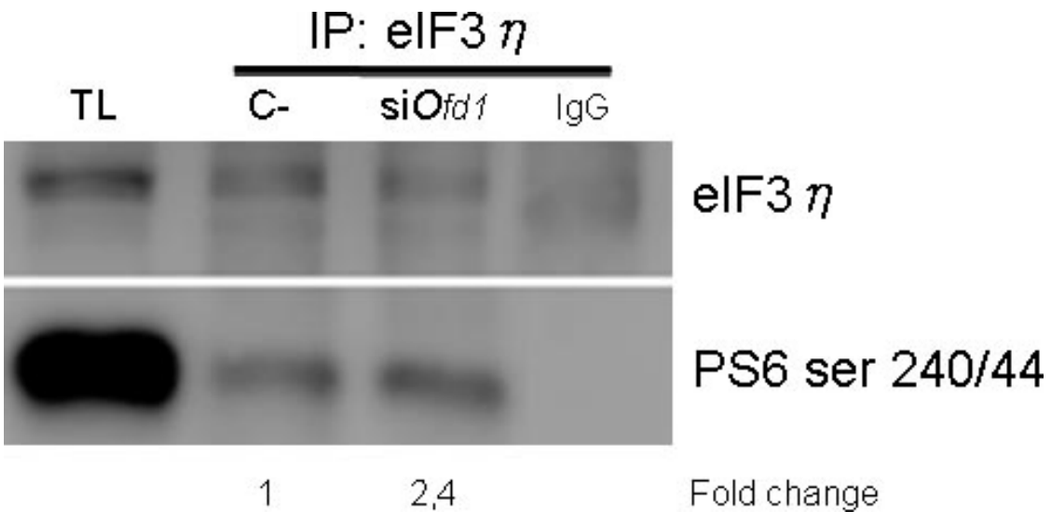

Figure 31. Analysis of PIC assembly. The amount of P-S6 bound to eIF3η in control (C-) and OFD1-silenced HEK293 (si*Ofd1*) cells was analyzed by Co-IP experiments. We used Rabbit Immunoglobuline G (IgG) as negative control for IP. Total lysate (TL) was loaded in the first lane. The fold change was calculated by using the Image J program.

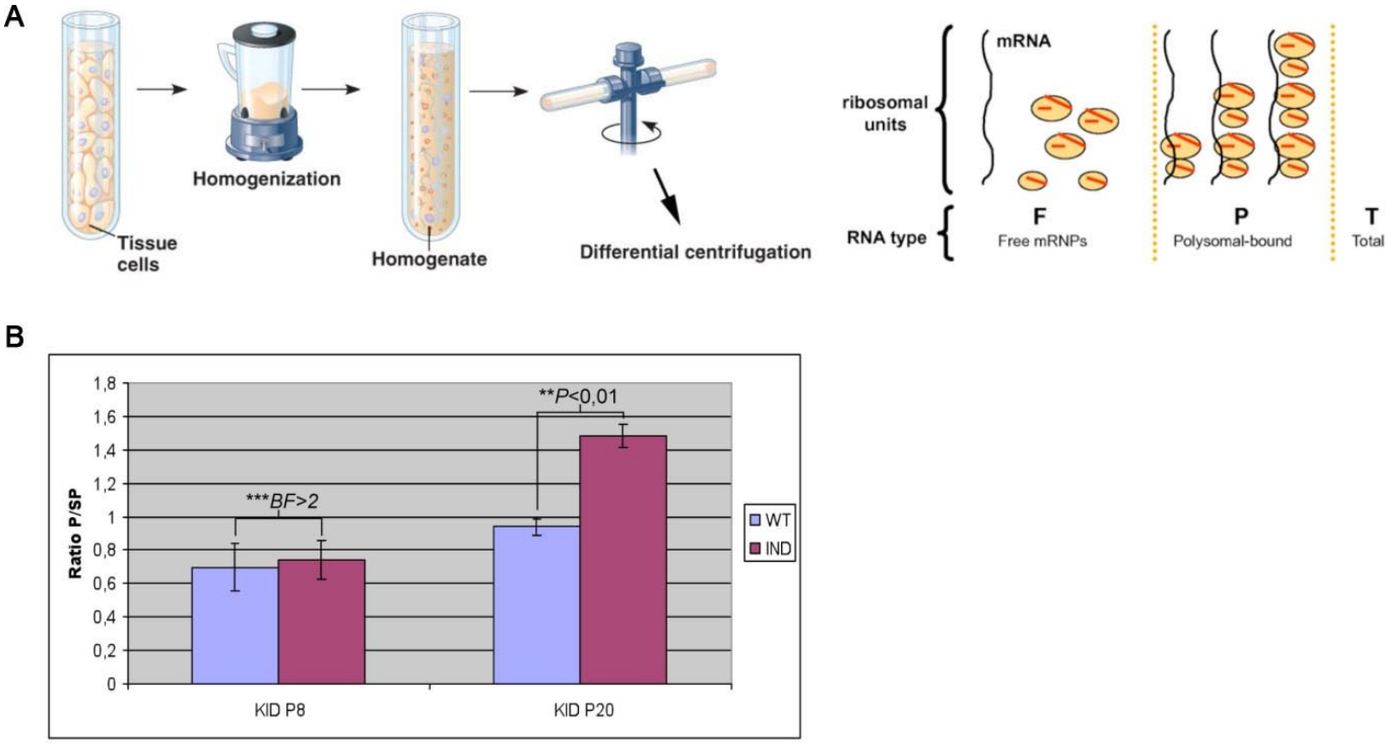

Figure 32. Analysis of the polysomal profile of renal extracts from *Ofd1$^{fl/y}$;CAGGcre$^{ER\text{-}TM}$* (IND) mice. (A) Description of Polysomes extraction (Ceppi *et al. Immunome Research* 2009). Cellular or tissue sample is homogenizated and the lysate is separated using sucrose-gradient fractionation after ultracentrifugation. This technique allows separation of free ribonucleoprotein particles (ribosome-free mRNA, F) from mRNAs bound to an increasing number of ribosomes (polysome-bound mRNA, P). (T) indicates the total remaining fractions in which no RNA is present. (B) The ratio between Polysomal RNA (P) and subpolisomal RNA (SP) was reported for both WT animals (violet) and *Ofd1$^{fl/y}$;CAGGcre$^{ER\text{-}TM}$* (IND) mutants (purple). The RNA was obtained from Kidney (KID) of IND mutants at a precystic (P8) and at a cystic (P20) stage. The significance vas calculated with *Bayes Factor* calculation (BF) at P8 and *p-value* calculation at P20.

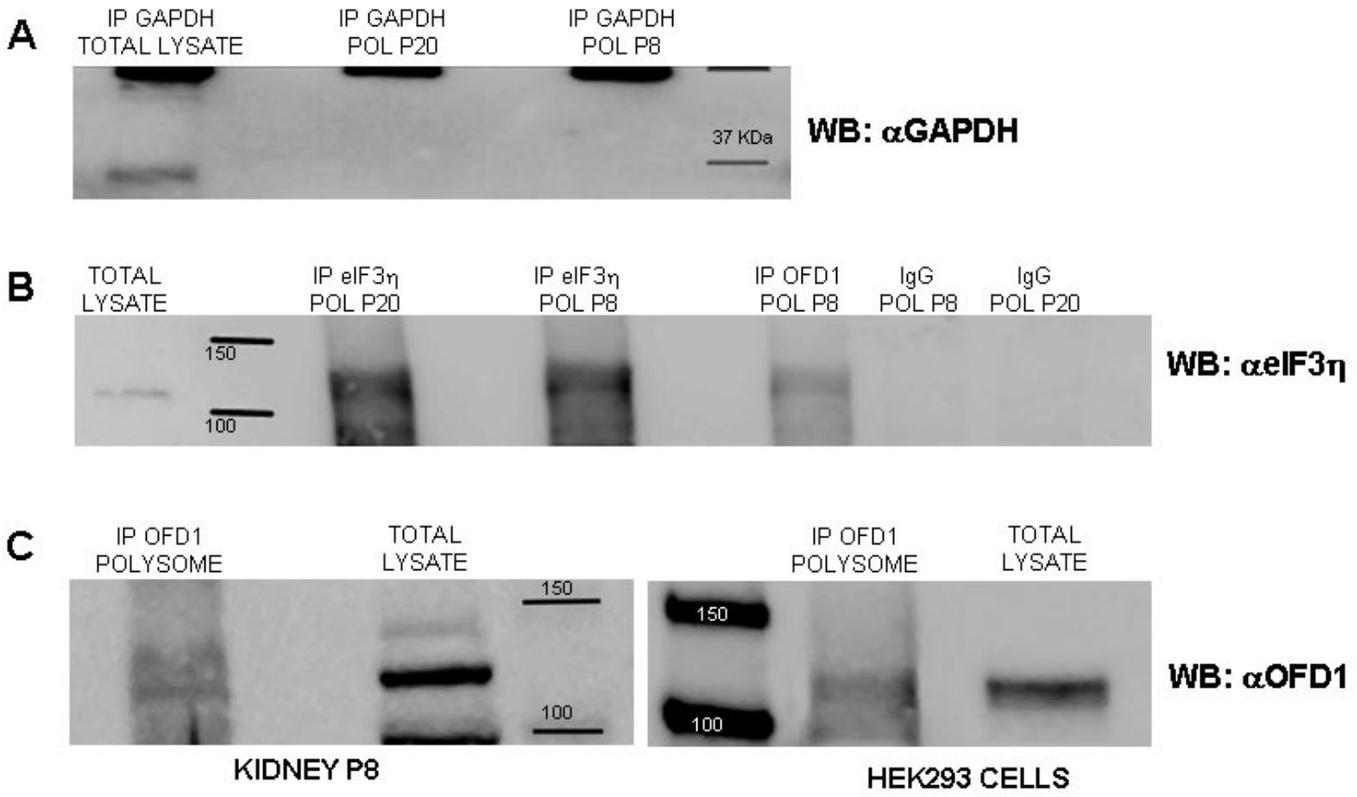

Figure 33. OFD1 is present in polysome fractions and coimmunoprecipitates with eIF3η. (A) We analyzed by immunoprecipitation the presence of the GAPDH protein in total renal lysate (first lane) and in polysomal (POL) fractions both at P20 (second lane) and P8 (third lane). GAPDH is exclusively detected in total lysate from kidney. (B) eIF3η is detected in POL fractions at both stages analyzed (second and third lanes). Co-IP between OFD1 and eIF3η confirmed that the interaction occurs also *in vivo* (fourth lane). (C) Immunoprecipitation experiments performed in both HEK293 cells and renal lysates showed that OFD1 is present in polysomal fractions.

A

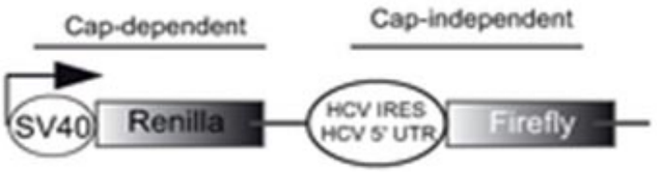

B

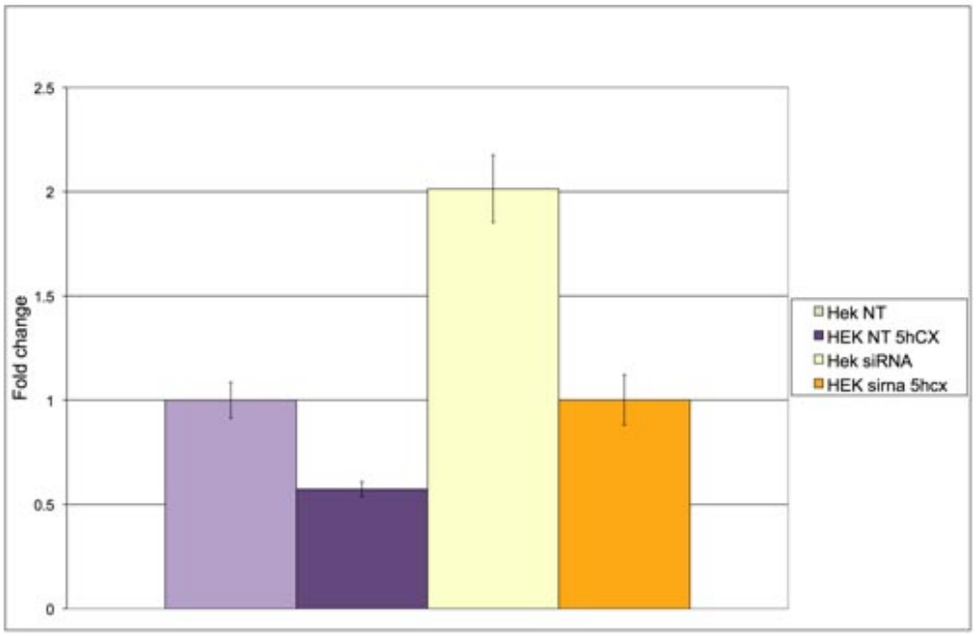

Figure 34. Cap-dependent translation is impaired in *OFD1*-silenced HEK293 cells. (A) Structure of the bicistronic reporter plasmid allowing cap-dependent expression of renilla luciferase and expression of firefly luciferase dependent on HCV IRES (Holz et al., 2005). (B) Cap-dependent translation is insulin stimulated and rapamycin sensitive. HEK293 cells were transfected in triplicate with the reporter plasmid. 48 hours post-transfection, luciferase activities were measured by a dual-luciferase assay, and the renilla/firefly luciferase light-unit ratio was calculated. The ratio was higher in *OFD1*-silenced cells (Hek siRNA-light yellow bar) compared with controls (Hek NT-violet bar). Both control and *OFD1*-silenced cells were treated with cycloheximide (CX) for 5 hours. The rate of degradation was comparable between control (HEK NT 5hCX-dark violet bar) and silenced (HEK siRNA 5hcx-orange bar) cells, suggesting that normal degradation occurred. Data are presented as the mean ± standard error. *p-value*<0.05.

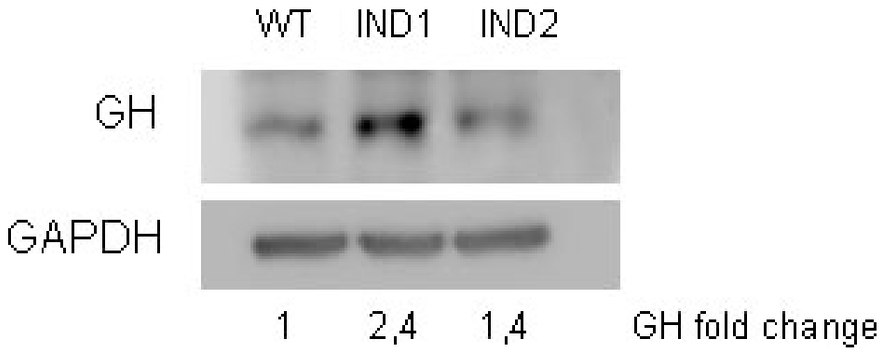

Figure 35. Growth hormone (GH) levels are impaired in *Ofd1*$^{fl/y}$;*CAGGcre*$^{ER-TM}$ (IND) mutants at P8. GH levels were analyzed by western blot. We observed an increased amount of GH in IND mutants compared to WT. The fold change was calculated by using the Image J program. IND1 and IND2 are two siblings of the same littermate.

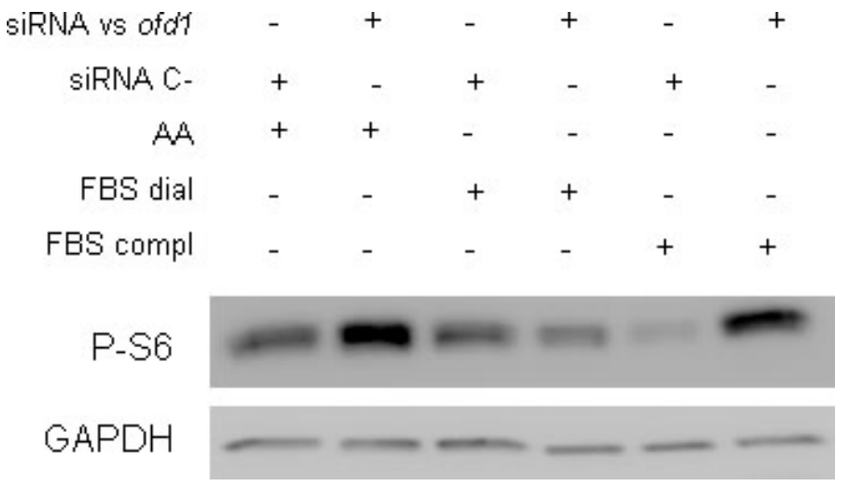

Figure 36. *Ofd1*-depleted cells were more sensitive to AA stimulation. Control and OFD1-silenced HEK293 cells were starved and re-stimulated with AA alone (AA), AA and nutrients (FBS compl), and nutrients alone (FBS dial). After 30 minutes of stimulation, the levels of P-S6 were observed by western blot. *Ofd1*-depleted cells were more sensitive to AA addition (second lane) compared to control (first lane). *Ofd1*-depleted cells (lane 4) and controls (lane 3) show comparable levels of P-S6 after dialyzed FBS (FBS dial, nutrients without AA) addition. When the stimulation was induced by complete FBS (FBS compl, nutrients plus AA) the levels of P-S6 are higher in *Ofd1*-depleted cells (lane 6) compared to control cells (lane 5).

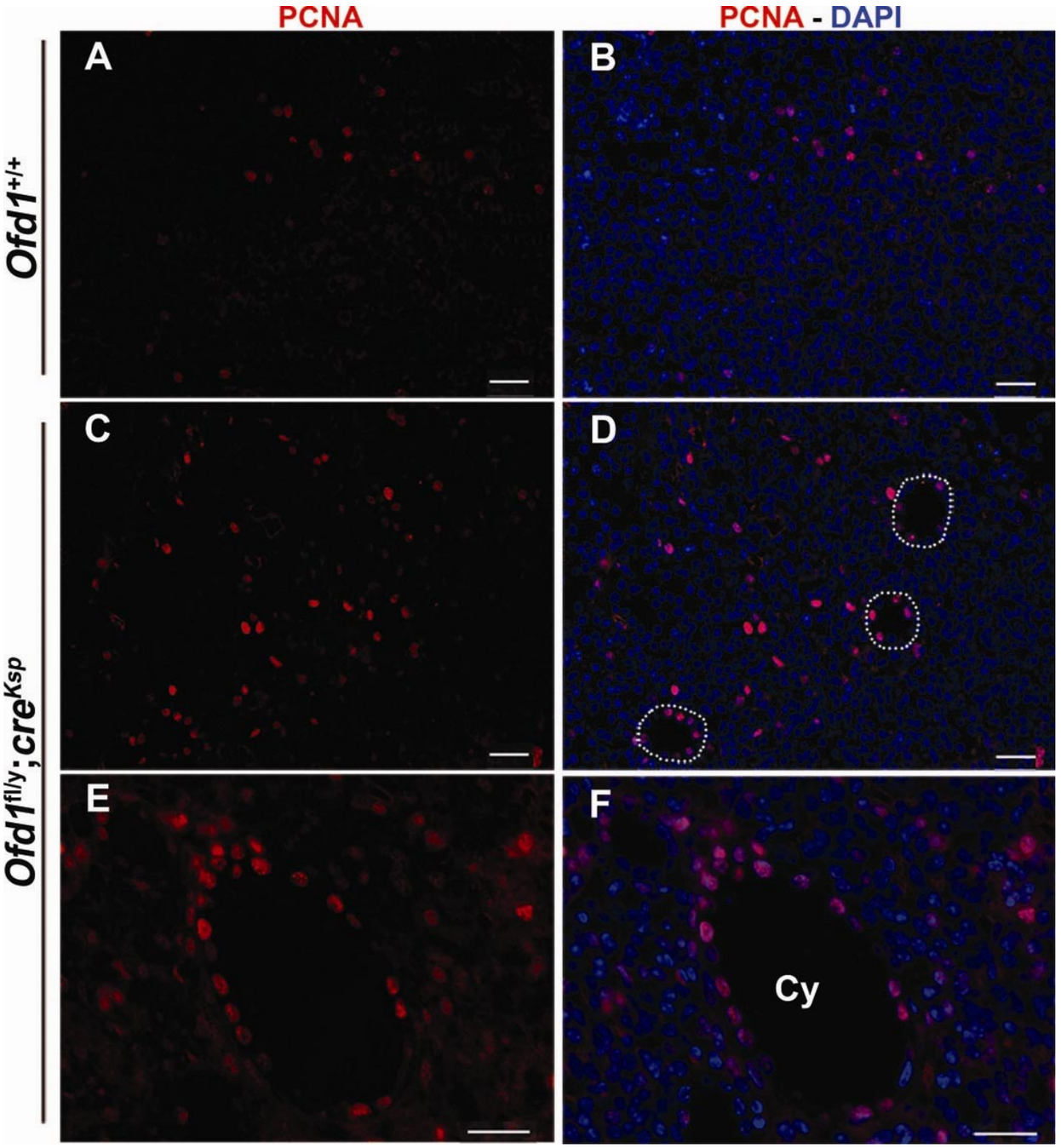

Figure 37. Staining with PCNA (red) reveals an increase of proliferating renal cells from *Ofd1*$^{fl/y}$;*cre*^{Ksp} (*Ksp*) mutants. The number of cell positive at PCNA staining was increased in *Ksp* mutants (C and D) compared with control animals (A and B) at 21. In D cysts are outlined by dotted lines and some of the cells lining the cysts are positive for the staining. The same result is evident in cysts (Cy) shown in E and F where images were taken at higher magnification. Nuclei were stained with DAPI (blue) in B, D, and F. Bars=10 μm (A-F).

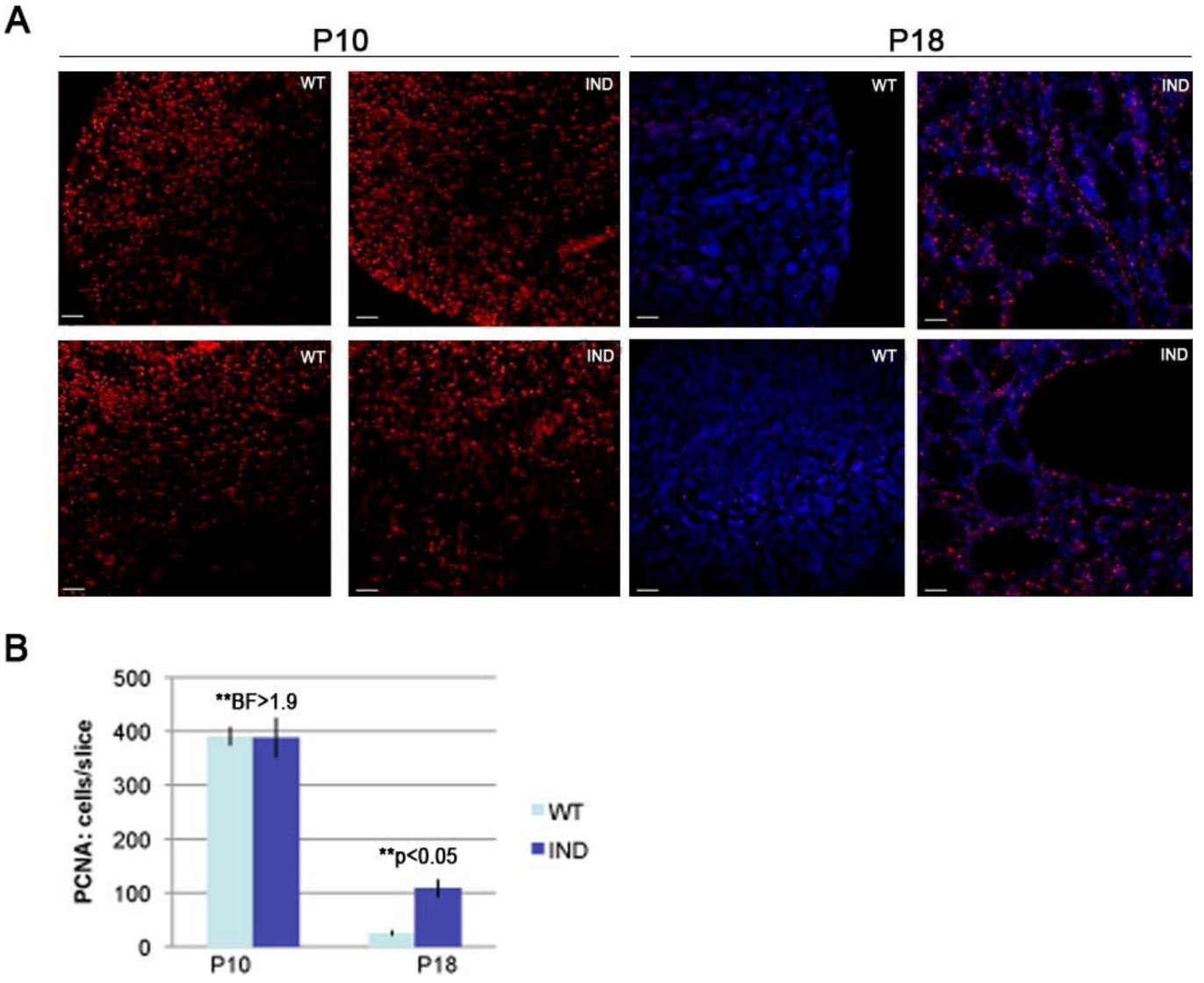

Figure 38. PCNA staining reveals an increased number of positive cells in *Ofd1$^{fl/y}$;CAGGcre^{ER-TM}* (IND) mutants at P18. (A) PCNA staining in renal sections at P10 (panels on the left) reveals the presence of cycling cells both in WT and IND mice. At P18 (panels on the right) PCNA positive cells in the WT animals are reduced when compared to PCNA positive cells present in the IND mice both in cystic and not dilated tubules. (B) At P10 the number of positive cells was comparable between WT and IND mice, while at P18 a significant difference was observed. Bayes Factor (BF) and T-Test were used to calculate the significance. BF>1.9; p-value<0.05. Bars=100um.

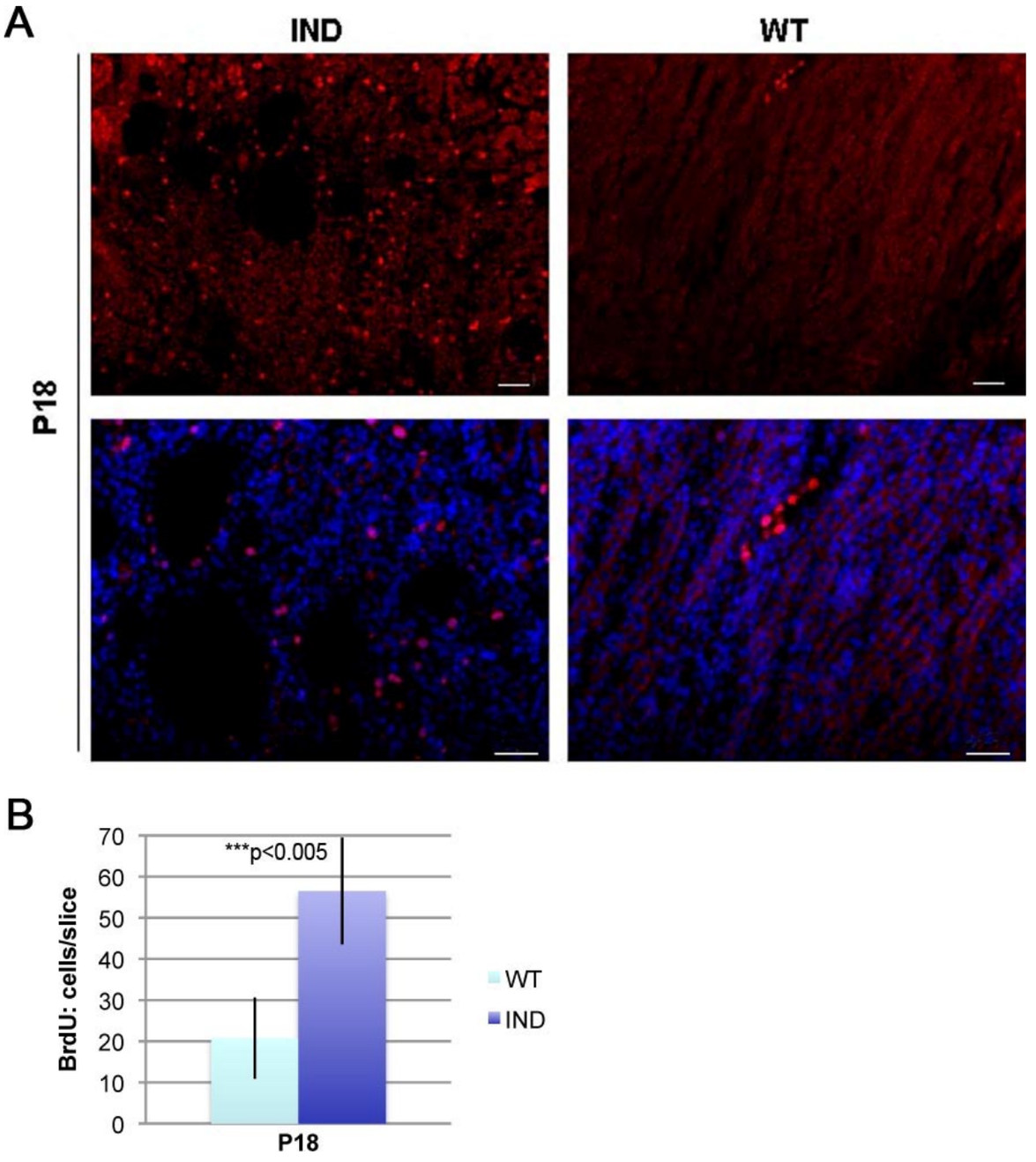

Figure 39. BrdU staining on renal sections reveals an increased number of cells in S-phase in *Ofd1$^{fl/y}$;CAGGcre$^{ER\text{-}TM}$* (IND) mice at P18. (A) BrdU staining at P18 revealed an increased number of positive cells in IND mice compared to WT animals. This observation was quantified in (B). T-test was used to calculate the p-value. p-value<0.005. Bars=50um.

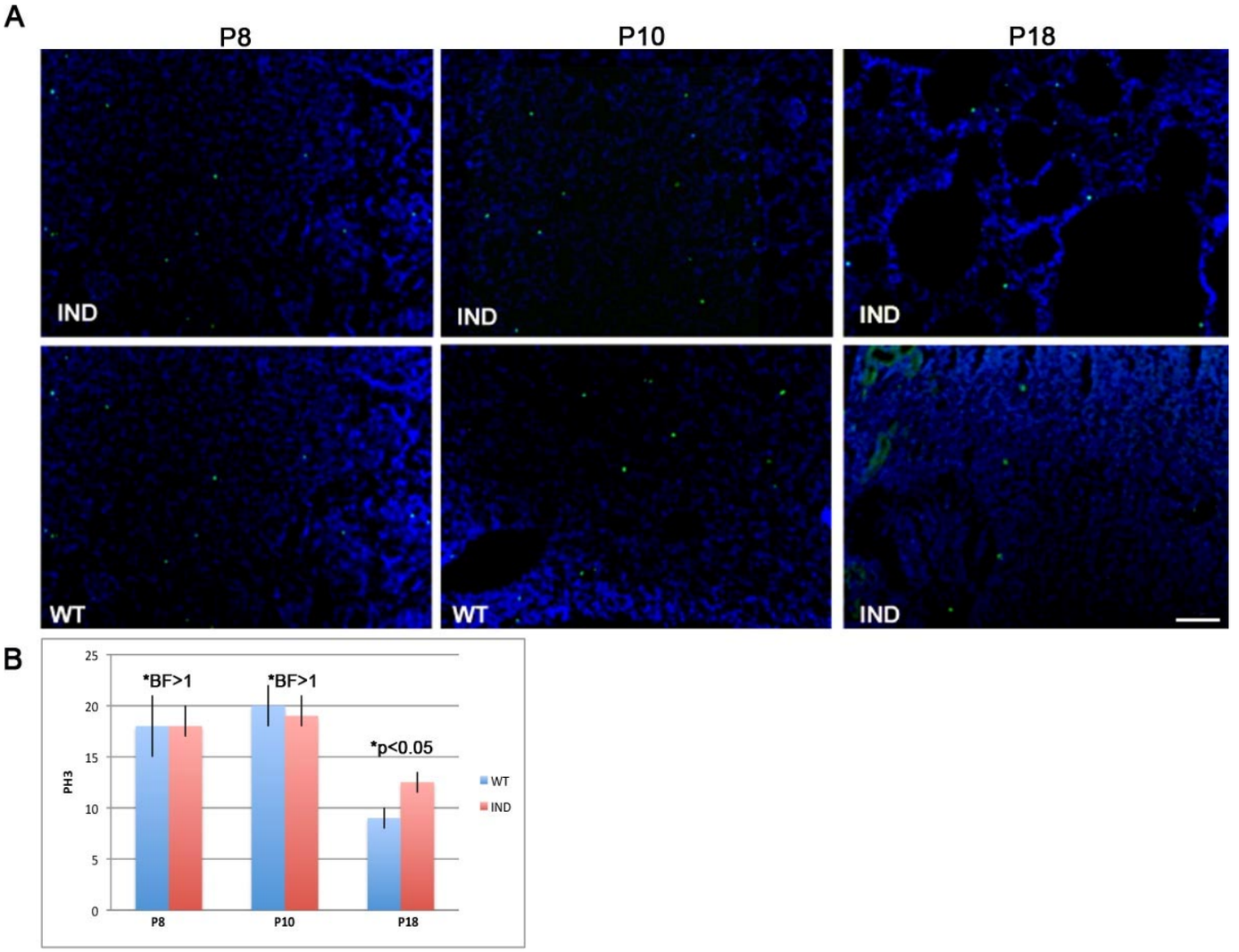

Figure 40. PH3 staining at different stages in WT and *Ofd1$^{fl/y}$;CAGGcre^{ER-TM}* (IND) mice. (A) PH3 staining was performed at P8, P10 and P18. (B) The number of positive cells was comparable between WT and IND mice at P8 and P10. A slight increase of mitotic cells was observed in IND mice at P18 compared to WT. Bar=100um.

i

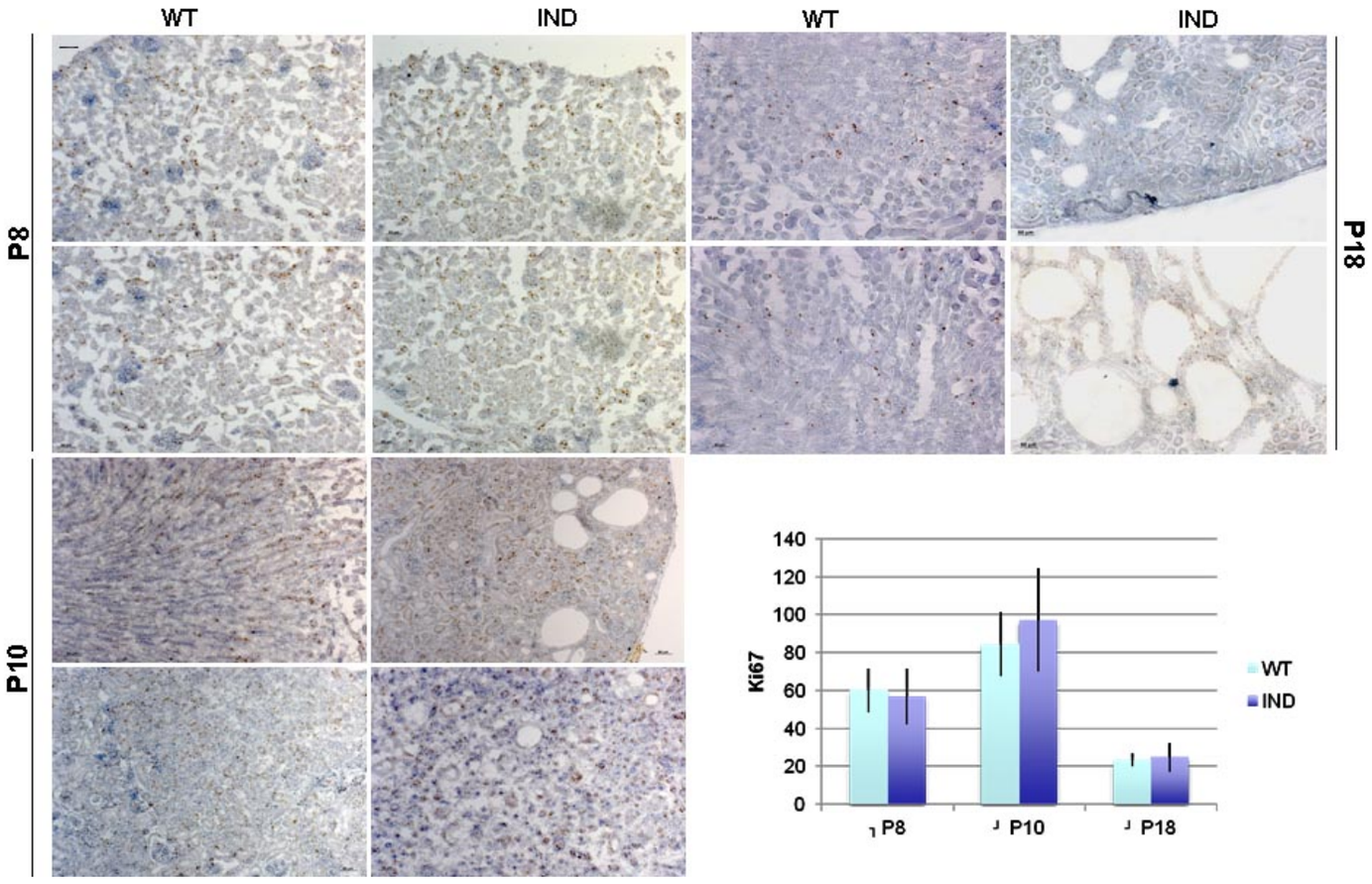

Figure 41. Ki67 staining in *Ofd1$^{fl/y}$;CAGGcre^{ER-TM}* (IND) mice. (A) ICH experiments on renal sections with an antibody against Ki67 revealed that at the different stages analyzed (P8, P10 and P18) the number of positive cells was comparable between WT and IND mice. (B) We counted the cells and the significance was calculated with the Bayes Factor calculation. BF>2. Bars=50um.

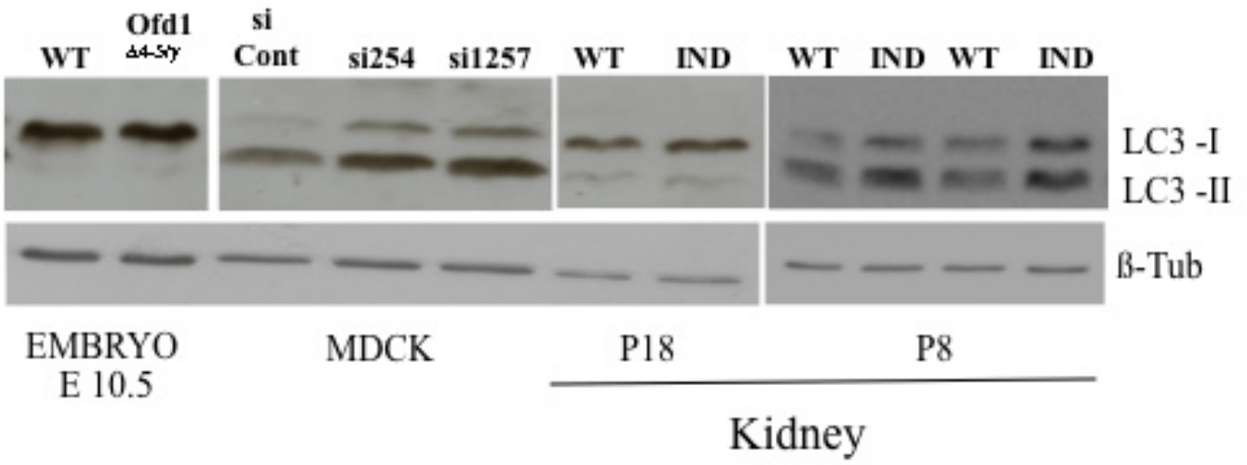

Figure 42. Analysis of LC3 levels in Ofd1-depleted models. Western blot analysis with an antibody against LC3 I and II revealed that LC3 levels were comparable between total lysates from Ofd1$^{+/+}$ control and Ofd1$^{\Delta 4\text{-}5/y}$ null mutants (embryos collected at E10.5) and between WT and lysates from kidneys from *Ofd1*$^{fl/y}$*;CAGGcre*$^{ER\text{-}TM}$ (IND) mutants at P18. Differences were detected in MDCK *Ofd1*-silenced cells and in IND mutants at P8 compared to controls.

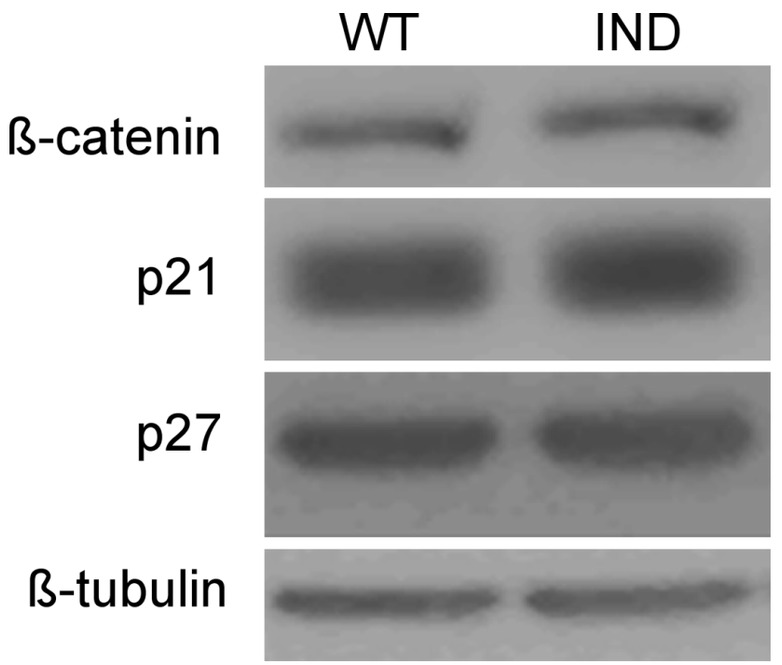

Figure 43. Western Blot analysis of pathways commonly involved in renal cystic disease at P20. We analyzed the levels of β-catenin protein as readout of the Wnt canonical pathway, while p21 and p27 were used as readout of the JAK-STAT pathway. No differences were observed in total protein levels comparing whole lysates from WT and *Ofd1*$^{fl/y}$;CAGGcre$^{ER\text{-}TM}$ (IND) mutants.

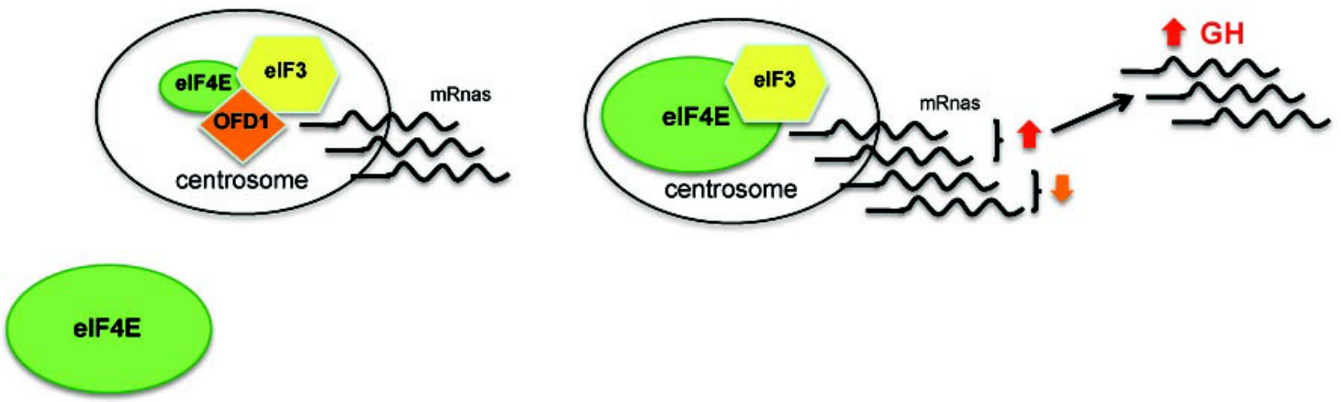

Figure 44. Schematic representation of the possible role of OFD1 in protein synthesis. We propose that OFD1 is part of the preinitiation complex (PIC) of translation at the centrosome where controls the formation of the PIC and the regulation of the translation of specific targets such as GH. In the absence of OFD1 eIF4E accumulates at the centrosome and the translation of specific targets is impaired.